THE STRESS RESPONSE AND CIRCADIAN REGULATION OF TRANSLATION IN NEUROSPORA CRASSA

A Dissertation

by

STEPHEN Z. CASTER

Submitted to the Office of Graduate and Professional Studies of
Texas A&M University
in partial fulfillment of the requirements for the degree of

DOCTOR OF PHILOSOPHY

Chair of Committee,	Deborah Bell-Pedersen
Committee Members,	Daniel J. Ebbole
	Paul Hardin
	Matthew Sachs
	Terry Thomas
Head of Department,	Dorothy Shippen

August 2016

Major Subject: Genetics

ABSTRACT

Stress response pathways function to allow cells to adapt to changes in the environment. In *Neurospora crassa*, acute osmotic stress activates the conserved p38-like osmosensing mitogen-activated protein kinase (OS MAPK) pathway. When activated, the terminal MAPK, OS-2 can activate transcription factors and kinases. We show an acute osmotic stress activates OS-2, which phosphorylates and activates the conserved kinase RCK-2. RCK-2 phosphorylates and inactivates the highly conserved eukaryotic elongation factor 2 (eEF-2). To determine if this is a mechanism for translational regulation of mRNAs, I examined ribosome profiling and RNAseq data from osmotically stressed WT and Δ*rck-2* cultures. I found that RCK-2/eEF-2 regulate 69 constitutively expressed mRNAs at the level of translation. I also examined ribosome profiling and RNAseq data from cultures given light exposure, and found that 36 constitutively expressed mRNAs were regulated at the level of translation. In both cases, the translationally-controlled genes were enriched for metabolic processes, suggesting that rapid regulation of metabolism through translational control helps the organism overcome osmotic and light stress.

The circadian clock has a profound effect on gene regulation; however, little is known about the role of the clock in controlling translation. I show that clock signaling through the OS MAPK pathway promotes rhythmic phosphorylation of RCK-2 and eEF-2 in

constant conditions. Using a cell-free translation assay, I demonstrated that clock signaling to eEF-2 leads to rhythmic control of mRNA translation.

To determine the extent of clock regulation of translation *in vivo*, I examined ribosome profiling and RNAseq data from WT cultures over a circadian time course. 637 Neurospora mRNAs showed rhythmic ribosome occupancy, and 549 of these were from constitutively expressed mRNAs. To determine which of these translationally cycling mRNAs required RCK-2/eEF-2 regulation, I examined ribosome profiling and RNAseq data from Δ*rck-2* cultures over a circadian time course. I found 419 of the constitutive mRNAs with cycling ribosomal occupancy required clock regulation of RCK-2/eEF-2. While the regulation of initiation was thought to be the main control point of translation, these data revealed a major role for eEF-2 activity and elongation in translation control following stress and by the circadian clock.

DEDICATION

I would like to dedicate my dissertation to my family, especially my mother and sister who were always there for support and guidance. I would also like to dedicate this to my grandparents, who taught me what it means to be strong.

ACKNOWLEDGEMENTS

I would like to acknowledge the members of the Bell-Pedersen lab, both past and present for their continuous support and feedback. I would particularly like to thank Jay Dunlap for collaborative support, as well as Bill Belden for the unique opportunity to learn how to analyze big data. I would like to thank all the students and faculty in both the Texas A&M Center for Biological Clocks Research and the Genetics department. I would also like to thank my committee for their support and advice over these many years. And lastly, I would like to thank Deborah Bell-Pedersen for all of her help, support, and continuous effort to make our lab a successful one.

TABLE OF CONTENTS

Page

LIST OF FIGURES

Page

LIST OF TABLES

Page

CHAPTER I

INTRODUCTION

Circadian Clock

The circadian clock acts as an endogenous mechanism that regulates diverse biological functions in many organisms, from prokaryotes to eukaryotes (1). The clock regulates daily rhythms in biological processes ranging from sleep-wake cycles to metabolism and gene expression. Disruption of the circadian clock has profound effects on human physiology, and can lead to metabolic disorders and tumor development (2, 3). Evidence for the circadian clock was first reported in 1729 by Jean Jacques d'Ortous deMairan in which he observed leaf movement, even in the absence of light (4, 5). However, it was not until the 1950s and 1960s that the study of biological clocks began in earnest, and over the subsequent decades, the field of chronobiology has expanded into many varieties of organisms ranging from cyanobacteria to humans (5).

The key properties for a circadian clock are defined as: i) the persistence of rhythms in constant environmental conditions (e.g., constant darkness) with a period of about 24 h, also called the free-running period; ii) temperature compensation (i.e., a change in temperature does not affect the period length); and iii) the clock can be reset by environmental input signals. The molecular clock consists of genes that encode positive element(s) that activate downstream negative element(s) that in turn inhibit the activity

of the positive element(s). These elements form an auto-regulatory feedback loop that controls daily rhythms (1, 6).

The Circadian Clock in *Neurospora crassa*

Many fundamental properties of the clock have been discovered using the simple eukaryotic fungus *Neurospora crassa* as a model system (7). When Neurospora is grown in constant conditions (i.e., in constant darkness (DD) at 25° C), the positive components of the core oscillator, WHITE COLLAR-1 (WC-1) and WC-2, heterodimerize to form the WHITE COLLAR COMPLEX (WCC). WC-1 is a zinc finger DNA transcription factor with LOV (light, oxygen, and voltage-sensing) and PAS (Per-ARNT-Sim) domains (8, 9). In addition to being a key component of the circadian clock, WC-1 is also a blue-light photoreceptor (10, 11). WC-2 is also a zinc finger transcription factor, with a single PAS domain (12). In the clock mechanism, WCC activates transcription of *frequency* (*frq*), a negative element (13).

The *frq* gene acts as the main regulator of the WCC and encodes both a long and short isoform of FRQ protein (14). FRQ accumulates over time and dimerizes, forming a complex with FREQUENCY-INTERACTING RNA HELICASE (FRH) called the FCC. FRH stabilizes FRQ, preventing its rapid degradation due to the intrinsically disordered properties of FRQ protein (15). The FCC inhibits the activity of the WCC by recruiting casein kinase 1a (CK1a) to the WCC, which results in hyperphosphorylation of the WCC (16). Hyperphosphorylated WCC is stable but inactive, which in turn leads to

diminished transcription of *frq*. Over time FRQ is progressively phosphorylated and interacts with FWD-1, an F-box/WD-40 repeat-containing protein that acts as a substrate for the SCF (Skp1-Cul1-F-box-protein) ubiquitin ligase (17, 18). FRQ is then ubiquitinated and degraded, and the WCC becomes dephosphorylated and active again, through the activity of protein phosphatase 2A (PP2A) to restart the cycle (19).

Clock Regulation of Output Pathways in Neurospora

In addition to the WCC binding to the *frq* promoter, the WCC also binds to approximately 5% of all genes in Neurospora, most of which are both clock- and light-regulated (20). These genes encode transcription factors, as well as various output pathway components and terminal clock-controlled genes (ccgs) (6). Circadian regulation of the first tier transcription factors leads to clock control of approximately 40% of Neurospora genes.

One of the identified output pathway components, *os-4*, has WCC binding sites or light response elements (LREs) found in the promoter region. OS-4 is the mitogen activated protein kinase kinase kinase (MAPKKK) of the osmosensing (OS) MAPK pathway. MAPK pathways consist of serine/threonine MAPKs that link extracellular signals to regulate many cellular processes including, but not limited to stress response, apoptosis and survival (21). The OS MAPK pathway in Neurospora is important for cell adaptation in conditions of high osmolarity, and phosphorylation/activation of the terminal MAPK (OS-2) is clock-controlled (22).

Clock regulation of MAPK pathways and cellular processes provides an adaptive advantage in anticipation of daily environmental stressors (20, 23, 24). The WCC rhythmically binds to the promoter of *os-4*, and OS-4 protein accumulates rhythmically. When the LREs are deleted in the *os-4* promoter, *os-4* mRNA is arrhythmic and that in turn results in constitutive phosphorylation of the downstream MAPK OS-2 (25). Following osmotic stress, phosphorylated OS-2 (P-OS-2) can interact with other proteins, including transcription factors, kinases, and chromatin remodeling proteins, leading to activation or repression of target genes (26). However, not much is known about the downstream effects of clock regulation of P-OS-2.

Post-transcriptional Control by the Circadian Clock

Depending on the organism and tissue, between 10 - 40% of the eukaryotic genome is under control of the clock at the level of transcription (27-32). These transcripts peak in abundance at all possible phases of the circadian cycle, implicating the action of a network of transcription factors controlling phase. Such studies led to the dogma that circadian output is primarily controlled at the transcriptional level. However, some mammalian genes show post-transcriptional control of rhythmicity (33, 34), including clock control of splicing (35), polyadenylation (36, 37), and deadenylation (38, 39). The extent of this control, and the mechanisms for many of these events, have not been fully elucidated. In addition, recent proteomic analysis of rhythmically accumulating soluble

proteins in mouse liver showed that up to 50% of the proteins examined had robust rhythms in abundance, but no apparent rhythms in the associated mRNA levels (40).

Consistent with clock control of translation, the clock regulates the levels (eIF1, eIF4A2, eF4G1, eIF5, eEF2, eEF1A1) and phosphorylation state (eIF4E, eIF4G, eIF4B, 4EBP1) of translation initiation factors in mouse liver (41, 42), and the clock has been implicated in regulating the translation efficiency of mRNAs with specific 5'-terminal oligo pyrimidine tract (5'-TOP) sequences or with translation initiator of short 5'-UTR (TISU) motifs (43). Furthermore, circadian rhythms can persist in the absence of transcription, as exemplified by the non-transcriptional time-keeping mechanism in the cyanobacterial Kai oscillator, and the evolutionarily conserved rhythms in post-translational modification of the antioxidant peroxiredoxin proteins (44).

Also consistent with clock control of translation, individual genes from a variety of organisms have rhythms in protein levels that arise from mRNAs that accumulate constitutively over the course of the day. Examples include LBP in Gonyaulax (45), Eip74EF in Drosophila (46), Nocturnin in Xenopus retina (38), Pdia3, Cat, and Serpina1d in the mouse liver (40), and WC-1 in Neurospora (47). For LBP and Eip74EF, translational regulation is due to rhythmic RNA-binding protein interactions at the 3' UTR; however for the others, the mechanisms of circadian post-transcriptional control have not been fully elucidated. Rhythmic antisense RNA and/or miRNA expression is also implicated in translational control of core clock proteins, including antisense RNA

to *frq* in Neurospora, antisense RNA to *per* in Drosophila, and miR-141 control of *Clock* in mice (33, 34). In mouse liver, the clock controls mRNA levels for several translation initiation factors, ribosomal RNAs, and ribosomal protein mRNAs (41), suggesting that aspects of ribosome biogenesis are clock-regulated. These data, although limited, indicate that clock regulation of translation may be a widespread phenomenon.

Taken together, these data show that a wholly transcriptional model for rhythmic gene regulation cannot account for the extent of rhythms of protein expression, and point to important roles for post-transcriptional, translational, and/or post-translational mechanisms in generating circadian output. Yet, while we know that rhythmic mRNA does not necessarily reflect rhythmic protein expression, and the phase relationships between mRNA levels and protein are not always overlapping, we lack basic information on how the clock controls these fundamental post-transcriptional control mechanisms. Elucidating the rhythmic proteome and the translational control points that regulate circadian protein oscillations is a critical step needed to understand the molecular programs that drive circadian physiology and associated disease.

Clock Regulation of Translation in Neurospora

In yeast, the homolog of Neurospora OS-2, Hog1, directly phosphorylates and activates a conserved serine/threonine kinase, Rck2. The activation of Rck2 occurs when Hog1 phosphorylates serine and threonine residues within the C-terminal autoinhibitory domain. (48, 49). Activated Rck2 then directly phosphorylates elongation factor-2 (EF-

2) (50-52). eEF-2 is the major regulator of peptide chain elongation in all eukaryotic cells, critical for cell growth and proliferation (53). eEF-2 activity is increased in several human tumors and cancer cell lines, including glioblastoma, gastrointestinal, breast, and lung cancers (54-57). eEF-2 activity is also associated with cell cycle progression, cellular differentiation, and development (58-60). Interestingly, while phosphorylation of eEF-2 (P-eEF-2) is primarily associated with translation repression, in Aplysia and mouse neurons, P-eEF-2 promotes translation of some mRNAs, while repressing others (61, 62)

N. crassa RCK-2 was identified by comparing *S. cerevisiae* Rck2 to the Neurospora genome. A protein was identified encoded by NCU09212 that had 40% amino acid identity to yeast Rck2, with the majority of the sequence identity occurring within the catalytic domain (Figure 1A). This domain is conserved throughout eukaryotes and is homologous to mammalian MAPK-activated protein kinase 2 (MAPKAP-K2). It was previously shown that p38, the mammalian homolog of Neurospora OS-2, directly phosphorylates MAPKAP-K2, similar to yeast (63).

N. crassa eEF-2 was also identified by comparison of Neurospora proteins to EF-2 from yeast. The protein encoded by NCU07700 has 79% identity to yeast EF-2 (Figure 1B). This elongation factor is highly conserved throughout eukaryotes, and is homologous to mammalian eEF-2. During translation elongation, eEF-2 is responsible for mediating the

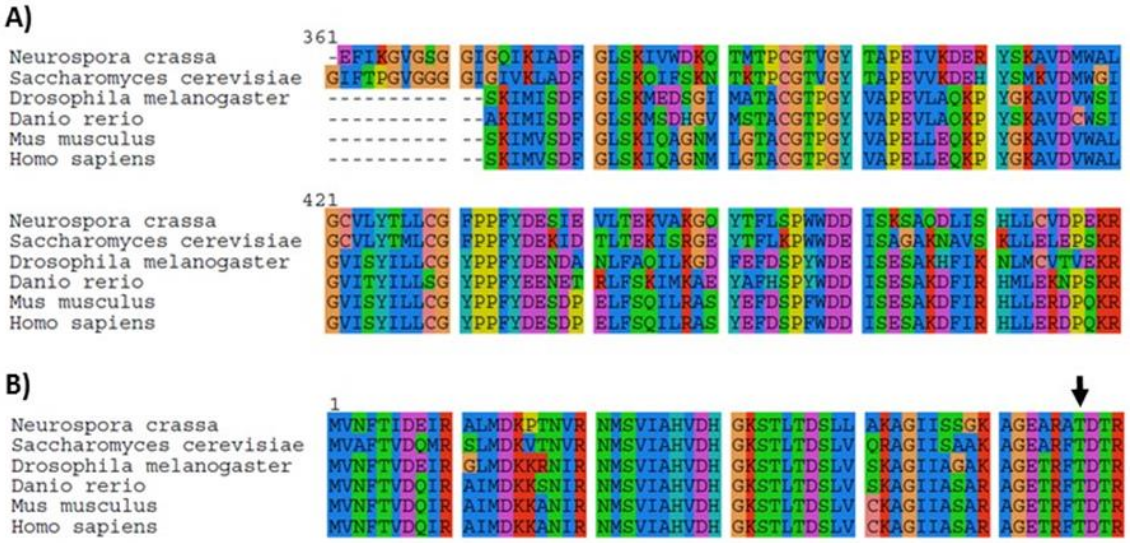

Figure 1. Sequence alignment of *N. crassa* RCK-2 and eEF-2. Multi-sequence alignment of the *N. crassa* RCK-2 catalytic domain (A) and eEF-2 N-terminus (B) to homologs in the indicated organisms. The arrow indicates the conserved threonine residue at amino acid 56 in eEF-2 that is phosphorylated.

translocation of the peptidyl-tRNA from the A-site to the P-site of the ribosome (64). eEF-2 can be inactivated through phosphorylation of Thr56, effectively stalling translation elongation, and inhibiting translation (65-67). Work in mammals has shown that signaling through the p38 pathway and MAPKAP-K2 leads to phosphorylation of eEF-2 kinase (53, 68). When eEF-2 kinase is activated, it phosphorylates and inactivates eEF-2 (69). While we were unable to identify eEF-2 kinase in *N. crassa*, our work demonstrates that RCK-2 can directly interact with and phosphorylate eEF-2 in the absence of any known eEF-2 kinase (see Chapter II).

Objectives

The clock provides an endogenous mechanism for anticipation of daily environmental stresses. Many studies have focused on cataloging rhythmic mRNA, and determining how the clock regulates rhythmic mRNA levels through the activity of clock controlled transcription factors (20, 70). However, little is known about how the clock regulates translation. I propose that clock signaling through the OS MAPK pathway leads to rhythmic phosphorylation and activation of RCK-2. RCK-2 then rhythmically phosphorylates eEF-2, acting as a mechanism for clock regulation of translation of specific mRNAs. The following hypotheses will be tested in order to validate this proposal:

1. RCK-2 and eEF-2 are part of the osmotic stress response pathway. To test this hypothesis, I first examined the response of RCK-2 and eEF-2 activity following an osmotic stress. I found that RCK-2 protein is induced and highly phosphorylated following osmotic stress, and that this response required OS-2. I also found that eEF-2 is highly phosphorylated following osmotic stress, and that phosphorylation of eEF-2 is partially due to OS-2 activation of RCK-2. These data suggested that RCK-2 and eEF-2 are part of the stress response pathway, but eEF-2 phosphorylation can be regulated by other kinase(s).

2. Clock signaling through the OS pathway, leads to rhythmic phosphorylation of RCK-2 and eEF-2, acting as a mechanism for clock regulation of translation

elongation. To test this hypothesis, I examined phosphorylation of RCK-2 and eEF-2 over a circadian time course. I discovered that both RCK-2 and eEF-2 phosphorylation are clock-controlled, and the rhythm in accumulation of phosphorylated RCK-2 and eEF-2 requires clock signaling through the OS pathway. Using translation extracts programmed with luciferase mRNA in an *in vitro* assay, I found that clock control of the levels of phosphorylated eEF-2 leads to rhythmic repression of translation, and that clock signaling through RCK-2 and eEF-2 leads to repression of translation elongation.

3. Because not all Neurospora proteins cycle in abundance, I hypothesized that clock control of the levels of phosphorylated eEF-2 does not affect all mRNAs. In order to test this hypothesis, I performed ribosome profiling (to determine which mRNAs are being actively translated) and RNAseq (to identify all mRNAs) following an osmotic stress, a light pulse, and over a circadian time course. I identified 194 genes that were significantly up-regulated or down-regulated at the level of ribosomal occupancy following an osmotic stress, and showed that 69 of these genes required RCK-2 for regulation by osmotic stress. Using functional categorization (FunCat) analyses, I found that these genes were primarily enriched for metabolic processes. Following a light pulse, I identified 36 genes that were induced or repressed only at the level of translation. These genes were also enriched for metabolic processes. When I examined circadian regulation of mRNA translation by ribosome profiling, I identified 549 mRNAs

that have rhythmic ribosomal occupancy, but constitutive mRNA expression. Some of these genes were also enriched for metabolic processes. Of these genes, 419 were arrhythmic in Δ*rck-2* cells, demonstrating that the clock is regulating a specific set of mRNAs at the level of translation through control of the activity of RCK-2 and eEF-2.

The subsequent chapters will describe the results of my research. Chapter II is a manuscript that has been accepted by PNAS (Caster et al., 2016). Chapter III is a combination of 3 papers that are currently in preparation that describe the results of ribosome profiling and RNAseq following osmotic stress, light treatment, and over a circadian time course. In chapter IV, I discuss the major findings of this research, the significance of these findings, future plans for the 3 papers in preparation, and future directions for this work. Appendix A consists of a list of strains used for these experiments, as well as tables generated from the sequencing data from chapter III. Appendix B provides information on the pipeline and script used to analyze both the ribosome profiling and RNAseq data. Appendix C describes a grant proposal discussing the ribosome code (i.e., ribosomes with distinct compositions translate specific mRNAs). In Appendix C, my contribution to the grant is specified.

CHAPTER II

CIRCADIAN CLOCK REGULATION OF mRNA TRANSLATION THROUGH EUKARYOTIC ELONGATION FACTOR eEF-2*

Introduction

Circadian rhythms are the outward manifestation of an endogenous clock mechanism common to nearly all eukaryotes. Depending on the organism and tissue, nearly half of an organism's expressed genes are under control of the circadian clock at the level of transcription (32, 70-72). However, mounting evidence indicates a role for the clock in controlling post-transcriptional mechanisms (73), including translation initiation (41, 74), while clock control of translation elongation has not been investigated.

The driver of circadian rhythms in *N. crassa* is an autoregulatory molecular feedback loop composed of the negative elements FREQUENCY (FRQ) and FRQ RNA-interacting helicase (FRH), which inhibit the activity of the positive elements WHITE COLLAR-1 (WC-1) and WC-2 (75-78). WC-1 and WC-2 heterodimerize to form the white collar complex (WCC), which activates transcription of *frequency* (*frq*) (11, 75, 79), as well as activating transcription of a large set of downstream target genes important for overt rhythmicity (20, 70). One gene directly controlled by the WCC is *os-*

*Reprinted with permission from "Circadian clock regulation of mRNA translation through eukaryotic elongation factor eEF-2" by S. Caster, K. Castillo, M. Sachs, D. Bell-Pedersen (2016) *Proc Natl Acad Sci* ©The National Academy of Sciences of the USA

4, which encodes the mitogen-activated kinase kinase kinase (MAPKKK) in the osmotically-sensitive (OS) MAPK pathway (25). Rhythmic transcription of *os-4* leads to rhythmic accumulation of the phosphorylated active form of the downstream p38-like mitogen-activated protein kinase (MAPK) OS-2 (22). In *Saccharomyces cerevisiae*, the homolog of OS-2, Hog1, directly phosphorylates and activates the MAPK-activated protein kinase (MAPKAPK) Rck2 after acute osmotic stress (48, 49). Activated Rck2 phosphorylates EF-2, and as a result, represses translation elongation for most mRNAs (50-52). Therefore, we hypothesized that circadian clock control of OS-2 activity in *N. crassa* leads to temporal control of translation elongation through rhythmic activation of RCK-2.

In support of this hypothesis, we show that clock control of OS-2 leads to rhythmic phosphorylation of RCK-2 and eEF-2 in cells grown in constant conditions. Consistent with the peak in phosphorylated eEF-2 during the morning, translation elongation rates are reduced in extracts prepared from cells harvested at this time of the day. Furthermore, clock-controlled translation of GST-3 protein from constitutive mRNA levels *in vivo* is dependent on rhythmic eEF-2 activity, whereas rhythms in accumulation of FRQ are not dependent on rhythms in phosphorylated eEF-2. Together, these data support clock regulation of translation elongation of specific mRNAs as a mechanism to control rhythmic protein accumulation.

Results

Phosphorylation of RCK-2 Protein Requires OS-2

Total Rck2 kinase levels, and Rck2 phosphorylation by Hog1, increase following osmotic stress in *S. cerevisiae* cells (50). Rck2 then phosphorylates and inactivates EF-2, leading to general repression of translation (50, 80). To investigate if a similar mechanism exists for regulation of translation in *N. crassa*, we identified *N. crassa* RCK-2 and eEF-2 through sequence homology. To determine if *N. crassa* RCK-2 functions in the osmotic stress response pathway, RCK-2 protein levels and phosphorylation state were measured following acute osmotic stress in WT or Δ*os-2* cells containing a C-terminal hemagglutinin (HA)-tagged RCK-2 protein (RCK-2::HA) grown in the dark for 24 h (DD24) and then subjected to acute osmotic stress. As in yeast, *N. crassa* RCK-2::HA protein levels increased following osmotic stress, and induction required OS-2 (Figure 2A). Two forms of RCK-2::HA protein were observed by SDS-PAGE in WT cells, but not in Δ*os-2* cells (Figure 2A). Consistent with the idea that the slower migrating form of RCK-2::HA was phosphorylated, the band disappeared when protein extracts were treated with λ-phosphatase, but persisted in extracts treated with λ-phosphatase and phosphatase inhibitors (Figure 2B). In yeast, phosphorylated Rck2 is observed in osmotically stressed, but not in unstressed cells (50). In contrast, phosphorylated RCK-2:HA (P-RCK-2) was present in unstressed *N. crassa* cells, suggesting that OS-2-dependent phosphorylation of RCK-2 was directed by different input signals to the OS MAPK pathway, possibly signals from the circadian clock.

eEF-2 Phosphorylation is Regulated by RCK-2

To determine if *N. crassa* eEF-2 activity is altered following an acute osmotic stress, the levels of phosphorylated eEF-2 (P-eEF-2) were examined using an antibody that recognizes P-eEF-2 at the conserved threonine 56 residue (Figure 3A). P-eEF-2 levels

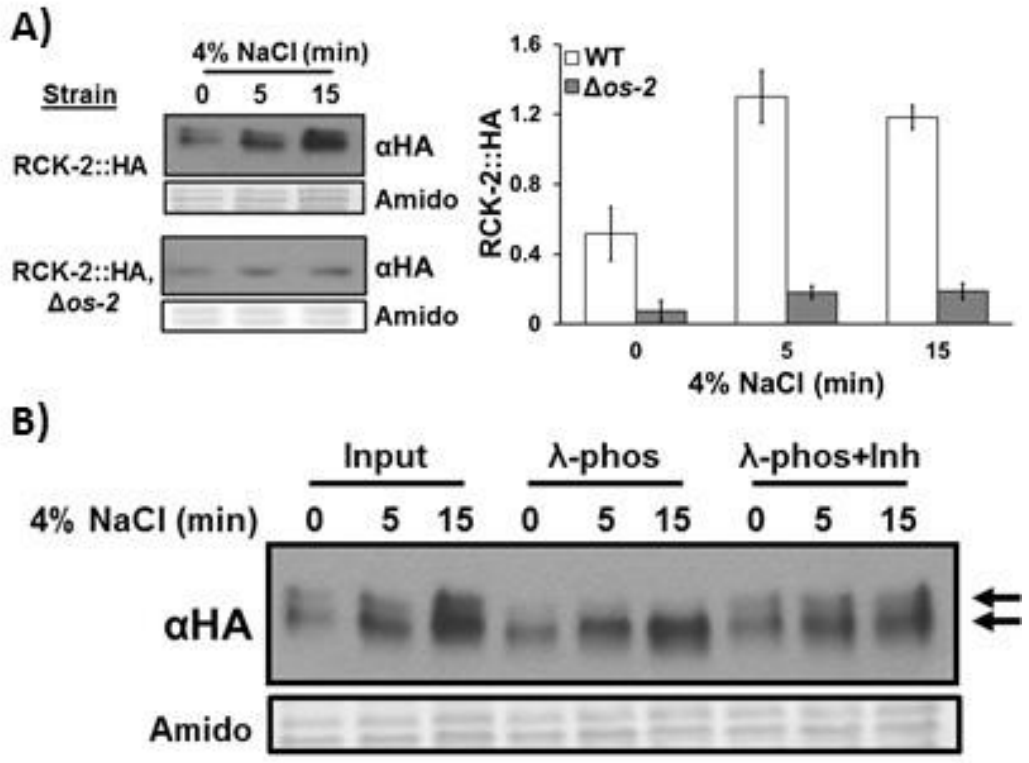

Figure 2. RCK-2 protein is induced by osmotic shock. A) Representative western blot of protein isolated from RCK-2::HA and RCK-2::HA, Δ*os-2* cells grown in the dark (DD) for 24 h (DD24) and incubated with 4% NaCl for the indicated times and probed with HA antibody (αHA). Amido stained proteins served as loading controls. The data are plotted to the right (mean ± SEM, n = 3). B) Western blot of protein from RCK-2::HA cells grown in the dark for 24 h and incubated with 4% NaCl for the indicated times, and given no further treatment (Input), treated with λ-phosphatase (λ-phos), or treated with λ-phosphatase plus phosphatase inhibitors (λ-phos+inh), and probed with HA antibody. The upper arrow points to the phosphorylated form of RCK-2, and the lower arrow to the unphosphorylated protein.

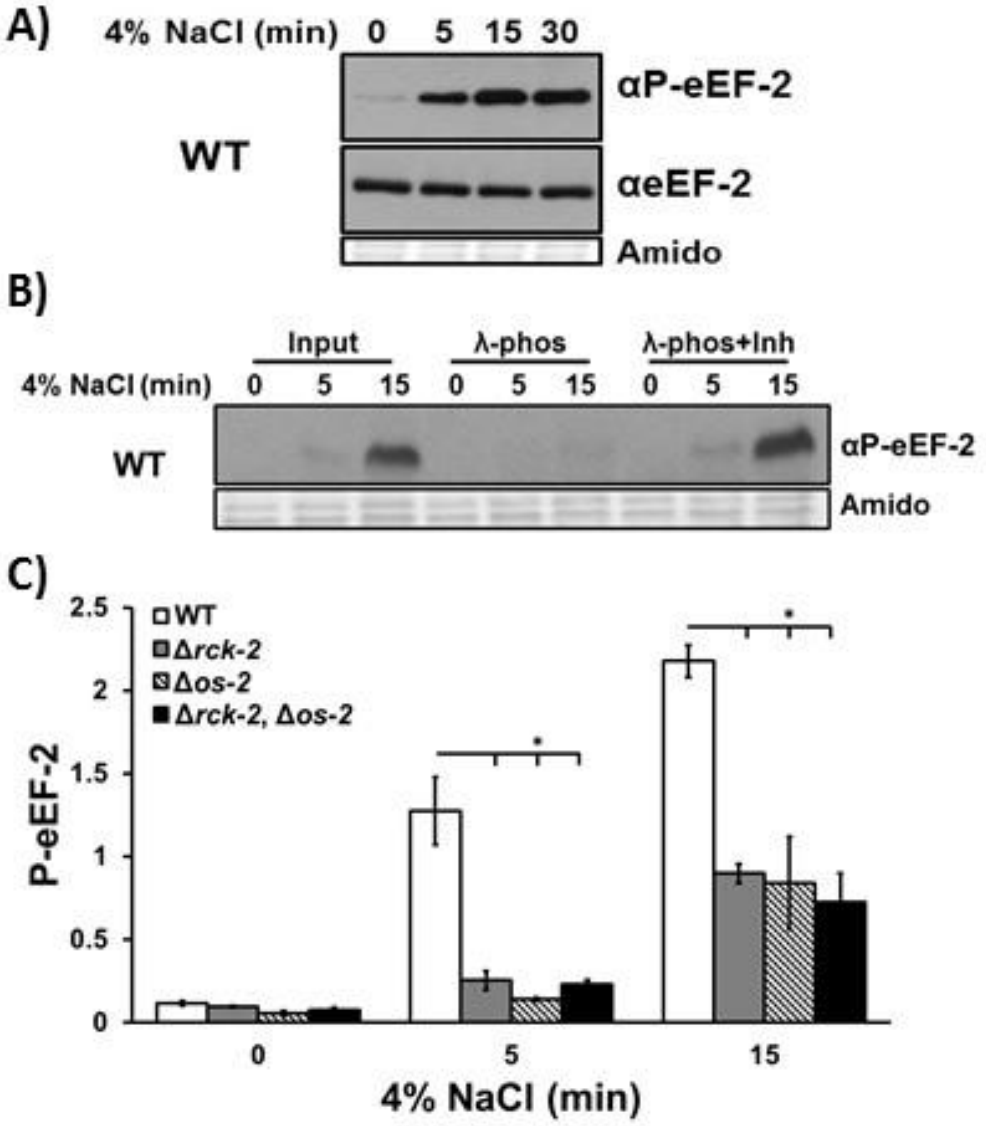

Figure 3. Osmotic stress-induced phosphorylation of eEF-2 is reduced in Δ*rck-2* cells. A) Western blots of protein extracted from WT cells grown in DD24 and treated with 4% NaCl for the indicated times and probed with phospho-specific eEF-2 antibody (αP-eEF-2) or total eEF-2 antibody (αeEF-2). The film was exposed for 15 s. B) Western blot of protein from WT cultures grown in DD24 and incubated with 4% NaCl for the indicated times, and given no further treatment (Input), treated with λ-phosphatase (λ-phos), or treated with λ-phosphatase plus phosphatase inhibitors (λ-phos+inh), and probed with αP-eEF-2. The film was exposed for 1.5 s. C) Plot of eEF-2 levels from WT, Δ*rck-2*, Δ*os-2*, and double mutant Δ*rck-2*, Δ*os-2* cells grown in DD24 and incubated with 4% NaCl for the indicated times (mean ± SEM, n = 3). The asterisks indicate a statistical difference ($p < 0.05$, student T-test). The western blots are shown in Figure 5.

increased within 5 min of addition of 4% NaCl to the cultures at DD24, whereas total eEF-2 levels, detected using an antibody generated to recognize all forms of eEF-2, were similar in untreated and salt-treated samples. To verify the specificity of the P-eEF-2 antibody, salt-treated samples were incubated with λ-phosphatase (Figure 3B). As expected, eEF-2 was not detected with P-eEF-2 antibody in the λ-phosphatase-treated samples, but was detected in samples treated with λ-phosphatase plus phosphatase inhibitors.

In *S. cerevisiae*, Rck2 directly phosphorylates eEF-2 (50). Immunoprecipitation of *N. crassa* RCK-2::HA with HA antibody resulted in co-immunoprecipitation of eEF-2 (Figure 4), suggesting that similar to *S. cerevisiae*, RCK-2 may directly phosphorylate eEF-2 in response to osmotic stress. Consistent with this idea, P-eEF-2 levels were significantly lower in Δ*rck-2* cells compared to WT cells following osmotic stress, such that P-eEF-2 levels were reduced up to 80% in Δ*rck-2* cells subjected to 5 min of salt stress (Figure 3C & 5). However, low-level phosphorylation of eEF-2 persisted in the absence of RCK-2, indicating that in addition to RCK-2, other kinase(s) can phosphorylate eEF-2. One possible candidate kinase was the MAPK OS-2. We examined the levels of P-eEF-2 in Δ*rck-2*, Δ*os-2*, and double Δ*rck-2*, Δ*os-2* mutant cells and found that the levels of P-eEF-2 in Δ*os-2* and the double Δ*rck-2*, Δ*os-2* mutant strain were similar to that observed in Δ*rck*-2 cells treated with NaCl for 5 or 15 min (Figure 3C & 5). Furthermore, levels of total eEF-2 in Δ*rck-2*, Δ*os-2*, and double Δ*rck-2*, Δ*os-2* mutant cells were similar to levels in WT cells (Figure 3C & 5), indicating that

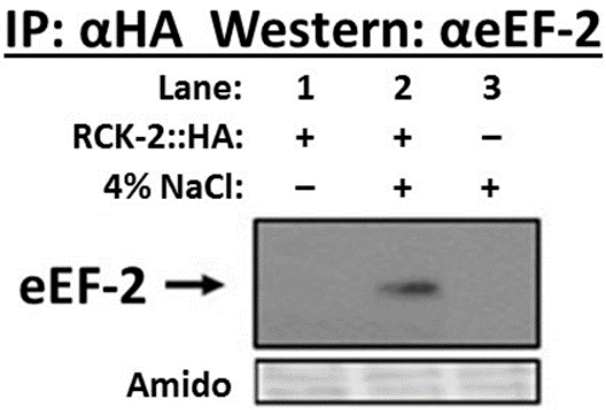

Figure 4. RCK-2 interacts with eEF-2 *in vivo*. Co-immunoprecipitation of RCK-2::HA (lanes 1 and 2) and control WT cells (lane 3) treated (+) or not (-) with 4% NaCl for 5 min was performed with HA antibody (αHA) and the blot was probed with αeEF-2. Amido stained proteins served as loading controls.

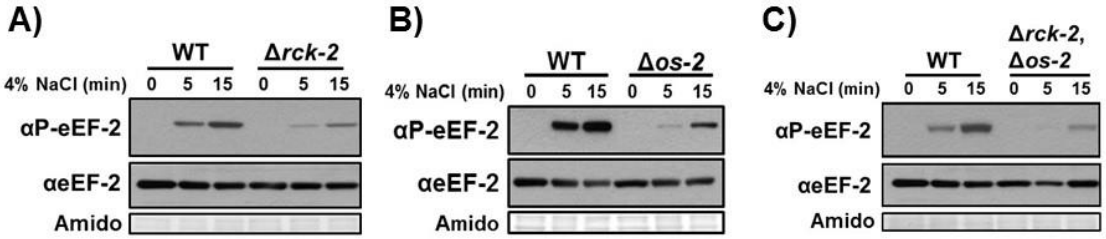

Figure 5. Osmotic stress-induced phosphorylation of eEF-2 is reduced in Δ*rck-2*, Δ*os-2*, and Δ*rck-2*, Δ*os-2* cells. Western blots of protein extracted from WT, Δ*rck-2* (A), Δ*os-2* (B), and Δ*rck-2*, Δ*os-2* (C) cells grown at DD24 and incubated with 4% NaCl for the indicated times and probed with αP-eEF-2 and αeEF-2. Amido stained proteins served as loading controls.

unidentified kinases phosphorylate eEF-2 following osmotic stress in the absence of RCK-2 and OS-2.

RCK-2 Phosphorylation is Regulated by the Circadian Clock

Based on clock control of the OS MAPK pathway (25, 81), and OS-2-dependent phosphorylation of RCK-2 (Figure 2A), I predicted that the circadian clock regulates the accumulation of phosphorylated RCK-2 (P-RCK-2) in constant environmental conditions. An antibody to detect phosphorylated RCK-2 was not available; however, P-RCK-2 could be separated from RCK-2 using PhosTag^{TM} gels (Figure 6A & B). P-RCK-2 levels cycled, and accumulation peaked during the late subjective night (DD28-32) (Figure 7A), slightly earlier than the peak accumulation of P-OS-2 (DD32-36) (25, 81). The earlier peak time in P-RCK-2 levels may be due to experimental error from using 4 h time points, or may reflect increased P-OS-2 activity during its accumulation. RCK-2 and P-RCK-2 levels were significantly reduced in Δ*os-2* cells harvested at DD24 (Figure 6C & D). The reduced levels of RCK-2 in Δ*os-2* cells in the dark suggested that in addition to control of RCK-2 phosphorylation, the OS pathway is necessary for normal expression of RCK-2. This regulation was not further investigated in this study. Consistent with clock regulation of P-RCK-2 levels through the OS-pathway, P-RCK-2 accumulation was low and arrhythmic in Δ*os-2* cells, and arrhythmic in Δ*frq* cells (Figure 7B, C & 6A).

eEF-2 Phosphorylation is Regulated by RCK-2 and the Circadian Clock

RCK-2 is required for normal induction of P-eEF-2 following acute osmotic stress (Figure 3C), and the clock controls rhythms in the levels of P-RCK-2 (Figure 7A).

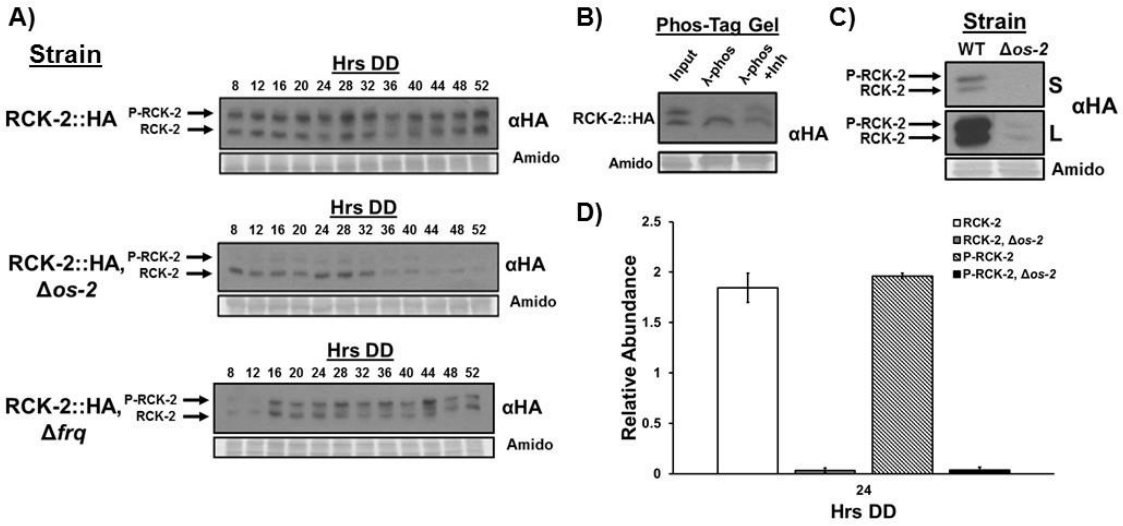

Figure 6. Visualization of phosphorylated RCK-2 using PhosTag™ gels. A) PhosTag™ western blots of the indicated strains containing RCK-2::HA grown in constant dark (DD), harvested every 4 h over 2 days (Hrs DD), and probed with HA antibody (αHA). Phos-Tag™ western blots separate P-RCK-2 from unphosphorylated RCK-2 (RCK-2) as shown by the arrows. The film exposure times were 1 s for RCK-2::HA in WT, 20 s for Δ*os-2*, and 4 s for Δ*frq* B) Western blot of RCK-2::HA DD12 samples that were untreated (Input), treated with λ-phosphatase (λ-phos), or treated with λ-phosphatase plus phosphatase inhibitors (λ-phos+Inh), separated on a PhosTag™ gel, and probed with HA antibody. C) 2 s (S) and 1 m (L) exposure of a representative Phos-Tag™ western blot using RCK-2::HA (WT) and RCK-2::HA, Δ*os-2* (Δ*os-2*) DD24 samples probed with αHA. P-RCK-2 and unphosphorylated RCK-2 are indicated by the arrows. The data are plotted below (D) (mean ± StDev, n = 2). Amido stained proteins served as loading controls.

Therefore, we predicted that eEF-2 phosphorylation would be clock-controlled. Consistent with this idea, the levels of P-eEF-2, but not eEF-2, cycled over the course of the day, with peak P-eEF-2 levels in the subjective morning (DD36) (Figures 8A, 9 & 10), slightly lagging the peak in P-RCK-2 levels (Figure 7A). This delay may be due to experimental error introduced by using 4 h time points, or due to the activity of phosphatases. P-eEF-2 levels fluctuated over time, but circadian rhythmicity was

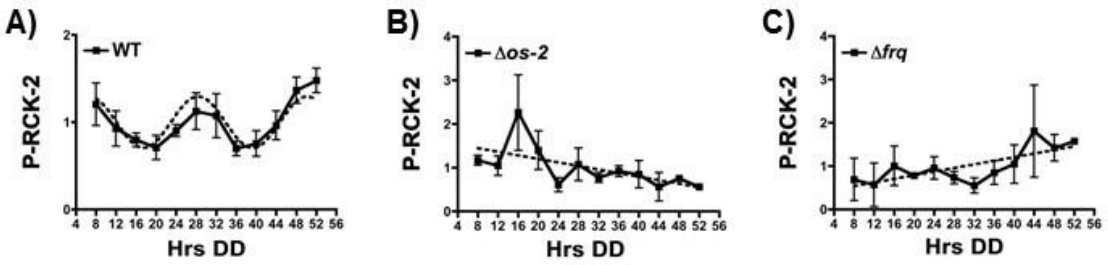

Figure 7. Rhythmic RCK-2 phosphorylation is regulated by clock signaling through the OS-2 pathway. Plots of levels of phosphorylated RCK-2 protein (P-RCK-2). Protein was extracted from the indicated cultures grown in DD and harvested every 4 h over 2 days (Hrs DD). A) RCK-2::HA (WT); B) RCK-2::HA, Δ*os-2* (Δ*os-2*); C) RCK-2::HA, Δ*frq* (Δ*frq*). P-RCK-2 levels were determined using PhosTag™ gels (Figure 6A & B). The plots represent the average P-RCK-2 signal normalized to total protein for each genotype, and thus does not reflect differences in P-RCK-2 levels in the strains. Rhythmicity of P-RCK-2 in WT cells was determined using F-tests of fit of the data to a sine wave (dotted black line; $p < 0.0001$, $n = 4$). The levels of P-RCK-2 were arrhythmic in Δ*os-2* ($n = 3$), and Δ*frq* ($n = 2$) cells as indicated by a better fit of the data to a line (dotted black lines).

abolished in Δ*rck-2*, Δ*os-2* and Δ*frq* cells (Figures 8B-D & 9). P-eEF-2 could be detected in both Δ*rck-2* (Figure 8E) and Δ*os-2* cells (Figure 9) in DD, consistent with additional kinases phosphorylating eEF-2. However, P-eEF-2 levels in Δ*rck-2* cells at DD36 (the time of peak P-eEF-2 levels in WT cells) were low, and at levels similar to the trough levels of P-eEF-2 in WT cells at DD24 (Figure 8E). Together, these data confirmed that clock signaling through the OS MAPK pathway and RCK-2 are necessary for rhythmic accumulation of P-eEF-2.

The extent of clock control of P-eEF-2 levels was measured by comparing the amount of P-eEF-2 from WT and Δ*rck-2* cells harvested at the trough (DD24) and peak (DD36) of P-eEF-2 accumulation (Figure 8E). A 2-fold increase in P-eEF-2 was observed at DD36

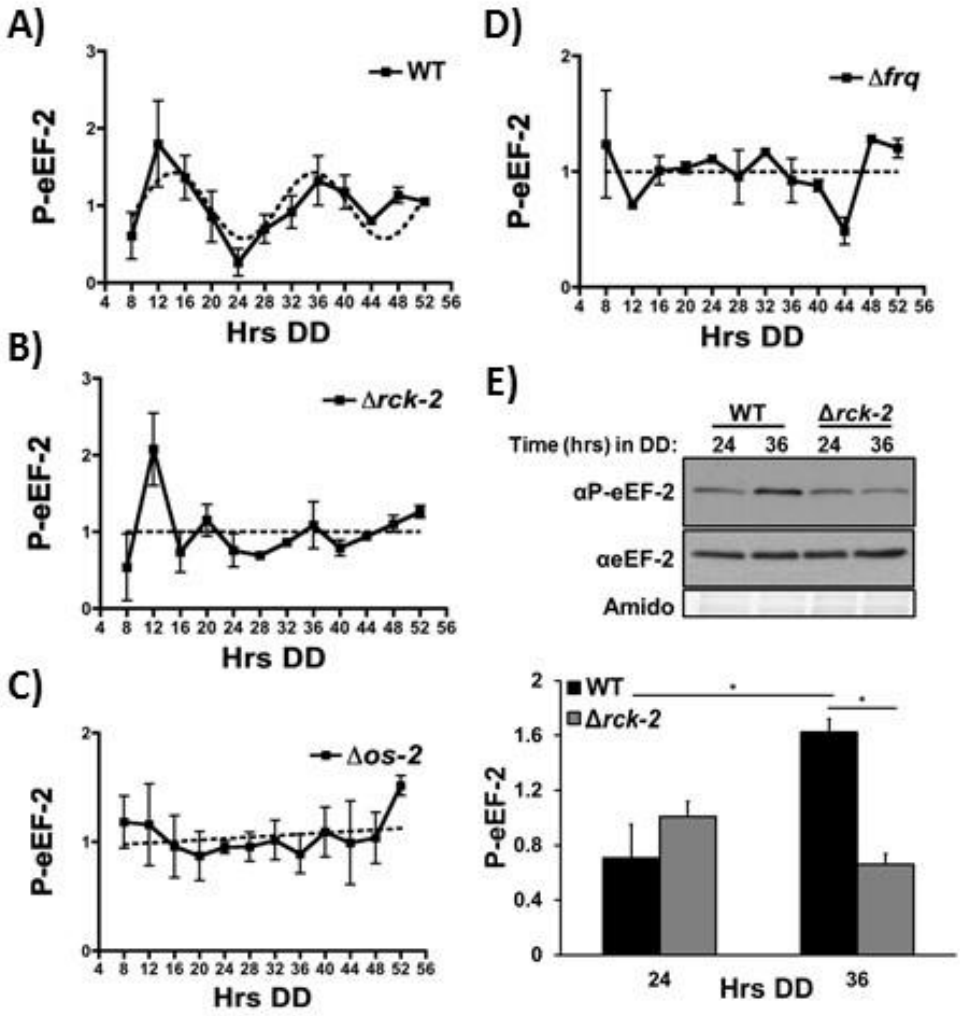

Figure 8. Clock control of eEF-2 phosphorylation requires signaling through the OS MAPK pathway and RCK-2. Plots of the abundance of P-eEF-2. Protein was extracted from the indicated strains grown in DD and harvested every 4 h over 2 days (Hrs DD): A) wild-type (WT); B) Δ*rck-2*; C) Δ*os-2*; and D) Δ*frq*. Protein was probed with αP-eEF-2 (Figure S5). Plots of the data are shown (mean ± SEM, n = 3) and represent the average P-eEF-2 signal normalized to total protein for each genotype as in Figure 3. Rhythmicity of P-eEF-2 in WT cells was determined using F-tests of fit of the data to a sine wave (dotted black line; $p < 0.0001$), while P-eEF-2 levels were arrhythmic in Δ*rck-2* (n = 3), Δ*os-2* (n = 3), and Δ*frq* (n = 2) cells as indicated by a better fit of the data to a line (dotted black lines). E) Representative western blot of protein extracted from the indicated strains grown in DD for 24 and 36 h and probed with αP-eEF-2 and αeEF-2. The film was exposed for 10 s. Amido stained proteins served as loading controls. The data are plotted below (mean ± SEM, n = 3). The asterisks indicate a statistical difference ($p < 0.05$, student T-test).

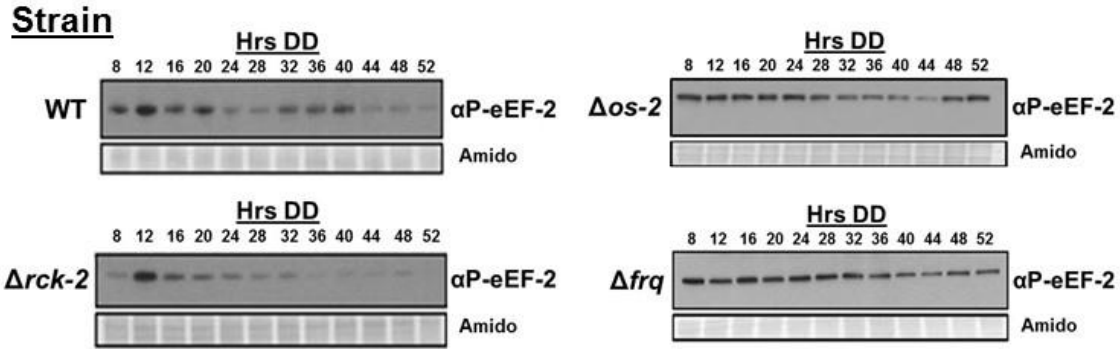

Figure 9. P-eEF-2 accumulates rhythmically. Representative western blots of protein extracted from the indicated strains grown in constant dark (DD), harvested every 4 h over 2 days (Hrs DD), and probed with αP-eEF-2. Amido stained proteins served as loading controls.

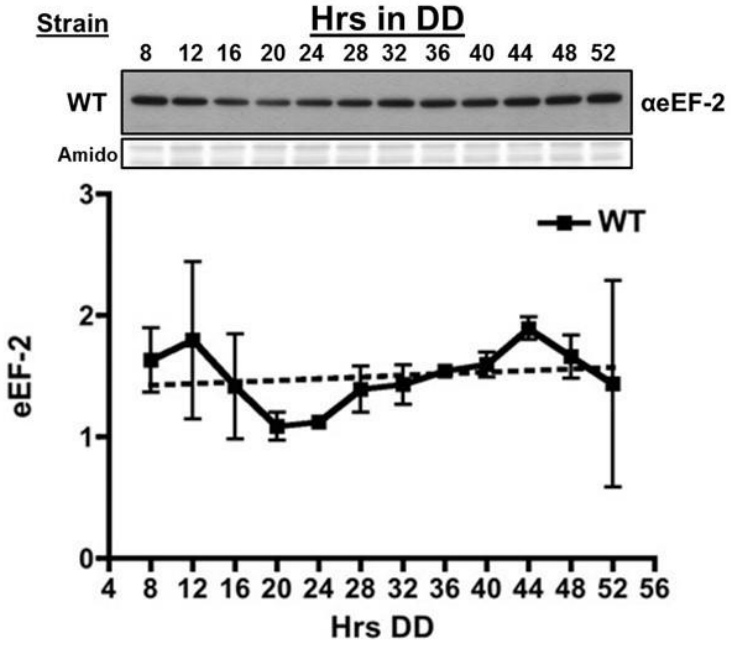

Figure 10. Constitutive accumulation of total eEF-2 levels over the day. Representative western blot of total protein from WT cells grown in constant dark (DD), harvested every 4 h over 2 days (Hrs DD), and probed with αeEF-2. Amido stained proteins served as loading controls. The data are plotted below, where the levels of eEF-2 in WT cells were found to accumulate constitutively, as indicated by a better fit of the data to a line (dotted black line; n = 2).

as compared to DD24 in WT cells, but not Δ*rck-2* cells. At DD36, P-eEF-2 levels were reduced by 60% in Δ*rck-2* cells as compared to WT cells, indicating that clock signaling through RCK-2 is responsible for over half of the total amount of P-eEF-2.

The Circadian Clock Controls Translation Elongation Rates in vitro*, and Rhythmic Protein Levels* in vivo*, Through Phosphorylation of eEF-2*

I predicted that mRNA translation would be highest when P-eEF-2 levels are lowest during the subjective evening (DD24), and lowest in the subjective late morning (DD36) when P-eEF-2 accumulation peaks (Figure 8A). To test this idea, I examined translation of *luciferase* (*luc*) mRNA in cell-free translation extracts isolated from WT and mutant cells harvested at DD24 and DD36. Consistent with this hypothesis, translation of *luc* mRNA in WT extracts was significantly higher at DD24 than at DD36 (Figure 11A). P-eEF-2 levels in Δ*rck-2* cells at DD24 and DD36 were similar to the trough levels at DD24 in WT cells (Figure 3C and 8E), and *luc* mRNA translation was high in Δ*rck-2* translation extracts at both times of day (Figure 11A). These data are consistent with (i) reduced P-eEF-2 levels increasing translation extract activity, and (ii) the necessity for clock signaling through RCK-2 to observe time-of-day-specific differences in the extracts' capacity to translate *luc* mRNA. The levels of *luc* mRNA translation were higher in Δ*rck-2* cell extracts at both times of the day as compared to the peak in WT extracts at DD24, despite finding that the steady-state levels of P-eEF-2 were similar to the WT level at DD24 (Figure 8E). This result suggested that RCK-2 regulates additional factors in cells that reduce mRNA translation, possibly by altering levels or

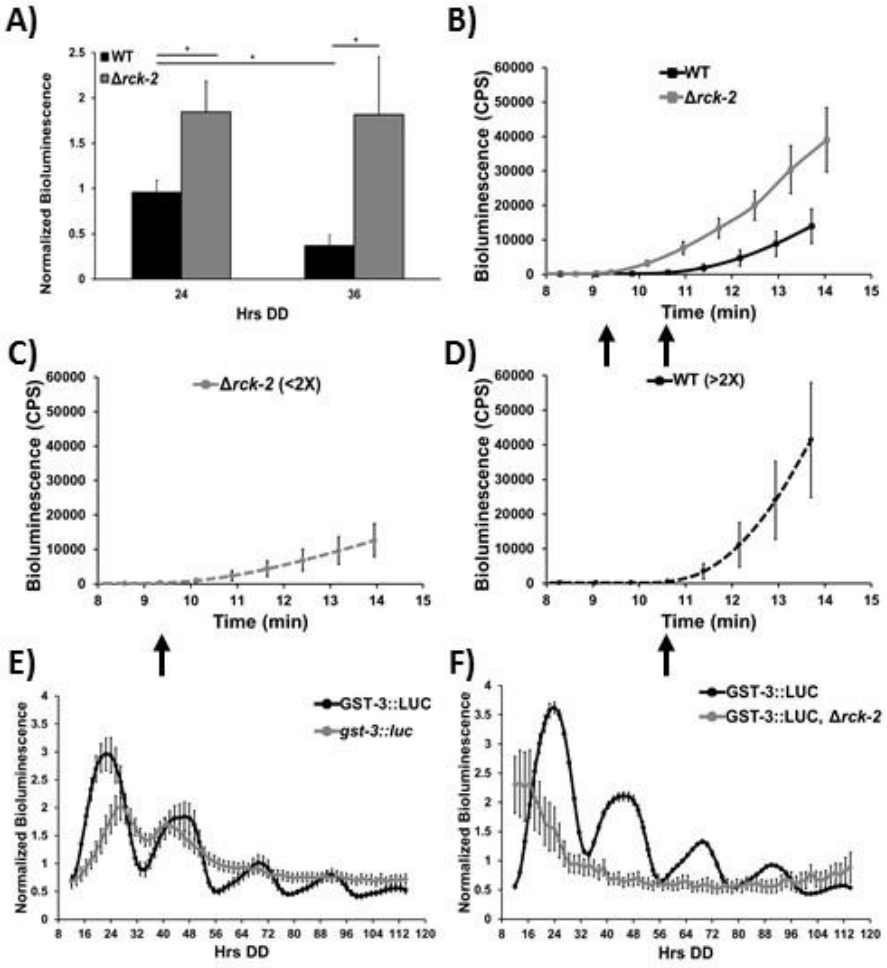

Figure 11. The circadian clock regulates translation elongation through RCK-2 and P-eEF-2. A) *In vitro* translation assay of *luciferase* (*luc*) mRNA using *N. crassa* cell-free extracts from wild-type (WT) and Δ*rck-2* strains grown in DD and harvested at 24 or 36 h (Hrs DD). The average (mean ± SEM) bioluminescence signal from WT (n = 4) and Δ*rck-2* (n = 4) are plotted. An asterisk represents a statistical difference ($p < 0.05$, student's T-test). B) *In vitro* translation assay of *luc* mRNA using *N. crassa* cell-free extracts from WT and Δ*rck-2* strains grown in DD for 36 h. The average amount (mean ± SEM, n = 3) of bioluminescence counts per second (CPS) from WT and Δ*rck-2* extracts are plotted. The average amount (mean ± SEM, n = 3) of bioluminescence from Δ*rck-2* cell-free extract programmed with a 2-fold decrease (<2X) of *luc* mRNA (C), and WT cell-free extract programmed with 2-fold more (>2X) *luc* mRNA (D). The time of first appearance of LUC is indicated with an arrow in B-D. E) Luciferase assay using GST-3::LUC translational (n = 15) and *gst-3::luc* transcriptional fusion strains (n = 24) kept in DD for 4.5 days. The average amount (mean ± SEM) of bioluminescence is plotted. F) Luciferase assay using GST-3::LUC translational (n = 20) and GST-3::LUC, Δ*rck-2* (n = 11) fusion strains kept in DD for 4.5 days. The average (mean ± SEM) bioluminescence signal is plotted.

activities of ribosomes, tRNAs, or translation factors. The nature of this regulation will be investigated in future studies.

To determine if rhythmic P-eEF-2 levels affect translation elongation rates, we used an *N. crassa* cell-free translation protocol (82, 83) that accurately reflects protein translation *in vivo* (82, 84). Firefly *luc* mRNA was used as the template in the cell-free system to determine the time of first appearance (TFA) of the luminescence signal. TFA is a measure of the time needed for the ribosome to complete protein synthesis and is indicative of translation elongation rate (83, 84). Changes in translation elongation rates as a function of eEF-2 phosphorylation were examined in cell-free extracts isolated from WT and Δ*rck-2* cells harvested at the time of peak P-eEF-2 levels in WT cells (DD36). As predicted, TFA was detected earlier in Δ*rck-2* than in WT extracts (Figure 11B), in line with reduced P-eEF-2 levels and increased elongation rates in Δ*rck-2* cells as compared to WT cells. In accordance with increased translation elongation rates in Δ*rck-2* extracts, the slope of LUC accumulation over time was two-fold higher in Δ*rck-2* extracts compared to WT extracts (Figure 11B). To determine TFA under conditions where LUC synthesis rates were overall similar, we examined the consequences of varying the concentration of mRNA used to program extracts. The rate of accumulation of LUC in Δ*rck-2* was comparable to that of WT when Δ*rck-2* was programmed with 2-fold less mRNA than WT (Figure 11C). Importantly, the TFA was still earlier than in WT extracts, consistent with an increased elongation rate in Δ*rck-2* extracts. Similarly, when WT extracts were programmed with 2-fold more mRNA than Δ*rck-2* (Figure

11D), the accumulation of LUC after TFA correspondingly increased to levels similar to Δ*rck-2*, but TFA was still delayed relative to Δ*rck-2*.

To examine if rhythmic accumulation of P-eEF-2 provides a mechanism to rhythmically control mRNA translation elongation *in vivo*, we assayed rhythmicity of a GST-3 (encoding glutathione S-transferase)::LUC translational fusion in WT and Δ*rck-2* cells. This gene was chosen based on constitutive *gst-3* mRNA accumulation (70), and evidence for rhythms of GST activity in mammalian cells (85). Consistent with the transcriptome data (70), a *gst-3* promoter::*luc* fusion was constitutively expressed in WT cells (Figure 11E). In contrast, GST:LUC protein levels cycled in WT, but not in Δ*rck-2* or Δ*frq* cells (Figure 11E & F, 12), demonstrating that clock signaling through RCK-2 and eEF-2 provides a mechanism to control translation elongation and protein accumulation. However, not all mRNAs are affected by rhythmic accumulation of P-eEF-2. We found that the levels and cycling of the core clock protein FRQ was not altered in Δ*rck-2* cells (Figure 13A & B).

Discussion

Increasing evidence points to the importance of the circadian clock in controlling mRNA translation, including rhythmic activation of cap-dependent translation factors (41, 74, 86-88), and specific RNA binding proteins that control the translation of core clock genes (89-93). While the initiation of translation has long been considered to be the

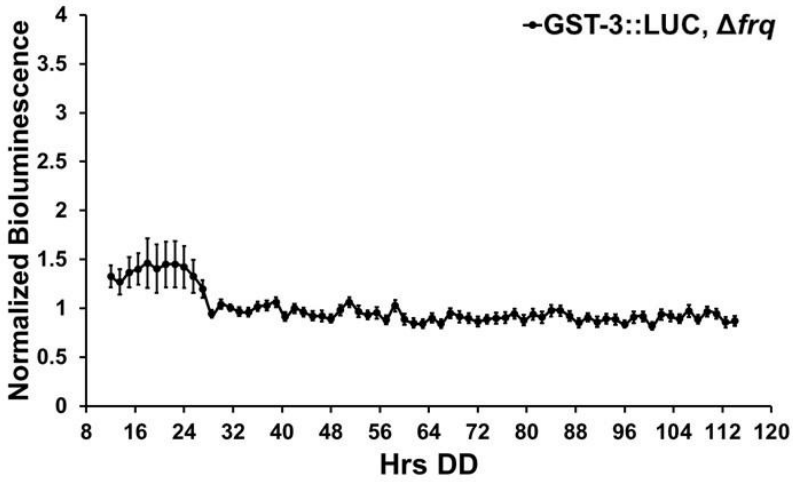

Figure 12. Rhythmic accumulation of GST-3 is abolished in a clock mutant strain. The average amount (mean ± SEM, n = 24) of bioluminescence from GST-3::LUC, Δ*frq* cells grown in the dark for the indicated times (Hrs DD) is plotted.

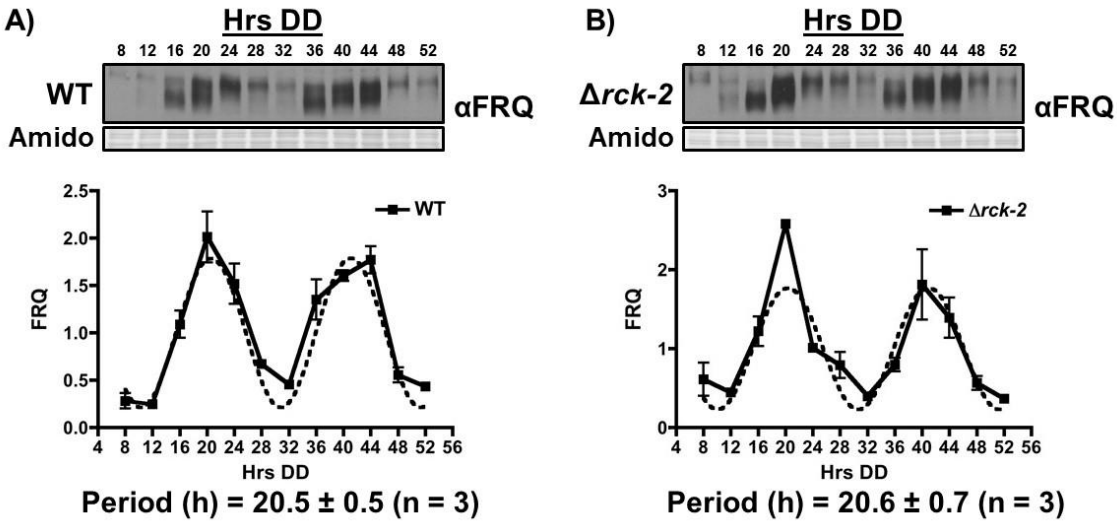

Figure 13. FRQ levels and rhythmicity in Δ*rck-2* cells are similar to WT cells. Western blots of protein extracted from WT (A) and Δ*rck-2* (B) cells grown in DD, harvested every 4 h over 2 days (Hrs DD), and probed with FRQ antibody (αFRQ). Amido stained proteins served as loading controls. The data are plotted below (mean ± SEM, n = 3). Rhythmicity of FRQ in WT and Δ*rck-2* cells was determined using F-tests of fit of the data to a sine wave (dotted black line; $p < 0.0001$). The period of the rhythms are given below.

primary control step in translation (94), a growing body of evidence points to translation elongation being regulated (95, 96), with phosphorylation and reduction in activity of eEF-2 being a central point in this control. Here, we showed that the *N. crassa* circadian clock, through rhythmic control of the OS MAPK pathway and downstream effector protein RCK-2, generates a rhythm in P-eEF-2 levels, peaking in the subjective day. This regulation leads to decreased translation activity and decreased translation elongation rates during the day *in vitro*.

N. crassa RCK-2 most closely resembles mammalian eEF-2 kinase MAPKAP-K2. Similar to RCK-2 in fungi, mammalian MAPKAP-K2 activity is controlled by the stress-induced p38 MAPK pathway (63, 97). MAPKAP-K2 phosphorylates and activates eEF-2 kinase (eEF-2K), which in turn phosphorylates and inactivates eEF-2 (53). In mammals, several different signaling pathways converge on eEF-2K to activate or repress its activity and ultimately control the levels of P-eEF-2. In response to environmental stress, hypoxia, and nutrient status, p38 MAPK and mTOR signaling pathways inhibit eEF-2K (98-100), while AMP-kinase and cyclic AMP (cAMP)-dependent protein kinase A signaling activate eEF-2K (101-104). *N. crassa* cells lack an obvious homolog of eEF-2K. While my data showing that eEF-2 and RCK-2 coimmunoprecipitate in total protein extractions is consistent with a direct interaction between the two proteins, I cannot exclude the possibility that phosphorylation of eEF-2 by RCK-2 may be indirect and mediated through an unidentified kinase that functions similarly to eEF-2K. However, because low levels of P-eEF-2 were observed in Δ*rck-2*,

Δ*os-2*, and in Δ*rck-2,* Δ*os-2* double mutants following osmotic stress (Figure 3C & 5), it appears that RCK-2 is the major pathway leading to phosphorylation of eEF-2, although other kinases, such as AMPK, PKA, and/or TOR-pathway directed kinases, may also have minor roles. Importantly, p38, as well as TOR, AMPK activity, and cAMP levels, are clock-controlled in higher eukaryotes (105-110), suggesting that clock control of translation elongation through rhythmic eEF-2 phosphorylation may be conserved. Furthermore, recent studies have shown that eEF-2 levels cycle in abundance in mouse liver (42, 111); however, it remains to be determined if rhythms in mammalian eEF-2 levels affect its activity.

Our studies have uncovered a new mechanism for circadian clock control of protein abundance through the effects of rhythmic accumulation of P-eEF-2 on protein synthesis. These data lead to additional questions, including (i) to what extent does clock control of translation elongation affect rhythmic protein levels, and (ii) what is the advantage of clock control of translation elongation to the organism? Recent ribosome profiling in mammalian cells revealed that ~10% of mRNAs with rhythmic ribosome occupancy lacked corresponding rhythmic mRNA levels (111, 112). These data support a role for the clock in controlling translation of specific, rather than all, mRNAs. Consistent with clock control of eEF-2 activity promoting rhythmic translation of specific mRNAs, rather than providing a mechanism to globally control translation, we show that RCK-2, which is needed for rhythms in P-eEF-2 levels, is not necessary for rhythms in accumulation of the clock protein FRQ (Figure 13), whereas rhythms in

GST-3 protein levels require RCK-2 (Figure 11). Although there may be several ways to achieve specificity, we speculate that a slow-down in translation elongation rate during the day could reduce the expression of mRNAs for which elongation is rate-limiting, while the expression of mRNAs for which initiation is rate-limiting, would either not be affected, or would show relatively increased translation rates as a result of increased availability of initiation factors.

The clock plays a major role in controlling metabolism (113), including energy metabolism (114) and its major currency, ATP (115-117). As translation is one of the most energy demanding processes in the cell, it makes sense to coordinate protein translation to times of day when energy levels are highest. In *N. crassa*, clock-controlled mRNAs generally peak at two phases, dawn and dusk, with dusk phase enriched for genes involved in ATP-requiring anabolic processes, and dawn-phase enriched for genes involved in ATP-generating catabolism (70, 71). Based on our data showing that the levels of P-eEF-2 peak during the day, we predict increased rates of mRNA translation at night, directly following the peak production of ATP during the day, and in coordination with other anabolic processes, including lipid and nucleotide metabolism. In addition, environmental stress to the organism peaks during the day (118). Linking translation elongation control to stress-induced and clock-controlled MAPK signaling, as well as to nutrient sensing pathways, likely provides an adaptive mechanism to partition the energy-demanding processes of translation to times of the day that are less stressful to the organism.

Materials and Methods

Strains and Growth Conditions

Vegetative growth conditions and crossing protocols were as previously described (25, 119). Unless otherwise indicated, the strains used in this study contained the *ras-1*^{bd} mutation (Table A1). RCK-2::HA homokaryotic strains (DBP 1254 *mat A, rck-2::3X HA::hph,* and DBP 1255; *mat a, rck-2::3X HA::hph*) were generated by transforming FGSC9718 (*mat a*, Δ*mus-51::bar+*) with pRCK-2::3X HA, and crossing transformants (*mat a*, Δ*mus-51::bar+*, *rck-2::3X HA*) with FGSC 2489 (*mat A*). pRCK-2::3X HA was generated by 3-way PCR (120) combining a 2.4 kb fragment of *rck-2* (without the translational stop codon), a 10X glycine linker – 3X hemagglutinin (HA) – hygromycin-B resistance gene (*hph*), and 1.5 kb of the 3' UTR of *rck-2*. The resulting PCR product was cloned into pCR™ – Blunt vector (#K2700-20, Thermo Fisher Scientific Inc., Waltham, MA, USA). Incorporation of 3X HA into the native locus was verified by PCR, and integration of the HA-tagged RCK-2 construct was confirmed by detection of a ~75 kDa HA-tagged protein (RCK-2::HA predicted size = 72.6 kDa) in the transformants by western blot. The GST-3::LUC translational fusion was generated by 3-way PCR using a fully codon-optimized luciferase gene (121), and co-transformed with either pBP15 (DBP301) into WT (FGSC 2489) and Δ*frq* (DBP 1320), or with pBARGEM7-2 (DBP 425) into Δ*rck2* (DBP 828). The *gst-3* gene was targeted for replacement by the GST-3::LUC construct via homologous recombination. Hygromycin or basta-resistant transformants were picked and screened for luciferase activity. To generate the P*gst-3::luc* transcriptional fusion, a 1.3-kb promoter region of *gst-3* was

amplified with primers *gst3*SpeI F (5' GGACGCTACTAGTTGACAAGATT 3') and *gst3*AscI R (5' CGATGGCGCGCCGTCTGACATGGTAACG 3'). The PCR product was digested with *Spe*I and *Asc*I, and cloned into plasmid pRMP57 containing the codon-optimized luciferase gene. The resulting plasmid (DBP 594), targeted to the *his-3* locus, was digested with *Pci*I, and co-transformed with either pBP15 (DBP 301) into wild-type 74-OR23-IV (FGSC 2489) and Δ*frq* (DBP 1320) cells, or with pBARGEM7-2 (DBP 425) into Δ*rck2* (DBP 828). Hygromycin or basta-resistant transformants were picked and screened for luciferase activity. Verification of gene deletions for the strains generated in this study was accomplished by PCR, and integration of HA-tagged constructs was confirmed by western blot. All strains containing the *hph* construct were maintained on Vogel's minimal media, supplemented with 200 μg/mL of hygromycin B (#80055-286, VWR, Radner, PA). Strains containing the *bar* cassette were maintained on Vogel's minimal media lacking NH_4NO_3 and supplemented with 0.5% proline and 200 μg/mL of BASTA (Liberty 280 SL Herbicide, Bayer, NC). Osmotic stress was carried out on cells grown in Vogel's minimal media, 2% glucose, 0.5% arginine, pH 6.0 and shaking in constant light (LL) for 24 h at 25°C. The cultures were transferred to constant dark (DD) for 24 h at 25°C and 4% NaCl was added 5, 10, 15, and 30 min prior to harvest. Tissue for RNA and protein extraction was harvested by flash freezing in liquid N_2. Circadian time course experiments were conducted as previously described (25) with cells synchronized by a light-to-dark transfer (25°C in LL to 25°C in DD).

Protein Extraction, Western Blotting, λ-protein Phosphatase Treatment, and Co-immunoprecipitation

To determine levels of RCK-2 phosphorylation, protein was extracted as previously described (122) with the following modification: the extraction buffer was 50 mM HEPES pH 7.4, 137 mM NaCl, 10% glycerol, 5 mM EDTA, 10 mM NaF, 1 mM PMSF, 1 mM sodium ortho-vanadate, 1 mM β-glycerophosphate, 1X aprotinin (#A1153, Sigma-Aldrich, St. Louis, MO), 1X leupeptin hemisulfate salt (#L2884, Sigma-Aldrich), and 1X pepstatin A (#P5318, Sigma-Aldrich). To assay levels of total eEF-2 and phosphorylation of eEF-2, protein was extracted as previously described for RCK-2 with the following modification: the extraction buffer contained 100 mM Tris pH 7.0, 1% SDS. FRQ protein was extracted as previously described for RCK-2 with the following modification: the extraction buffer was 50 mM HEPES pH 7.4, 137 mM NaCl, 10% glycerol, 5 mM EDTA, 10 mM NaF, 1 mM PMSF, 1 mM sodium ortho-vanadate, and 1 mM β-glycerophosphate. For samples that were separated on PhosTag™ acrylamide gels, the extraction buffer consisted of 50 mM HEPES pH 7.4, 137 mM NaCl, 10% glycerol, plus protease and phosphatase inhibitors.

Protein concentration was determined using the Bradford assay (#500-0112, Bio-Rad Laboratories, Hercules, CA). Protein samples (50 μg) were separated on 10% SDS/PAGE gels and blotted to an Immobilon-P nitrocellulose membrane (#IPVH00010, Millipore, Billerica, MA) according to standard methods. Phos-tag™ acrylamide gels consisted of 8% SDS/PAGE gels with the addition of 35 μM Phos-tag™ Acrylamide

AAL-107 (#300-93523, Wako Chemicals USA, Inc., Richmond) and 70 μM $MnCl_2$ according to the manufacturer's recommendations.

RCK-2::HA was detected using Rat monoclonal anti-HA primary antibody (#11867423001, Roche Diagnostics, Indianapolis, IN) in 5% milk, 1X TBS, 0.1% Tween-20 at a concentration of 1:1,000 and anti-Rat IgG-Peroxidase secondary antibody (#A5795, Sigma-Aldrich) at a concentration of 1:5,000. Total eEF-2 protein was detected using Rabbit anti-eEF-2 primary antibody (#2332S, Cell Signaling Technology, Beverley, MA) in 5% BSA, 1X TBS, 0.1% Tween-20 at a concentration of 1:5,000 and anti-Rabbit IgG HRP secondary antibody (#170-6515, Bio-Rad Laboratories) at a concentration of 1:10,000. Phosphorylated eEF-2 protein was detected using Rabbit anti-Phospho-eEF-2 (Thr56) primary antibody (#2331S, Cell Signaling Technology) in 5% BSA, 1X TBS, 0.1% Tween-20 at a concentration of 1:5,000 and anti-Rabbit IgG HRP secondary antibody (#170-6515, Bio-Rad Laboratories) at a concentration of 1:10,000. FRQ protein was detected using mouse monoclonal anti-FRQ primary antibody (supernatant from clone 3G11-1B10-E2, a gift from M. Brunner's lab) in 7.5% milk, 1X TBS, 0.1% Tween-20 at a concentration of 1:200 and anti-mouse IgG-Peroxidase secondary antibody (#170-6516, BioRad Laboratories) at a concentration of 1:10,000. Detection of all proteins was by chemi-luminescence using SuperSignal® West Pico Substrate (#34077, Thermo Scientific, Rockford, IL). Western blot signals were quantitated using ImageJ (NIH) and normalized to total protein levels from amido

stained protein gels. The ratio of signal to total protein for each sample/gel (value X) was averaged (Av), and each value of X was divided by the Av signal for plotting.

To verify phosphate-specific signals, 50 μg of protein were treated with 20 U of λ-protein phosphatase (#P0753S, New England Biolabs, Ipswich, MA) for 30 min at 30°C, followed by boiling for 5 min in 1X Laemmli sample buffer. Inhibition of λ-protein phosphatase was accomplished by adding 10 mM NaF, 1 mM sodium ortho-vanadate and 1 mM β-glycerophosphate to samples just prior to the addition of λ-protein phosphatase.

Co-immunoprecipitation was carried out using 25 μL of GammaBind™ G Sepharose™ beads (#17-0885-01, Ge Healthcare Bio-Sciences, Pittsburgh, PA) as recommended by the manufacturer. Rat monoclonal anti-HA antibody (1:100; #11867423001, Roche Diagnostics) was bound to prewashed beads overnight at 4°C. Total protein (2 mg) was added to the beads and incubated overnight at 4°C.

Cell-Free Extracts and in vitro *Translation for Assaying Luciferase*

Cell-free extracts were prepared from germinated conidia as previously described (123, 124). *In vitro* translation of *luc* mRNA was accomplished as previously described using capped pQ101-Luc mRNA (124, 125). Incubations were carried out for 45 min at 26°C, and the reactions were stopped by adding 1X passive lysis buffer (#E1941, Promega, Madison, WI). 50 μL of luciferase assay reagent (126) and 15 μL of sample reaction

were loaded per well on an OptiPlate™-96 F plate (#6005279, Perkin Elmer, Waltham, MA, USA), and bioluminescence was then immediately measured using a Victor^3-V multi-label counter (#1420-252, Perkin Elmer, Waltham, MA). Relative bioluminescence was determined by normalizing the bioluminescence (CPS) values to the average of each plate. To examine the rate of translation elongation, the reaction buffer was modified to include 5 μM amino acids, 25 mM firefly luciferin (#306, Prolume Ltd., Pinetop, AZ, USA) and 5 mM Coenzyme A (#309, Prolume Ltd., Pinetop, AZ, USA). 25 μL of cell-free extract, 5 μL (12 ng/μL) of *luc* mRNA, and 20 μL of reaction buffer were loaded per well on an OptiPlate™-96 F plate, and bioluminescence was continuously measured for up to 15 min.

In vivo Luciferase Assay

Each well of a 96-well plate was filled with 150 μl of solid assay media (1X Vogel's salt, 0.03% glucose, 0.05% arginine, 0.5 mg/ml biotin, 0.1M quinic acid,1.5% agar and 25 μM D-luciferin) (Gold Biotechnology, St Louise, MO) (pH = 6.0). Quinic acid was added to the media to increase the amplitude of the luciferase rhythms (127). The plates were air dried for 12 h in a sterile laminar flow hood. A conidial suspension ($2X10^5$ cells/ml) was prepared from slant cultures, and 5 μl was used per well. The plate was covered with a breathable membrane (Diversified Biotech, Dedham, MA). The cultures were grown at 30°C for 24 h and moved to an Envision Xcite plate reader at 25°C (Perkin Elmer, Boston, MA) for measuring bioluminescence. Luminescence was counted every 90 min for at least 5 continuous days.

Statistical Analysis

Rhythmic data was fit either to a sine wave or a line as previously described (25, 128). P-values represent the probability that the sine wave best fits the data. The student T-test was used to determine significance in changes in the levels of P-eEF-2 and bioluminescence. Error bars in all graphs represent the SEM from at least 3 independent experiments, unless otherwise indicated.

CHAPTER III

REGULATION OF mRNA TRANSLATION

Overview

In this section, I describe experiments that were performed to identify mRNAs that are being translationally regulated. By comparing ribosome profiling and transcriptome (RNAseq) data, I identified sets of genes that are being regulated at the level of translation, but not at the level of transcription, either following an osmotic stress, a light pulse, or over a circadian time course. These genes were enriched for metabolic process, and may represent a mechanism for clock regulation of metabolism.

Introduction

Stress response pathways act as a mechanism for cells to respond to extracellular stimuli (i.e., osmotic shock, light response, etc.) that may be detrimental or beneficial to their survival (129-131). After the cell encounters a stress, response pathways are activated which activate many downstream genes (132). Evidence suggests that genes are not just being regulated at the level of transcription following stress, but that specific mRNAs are translationally up- or down-regulated, in the absence of an increase or decrease in their total mRNA levels (52). In Neurospora, little is known about which constitutively expressed mRNAs are preferentially targeted to the translational machinery following an external stimuli (i.e., after osmotic stress or a light pulse) or if there is a mechanism for this specificity.

The circadian clock acts as an endogenous mechanism to regulate response pathways, allowing organisms to anticipate daily environmental stresses (128, 133). Depending on the organism and tissue, nearly half of an organism's expressed genes are under control of the circadian clock at the level of transcription (32, 70-72). Mounting evidence indicates a role for the clock in controlling post-transcriptional mechanisms (73), including translation initiation (41, 74), and translation elongation (chapter II). However, what clock regulation of translation means for protein accumulation on a genome wide scale, and the mechanism(s) for specifying which mRNAs are targeted for translational regulation are unknown.

The driver of circadian rhythms in *N. crassa* is an autoregulatory molecular feedback loop composed of the negative elements FRQ and FRH, which inhibit the activity of the positive elements WC-1 and WC-2 (75-78). WC-1 and WC-2 heterodimerize to form the WCC, which activates transcription of *frequency* (*frq*) (11, 75, 79), as well as activating transcription of a large set of downstream target genes important for overt rhythmicity and light responses (20). These genes encode transcription factors, as well as various output pathway components and terminal clock-controlled genes (ccgs) (6). One gene directly controlled by the WCC is *os-4*, which encodes the MAPKKK in the osmotically-sensitive OS MAPK pathway (25). Rhythmic transcription of *os-4* leads to rhythmic accumulation of the phosphorylated active form of the downstream p38-like MAPK OS-2 (22). We have previously demonstrated that this leads to rhythmic

phosphorylation of the stress response pathway components RCK-2 and eEF-2, which in turn leads to rhythmic regulation of translation elongation (chapter II).

To better understand which constitutively expressed mRNAs are being regulated at the level of translation, I helped develop, and performed, ribosome profiling experiments, coupled with RNAseq in Neurospora cells, to determine which mRNAs are being translated under various conditions. I predicted that following a stress or over a circadian time course, specific mRNAs would be targeted to the translational machinery, and some, but not all mRNAs will be regulated by signaling to eEF-2. In support of this hypothesis, I found genes that were up- or down-regulated only at the level of ribosomal occupancy following an osmotic stress, light pulse, or over a circadian time course. Furthermore, I found specific mRNAs whose ribosomal occupancy was regulated by RCK-2/eEF-2. Taken together, these data support the idea that stress and clock regulation of translation elongation act as mechanisms to control the synthesis of specific proteins, rather than as a general mechanism to regulate translation of all mRNAs.

Results

Translational Regulation Following an Osmotic Stress

To identify which mRNAs are being regulated at the level of translation by RCK-2 after an osmotic stress, ribosome profiling and RNAseq analyses were carried out for WT and Δ*rck-2* cells that were untreated, or treated with 4% NaCl for 30 min. The quality of the

sequencing libraries was checked using FastQC, a quality control tool for high throughput sequence data (Babraham Bioinformatics, GPL v3). My libraries match previously described data sets (111, 134), and an example of the FastQC output is provided in Figure 14, and is representative of all subsequent ribosomal profiling sequencing libraries. To test how well the replicate sample sets overlap, R studio was used to analyze my Cuffdiff data, generating scatter matrices as previously described

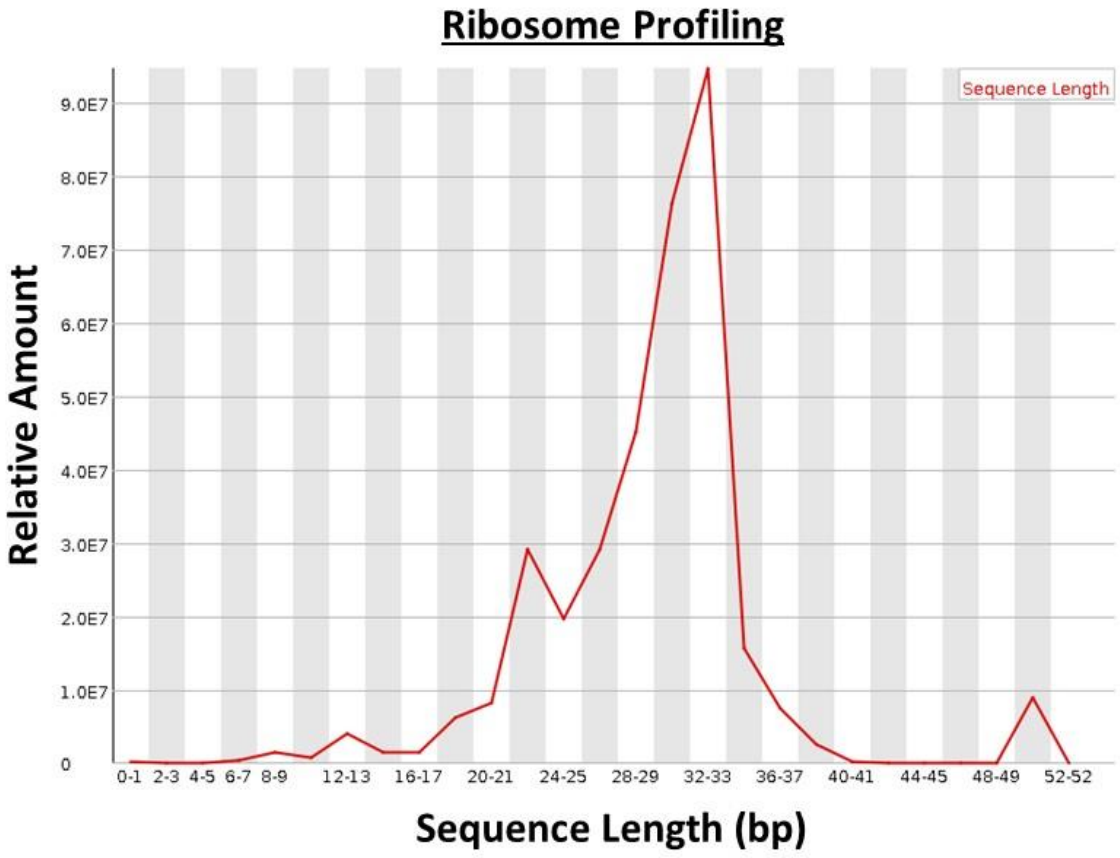

Figure 14. Distribution of sequence lengths. Representative plot of the distribution of sequence length, number of base pairs (bp), over all sequences for ribosome profiling, generated using FastQC.

(134, 135). For the ribosome profiling samples, when all time points were combined, the two data sets had a correlation coefficient or r^2 value of 0.5 (i.e., half of the data variability is explained when comparing the two groups) (Figure 15A). Further comparison of individual time points between replicates (i.e., 0 m replicate 1 compared to 0 m replicate 2) showed r^2 values ranging from 0.7 – 0.9, suggesting there is better correlation between the data sets when individual time points are compared and similar to previously published data (134). For the transcriptome samples, the replicates also overlap, with an r^2 value of 0.7 (Figure 15B). I also compared individual time points

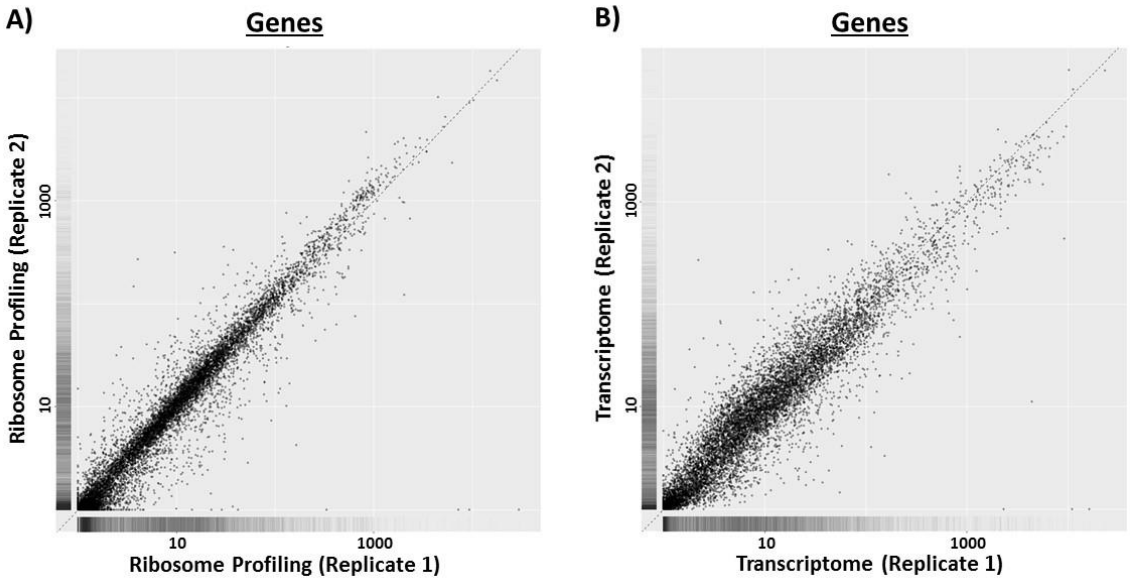

Figure 15. Comparison of sample replicates from cells treated and untreated with salt. Scatter matrices comparing two replicates from ribosome profiling (A) and transcriptome (B) sequencing data. Treated and untreated sample data from each replicate were combined using Tophat2. R studio was used to compare the individual replicates to each other and generate the scatter matrices.

between replicates and found that the r^2 values ranged from 0.7 – 0.8. Taken together, these data indicate that there is high correlation between the sequencing replicates.

To determine which genes were being either up- or down-regulated at the level of ribosomal occupancy, I first combined the replicates using Cufflinks and then used the resulting Cuffdiff data and R studio to generate lists of Neurospora genes with their associated fragments per kilobase of transcript per million mapped reads (FPKM) values. First, any NCUs with FPKM values less than 1 were removed. I then identified genes with a $\log_2$-fold change > 1 (induction) or < -1 (repression) when comparing the ribosome profiling WT time 30 m to time 0 m. 1,068 genes had at least a $\log_2$-fold change > 1 or < -1 in ribosomal occupancy following an osmotic stress. To identify which genes were being induced/repressed at the level of mRNA, Cuffdiff was used to determine which samples had at least a $\log_2$-fold change > 1 or < -1 when comparing the transcriptome WT time 30 m to time 0 m. I found 1,045 genes that had at least a $\log_2$-fold induction or repression in mRNA expression following an osmotic stress. 752 genes overlapped between the data sets (Figure 16), representing 70% of mRNAs targeted to the ribosomal machinery and 72% of the mRNAs. To increase the specificity of identified genes that are up- or down-regulated in ribosomal occupancy, but not in mRNA level, the threshold for mRNAs (transcriptome data) called as osmotically induced/repressed was changed to either a $\log_2$-fold change of > 0.75 or < -0.75. I compared the resulting list to my ribosome profiling data and found 194 mRNAs that

were up- or down-regulated at the ribosomal occupancy level. These genes are listed in Table A2 and A3.

I next used FungiFun (v5) and FunCat analyses to identify the functional characteristics of the 194 unique genes regulated only at the level of ribosomal occupancy. The analysis showed that the majority of the genes are significantly enriched for metabolic processes. FunCat analysis also revealed that the genes are involved in transcription and protein binding (Table 1). These data suggested that after an osmotic stress, mRNAs that are subject to higher or lower ribosome occupancy rates (with constitutive mRNA levels)

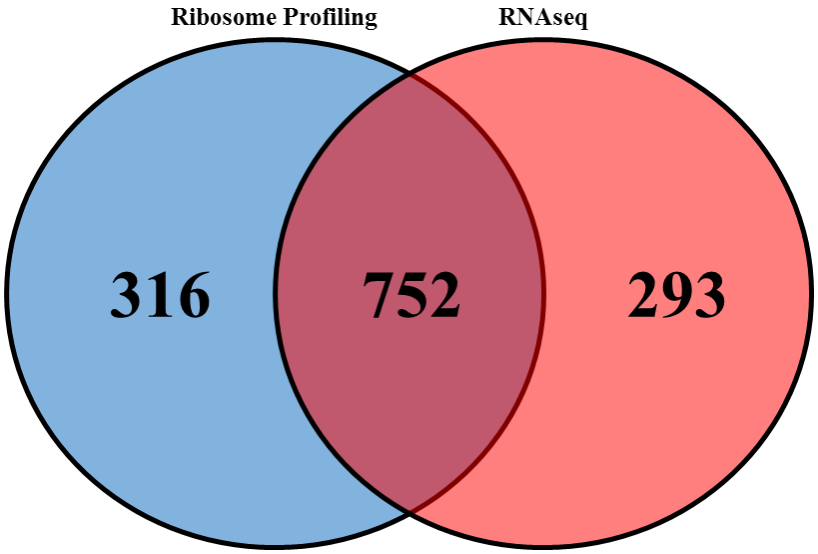

Figure 16. Comparison of ribosome profiling and transcriptome samples following an osmotic stress. Genes were identified that were either induced or repressed after a 30 min salt pulse from ribosome profiling sequencing data (blue circle) and RNAseq sequencing data (red circle). Center value represents the number of genes that overlapped between data sets.

are primarily involved in metabolic processes. To determine which of the mRNAs regulated at the level of ribosomal occupancy are due to RCK-2/eEF-2 regulation, I determined which of the 194 WT unique genes also had a $\log_2$-fold change > 1 or < -1 when compared to Δ*rck-2* cells from time 30 m to time 0 m. After removing this subset of genes, I identified 69 genes that are induced/repressed in WT, but not in Δ*rck-2* cells (Table A4 & A5). FunCat analyses of the genes with constitutively expressed mRNAs,

Table 1. FunCat analyses of genes that are induced/repressed only at the ribosomal occupancy level in WT cells following an osmotic stress. FunCat analyses of the most up- or down-regulated subsets of genes with a $\log_2$-fold change > 1 or < -1, for the ribosome profiling samples, and $\log_2$-fold change < 0.75 or > -0.75 for transcriptome samples. Categories were considered significant if $p < 0.05$.

Functional Category	Hits	p-value
membrane lipid metabolism	6	0.000179
cell wall	9	0.000785
protein with binding function or cofactor requirement (structural or catalytic)	11	0.002603
phospholipid metabolism	4	0.004008
modification with fatty acids (e.g. myristylation, palmitylation, farnesylation)	3	0.00565
transcription	4	0.009031
lipid, fatty acid and isoprenoid metabolism	13	0.011345
degradation of asparagine	1	0.016137
polysaccharide metabolism	7	0.018205
protein binding	4	0.018701
extracellular / secretion proteins	2	0.020604
glycolipid metabolism	2	0.029853
metabolism of primary metabolic sugar derivatives	2	0.029853
sphingolipid metabolism	1	0.032017
metabolism of glycosides	1	0.047644

whose up/down-regulation in ribosomal occupancy is due to RCK-2/eEF-2, were also involved in metabolic processes. Furthermore, they were also enriched for cell wall and extracellular protein degradation (Table 2). These data suggested that after an osmotic stress, RCK-2 is responsible for regulation of 35% of mRNAs that are subject to higher or lower ribosome occupancy rates (with constitutive mRNA levels). These genes are also primarily involved in regulating metabolic processes.

Table 2. FunCat analyses of genes that are induced/repressed due to RCK-2/eEF-2 only at the ribosomal occupancy level. FunCat analyses of the most upregulated subsets of genes with a $\log_2$-fold change > 1 or < -1, for the ribosome profiling samples, $\log_2$-fold change < 0.75 or > -0.75 for transcriptome samples, and $\log_2$-fold change < 1 or > -1 for Δ*rck-2* ribosome profiling samples. Categories were considered significant if $p < 0.05$.

Functional Category	hits	p-value
cell wall	4	0.009231
regulation of nitrogen metabolism	1	0.021662
extracellular protein degradation	1	0.027006
actin dependent transport	1	0.037612
nitrogen, sulfur and selenium metabolism	3	0.04648

Translational Regulation Following a Light Pulse

To determine which genes were induced or repressed at the level of translation following a light pulse, ribosome profiling and transcriptome data analyses were carried out on WT cells that were either untreated, or exposed to light for 15, 30, 45, 60, and 120 m. Samples were first validated for light induction, using RT-qPCR. A known light induced gene *al-1* (136), is induced in both replicates (Figure 17). I next examined if the sample

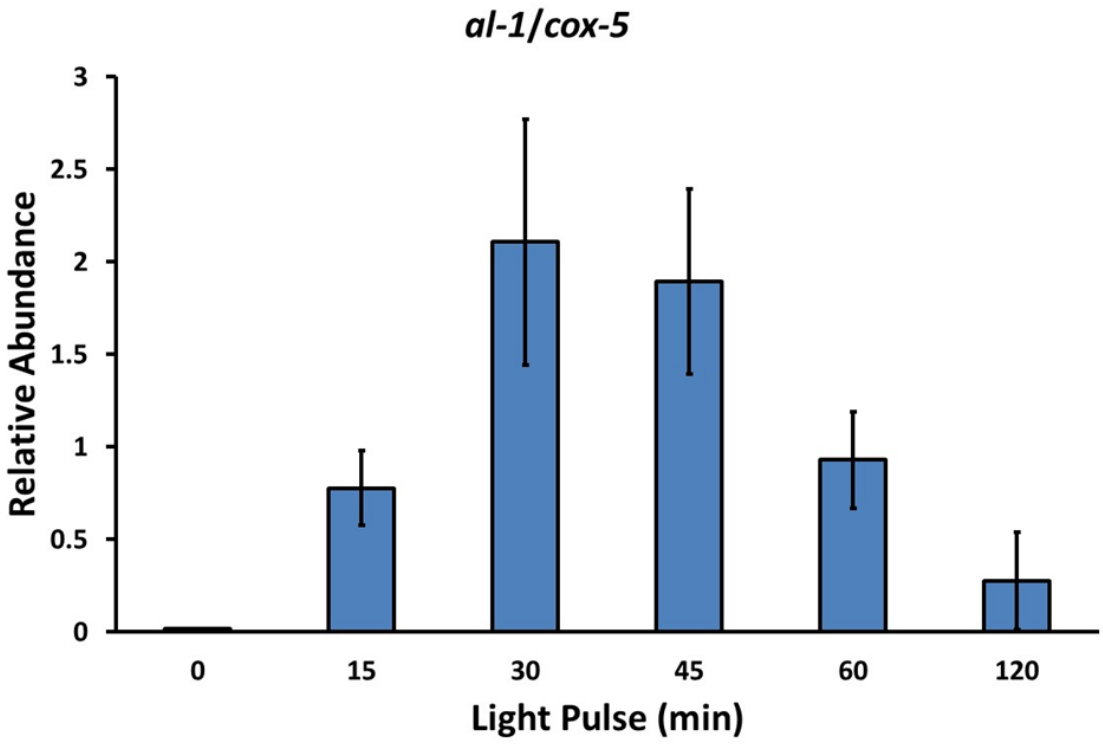

Figure 17. Validation of light induction experiment. RT-qPCR experiment from WT cells in DD24 given a light pulse for the indicated times, using *al-1* primers. The data (n = 2; mean ± StDev) were normalized to 1 and plotted. A non-light induced control (*cox-5*) was used to control for input DNA abundance.

replicates overlapped using Cuffdiff data and R studio. When all time points for each sample data set were combined, the ribosome profiling replicates did overlap with an r^2 value of 0.5 (Figure 18A), similar to what I observed with the osmotically stressed samples. Comparing the individual time points between each replicate (i.e., 0 m replicate 1 compared to 0 min replicate 2) the r^2 value increased to 0.6 – 0.8. For the transcriptome replicates, when all time points for each replicate were combined, the replicates did overlap, with an r^2 value of 0.8 (Figure 18B). When individual time points

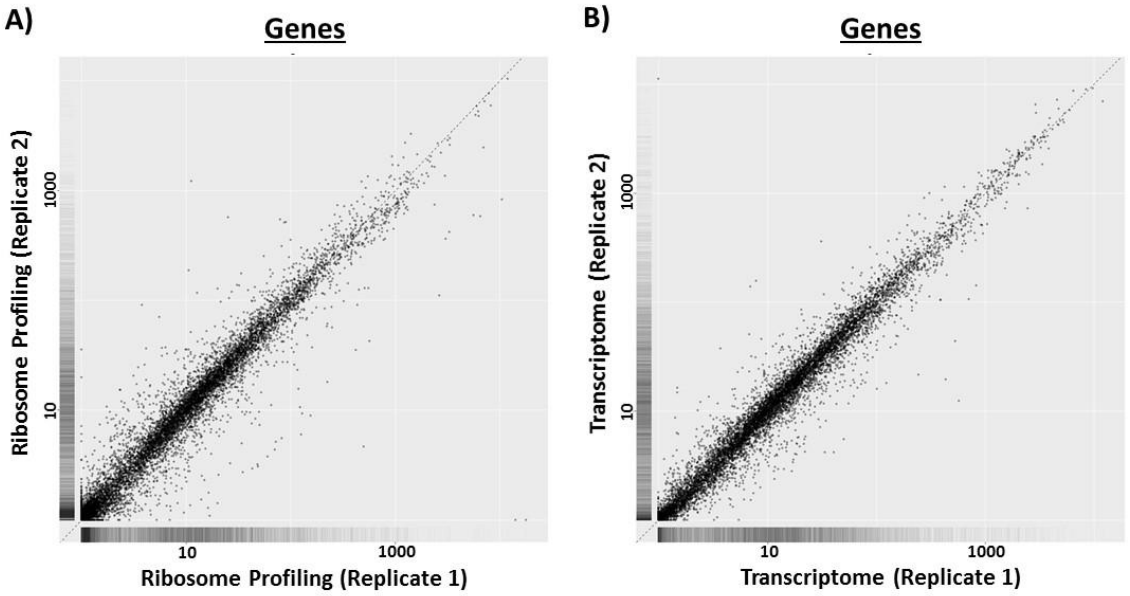

Figure 18. Comparison of sample replicates from cells kept in DD or exposed to light. Scatter matrices comparing two replicates from ribosome profiling (A) and transcriptome (B) sequencing data. Sample data from cells that were either kept in DD or exposed to a light pulse were combined using Tophat2. R studio was used to compare the individual replicates of the combined samples to each other and generate the scatter matrices.

were compared between replicates, the r^2 value ranged from 0.8 – 0.9. Taken together, these data indicate that there is high correlation between the sequencing replicates.

I then identified where the reads mapped to the genome for all replicates at all time points. Approximately 19% of reads for ribosome profiling mapped to the coding sequence (CDS), 3% mapped to the 5' and 3' untranslated regions (UTRs), and 78% mapped to ribosomal RNAs (rRNAs) or non-genic regions of the genome, similar to previous studies (137). For transcriptome samples, 40% of reads mapped to the CDS, 24% mapped to the 5' and 3' UTRs, and 36% mapped to rRNAs or non-genic regions of

the genome (Figure 19). Genes were then identified from ribosome profiling and transcriptome data sets that were induced or repressed after a light pulse. Using a cutoff p-value of 0.05 and a q-value or false discovery rate (FDR) of 0.2, 96 genes were identified at the ribosomal occupancy level that had at least a $\log_2$-fold change > 1 or < -1 following a light pulse at any time point (Figure 20A). 107 genes were identified that were induced/repressed at the transcriptome level (Figure 20B). When the two lists were compared, 60 genes overlapped between the two data sets (Figure 21 & 22), representing 63% of the ribosome profiling induced/repressed genes and 56% of the transcriptome induced/repressed genes. I continued to focus on the 36 genes that were

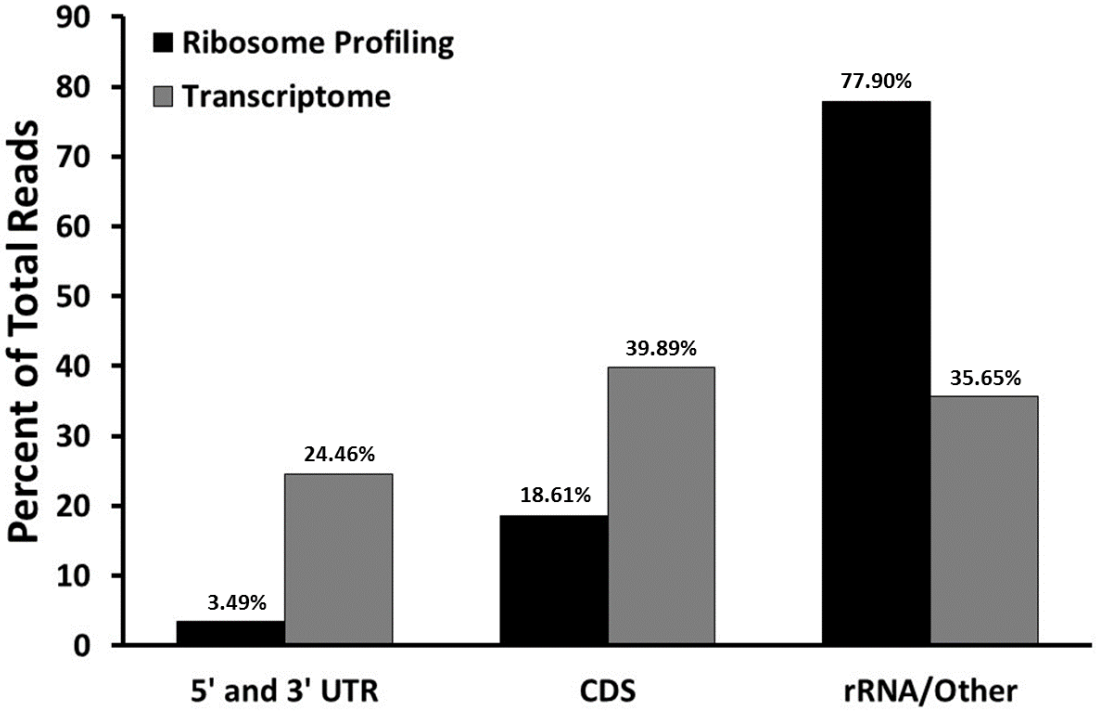

Figure 19. Analysis of reads mapped to the genome. Percentage of reads mapped to the Neurospora genome (v12) for ribosome profiling (black bars) and transcriptome (grey bars) samples.

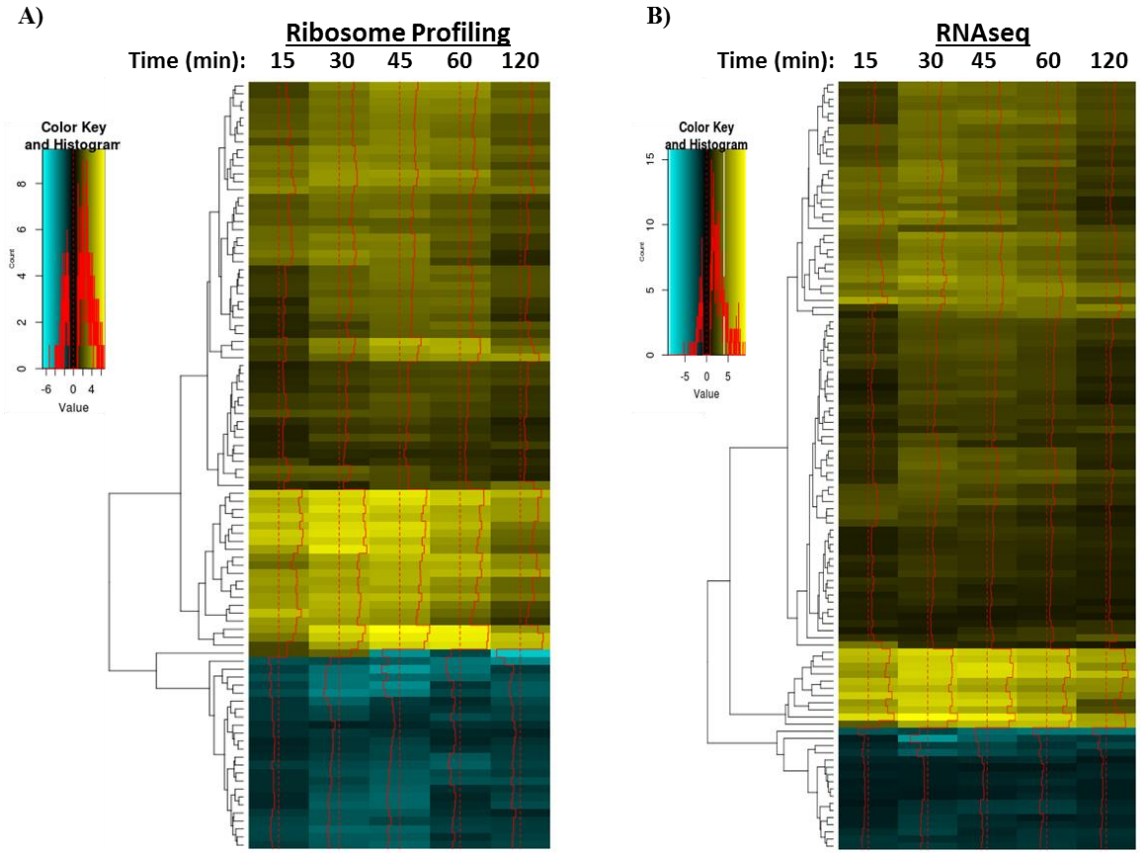

Figure 20. Heatmaps of induced and repressed genes. Log_2-fold change of 0 min time point compared to 15, 30, 45, 60, and 120 min for ribosome profiling (A) or transcriptome (B) samples showing genes with a log_2-fold change of > 1 or < -1. Euclidean clustering were generated using R studio and heatmap.2 with hclust, colors were specified using colorRampPalette.

induced/repressed only at the ribosomal occupancy level only (Table A6 & A7). Using FunCat analyses, I found that similar to the osmotic stress experiment, the 36 translational regulated mRNAs were enriched for metabolic processes. I also found that genes were enriched for virulence, defense and toxin transport (Table 3).

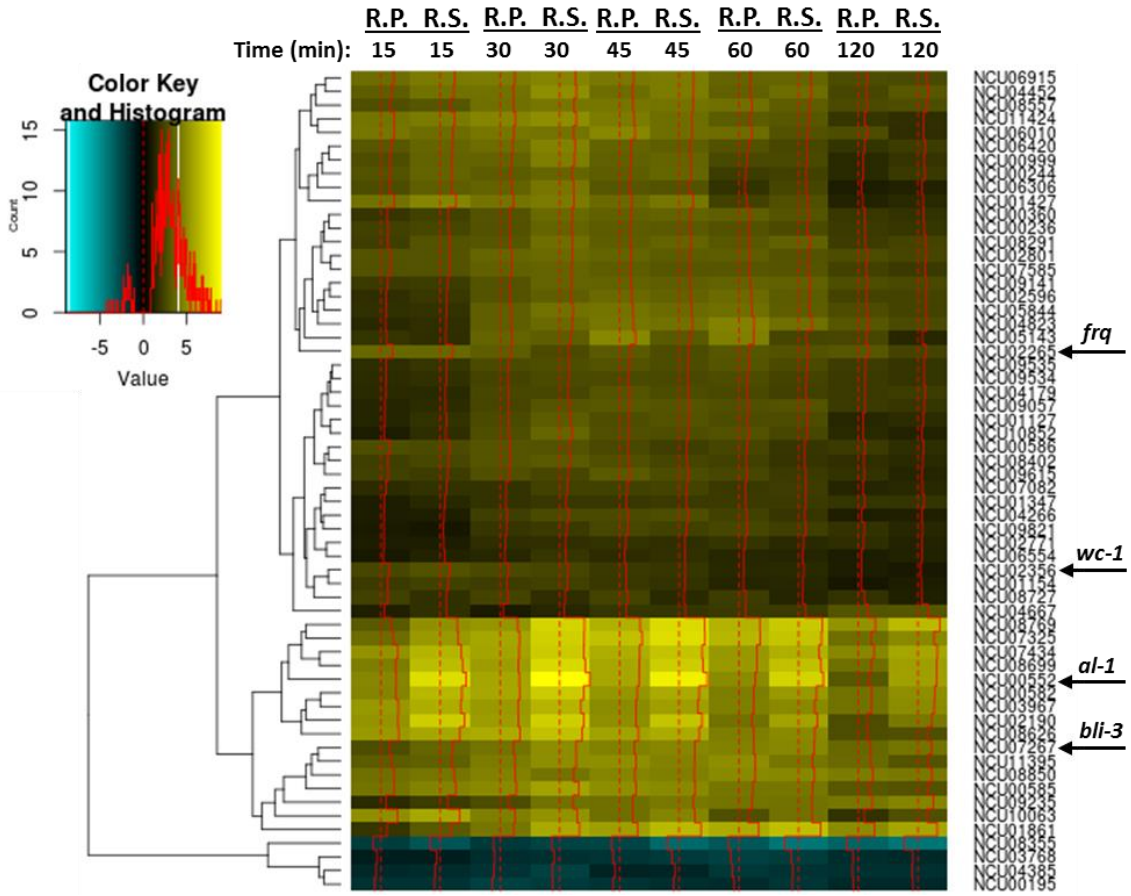

Figure 21. Comparison of ribosome profiling and transcriptome data sets. Heatmaps of commonly induced and repressed genes combined from ribosome profiling (R.P.) and transcriptome (R.S.) samples. Log_2-fold change of 0 min time point compared to 15, 30, 45, 60, and 120 min. A list of NCUs are given to the right of the graphs. Arrows indicate known light induced genes. Euclidean clustering were generated using R studio and heatmap.2 with hclust, colors were specified using colorRampPalette.

Taken together, these data suggested that mRNAs that are subject to higher or lower ribosome occupancy rates (with constitutive mRNA levels) in response to light are primarily from metabolic genes.

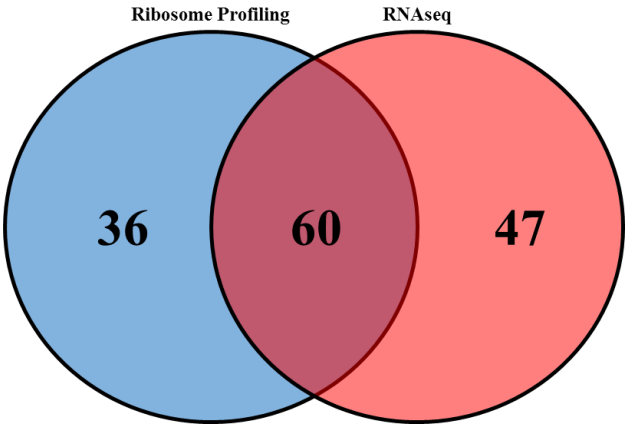

Figure 22. Comparison of ribosome profiling and transcriptome samples following a light pulse. Genes were identified that were induced/repressed after a 15, 30, 45, 60, and 120 min light pulse from ribosome profiling with a $\log_2$-fold change of > 1 or < -1 sequencing data (blue circle) and RNAseq sequencing data with a $\log_2$-fold change of > 1 or < -1 (red circle). Center value represents the number of genes that overlapped between data sets.

Table 3. FunCat analyses of genes that are induced/repressed only at the ribosomal occupancy level in WT cells following a light pulse. FunCat analyses of up-/down-regulated subsets of constitutively expressed mRNAs at the ribosome occupancy level following a light pulse. All light time exposures were compared to DD and were included if there was a significant induction/repression relative to DD ($p \leq 0.05$; $q \leq 0.2$). Categories were considered significant if $p < 0.05$.

Functional Category	hits	p-value
degradation of proline	1	0.011346
virulence, disease factors	2	0.012393
disease, virulence and defense	3	0.014062
drug/toxin transport	2	0.014832
biosynthesis of polyamines	1	0.016975
degradation of arginine	1	0.022574
siderophore-iron transport	1	0.022574
biosynthesis of proline	1	0.025363
metabolism of proline	1	0.033685
nucleotide-sugar metabolism	1	0.033685
biosynthesis of arginine	1	0.039197
metabolism of polyamines	1	0.041942
metabolism of alkaloids	1	0.041942
Type I protein secretion system (ABC-type transport systems)	1	0.041942
homeostasis of metal ions (Na, K, Ca etc.)	2	0.042064
cation transport (H+, Na+, K+, Ca2+ , NH4+, etc.)	2	0.045392
aminosaccharide anabolism	1	0.047411
cellular export and secretion	2	0.049515

Translational Regulation by the Clock

To identify which genes are rhythmic at the level of translation, ribosome profiling and transcriptome data analyses were conducted on WT cells over a circadian time course. To determine which of those genes are controlled by clock regulation of RCK-2, we performed ribosome profiling and transcriptome data analyses on Δ*frq* and Δ*rck-2* cells over a circadian time course. Before performing RNAseq and ribosome profiling, the multiple time series samples were tested for rhythmicity by assessing the accumulation of the core clock protein, FRQ. I found all experiments used for the data analyses were rhythmic (Figure 23A & B). I am still awaiting sequencing data from all of the replicates from the DD28 – 48 time points, and therefore currently include only the data for the

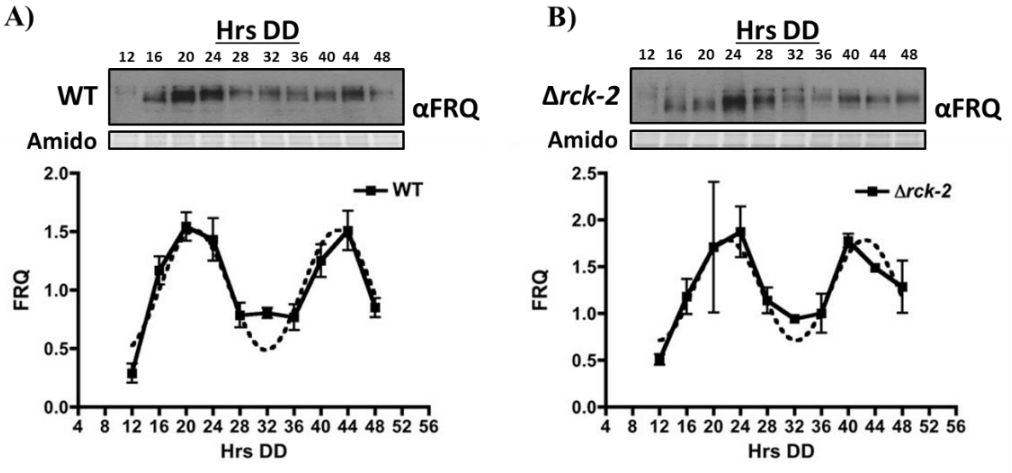

Figure 23. Rhythmic accumulation of FRQ levels over the day. Western blot of total protein from WT and Δ*rck-2* cells grown in constant dark (DD), harvested every 4 h over 2 days (Hrs DD), and probed with αFRQ. Amido stained proteins served as loading controls. The data are plotted below, where the levels of FRQ in both WT (mean ± SEM, n = 3) and Δ*rck-2* (mean ± StDev, n = 2) cells were found to accumulate rhythmically, as indicated by a best fit of the data to a sine wave (dotted black line).

first 6 time points (DD12 – DD32) from 3 WT replicates and 1 Δ*rck-2* replicate. Next, WT sample replicates were compared using Cuffdiff and R studio. I found that when all 6 time points for each replicate were combined, there was little overlap (Figure 24A), with an r^2 value of 0.2 when comparing replicate 1 (rep. 1) to rep. 2; an r^2 value of 0.6 when comparing rep.1 to rep. 3; and an r^2 value of 0.1 when comparing rep. 2 to rep. 3. Further analysis was performed, comparing the individual time points between each replicate (i.e., DD12 rep. 1 to DD12 rep. 2). The r^2 values when comparing rep.1 to rep. 2 ranged from 0.7 – 0.9, rep. 1 to rep. 3 from 0.2 – 0.9, and rep. 2 to rep. 3 from 0.1 – 0.9. For the transcriptome replicates, when all time points were combined, the r^2 value was 0.8 when comparing rep. 1 to rep. 2, 0.7 when comparing rep. 1 to rep. 3, and 0.6 when comparing rep. 2 to rep. 3 (Figure 24B). Further analysis comparing the individual time points for each replicate, revealed r^2 values of 0.6 - 0.9 when comparing rep.1 to rep. 2, 0.4 – 0.5 when comparing rep. 1 to rep. 3, and 0.2 – 0.4 when comparing rep. 2 to rep. 3. Taken together, these data indicate that there is little correlation between the ribosome profiling sequencing replicates, relative to the osmotic and light stress samples.

I proceeded to identify rhythmically cycling genes from our preliminary ribosome profiling and transcriptome data using JTK cycle (138), with a p-value cutoff of ≤ 0.06. 637 genes were identified with cycling mRNA ribosomal occupancy and 1,205 genes with cycling mRNAs. When the two lists were compared, I found that only 88 genes overlapped (Figure 25), representing 14% of the rhythmic ribosomal occupancy mRNAs

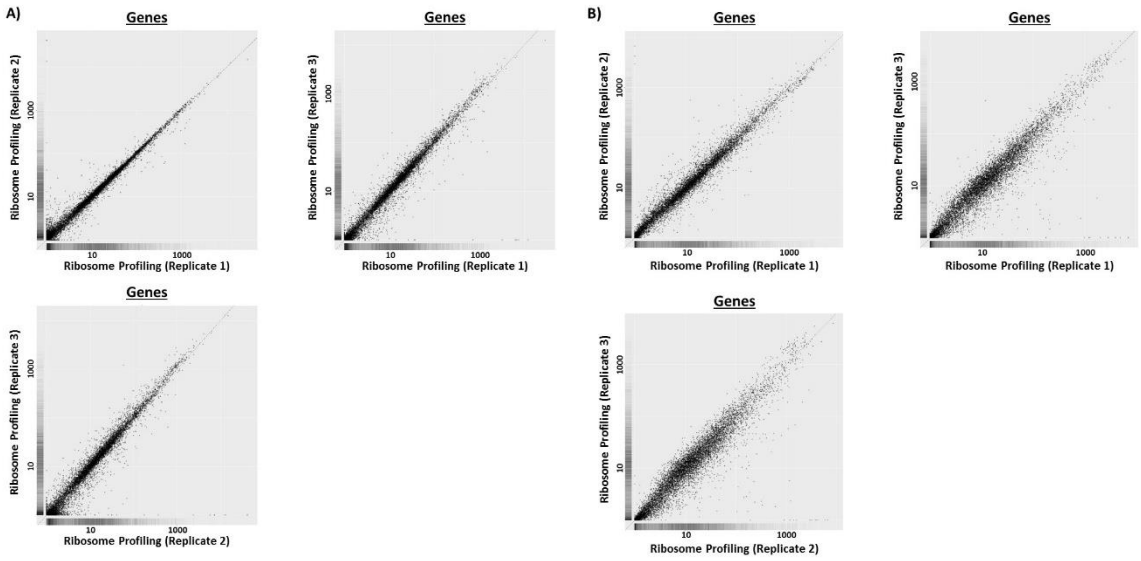

Figure 24. Comparison of time course replicates. Scatter matrices comparing each time course replicate to each other from ribosome profiling samples (A) or transcriptome samples (B) in WT cells

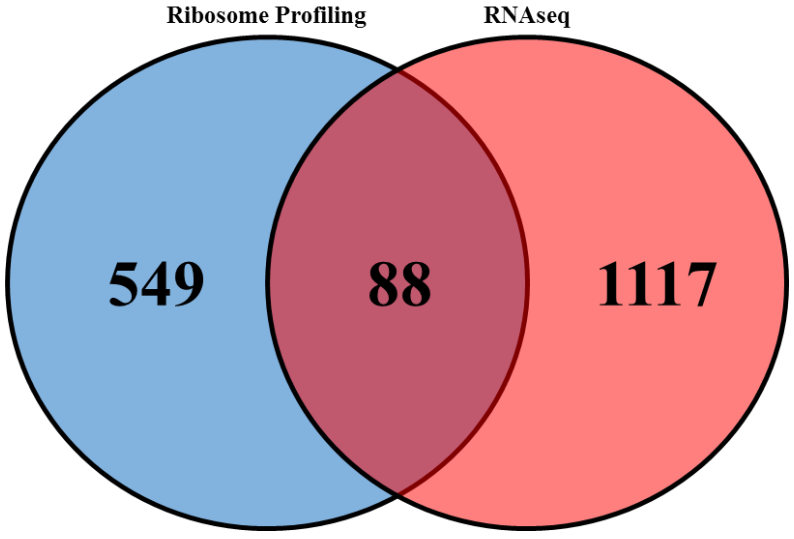

Figure 25. Comparison of ribosome profiling and transcriptome samples over a circadian time course. Genes were identified by JTK cycle that were rhythmic ($p \leq 0.06$) from ribosome profiling sequencing data (blue circle) and RNAseq sequencing data (red circle). Center value represents the number of genes that overlapped between data sets.

and 7% of the cycling mRNAs. I continued the data analysis and found that 549 genes had rhythmic ribosomal occupancy on non-cycling mRNAs (Table A8). I also found that approximately 60% of these peaked during the subjective evening/night. Using FunCat analyses, the 549 genes that have cycling mRNA ribosomal occupancy were examined further. FunCat analyses showed that the genes, similar to the salt induction and light induction experiments, were enriched for some metabolic processes (Table 4). Genes were also identified that encode for cation transport, osmosensing, and cell rescue.

Table 4. FunCat analyses of constitutively expressed mRNAs with rhythmic ribosomal occupancy in WT cells. FunCat analyses of constitutively expressed mRNAs with rhythmic ribosomal occupancy over a circadian time course. Rhythmicity was determined using JTK cycle ($p \leq 0.06$). Categories were considered significant if $p < 0.05$.

Functional Category	hits	p-value
nucleotide/nucleoside/nucleobase transport	4	0.010529
cation transport (H+, Na+, K+, Ca2+ , NH4+, etc.)	13	0.012767
electromagnetic waves resistance (e.g. UV)	2	0.015583
homeostasis of protons	6	0.021764
degradation of tyrosine	3	0.028192
stress response	10	0.033347
osmosensing and response	5	0.035185
tubulin dependent transport	2	0.03631
cell rescue, defense and virulence	21	0.03783
spindle pole body/centrosome and microtubule cycle	4	0.040235
C-compound and carbohydrate metabolism	29	0.048517
sugar transport	3	0.049139

To identify which of the 549 genes cycling at the level of ribosomal occupancy are regulated by clock control of RCK-2, I next analyzed ribosome profiling and transcriptome data set from Δ*rck-2* cells. Using JTK cycle and a p-value = 1 (not significantly cycling), 6,821 genes did not cycle in ribosomal occupancy in Δ*rck-2* cells. When this list was compared to the 549 genes from WT cells, 419 or 76% of the genes overlap (Figure 27 & Table A9). These genes represent mRNAs whose cycling in ribosomal occupancy is abolished in Δ*rck-2*. Since *rck-2* disrupts clock signaling to eEF-2 as previously described, I hypothesize that clock regulation of eEF-2 activity is necessary for these genes to maintain rhythmicity at the level of translation. However, the mechanism for selection of these mRNAs for regulation by rhythmic P-eEF-2 is unknown.

The function of the 419 genes regulated by RCK-2/eEF-2 were determined using FunCat analyses. Genes were found to be enriched for nucleotide transport, ribosomal proteins, and glycogen anabolism (Table 5). Taken together, these data suggested that the clock is signaling through RCK-2/eEF-2 to translationally regulate specific genes, potentially acting as a mechanism to regulate ribosome biogenesis (i.e., through control of ribosomal proteins) and glycogen metabolism.

Discussion

Translational Regulation Following an Osmotic Stress

Following acute osmotic stress, Neurospora cells activate the highly conserved p38-like

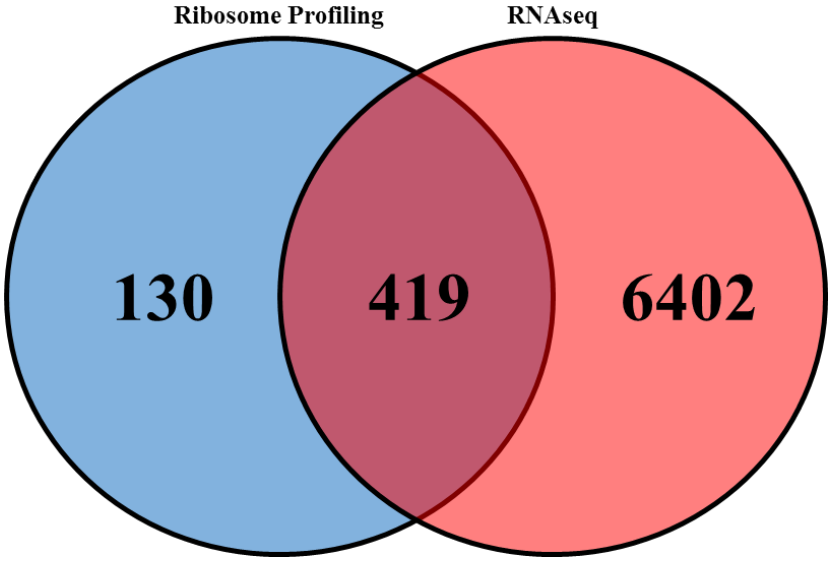

Figure 26. Venn diagram showing the comparison of WT and Δ*rck-2* rhythmic ribosomal occupancy. Genes were identified by JTK cycle that were rhythmic ($p < 0.06$) from ribosome profiling sequencing data in WT cells (blue circle) and arrhythmic in Δ*rck-2* cells (red circle). Center value represents the number of genes that overlapped between data sets.

Table 5. FunCat analyses of constitutively expressed mRNAs with rhythmic ribosomal occupancy regulated by RCK-2/eEF-2. FunCat analyses of constitutively expressed mRNAs with rhythmic ribosomal occupancy from WT cells that do not cycle in Δ*rck-2* cells. Rhythmicity was determined using JTK cycle ($p \leq 0.06$). Categories were considered significant if $p < 0.05$.

Functional Category	hits	p-value
nucleotide/nucleoside/nucleobase transport	4	0.004115
degradation of tyrosine	3	0.013904
ribosomal proteins	1	0.020699
sugar transport	3	0.024903
5'-end processing	2	0.039017
glycogen anabolism	1	0.040579

OS MAPK pathway. The OS pathway in turn activates downstream kinases and transcription factors (26, 139), including the previously described serine/threonine kinase RCK-2. RCK-2 in turn phosphorylates and inactivates eEF-2. To determine the role of eEF-2 regulation on translation following acute osmotic stress, I performed ribosome profiling and RNAseq on WT and Δ*rck-2* cells, before and after treatment with salt. From preliminary sequence analyses, I found that specific mRNAs are being translationally regulated in WT cells following acute osmotic stress, with genes enriched for metabolic processes. I also found that a subset of the translationally regulated mRNAs are controlled by RCK-2/eEF-2 and enriched for metabolic processes. These data suggested that following acute osmotic stress, components of primary metabolic pathways are translationally controlled. Since metabolism is responsible for vital processes essential for cell survival and growth, it is not surprising that during the stress response, metabolic genes are being regulated not only at the level of transcription, as previously described (139, 140), but also at the level of translation. I suggest that by controlling both transcription and translation, cells are provided with an adaptive advantage by (i) up-regulating transcription of genes needed for adaptation; (ii) turning off transcription of non-essential genes; (iii) targeting mRNAs to the ribosomal machinery for rapid synthesis of necessary proteins; and (iv) stopping translation of non-essential mRNAs to conserve energy. Previous work has demonstrated that following an osmotic stress the translational response in both mammals and yeast exceeds that of the transcriptional response (141, 142), I therefore suggest that by rapidly responding to an osmotic stress, and instantaneously turning off translation of mRNAs not required for

cell survival, Neurospora conserves energy and is provided with an adaptive advantage. While my data provides information on the translational regulation of mRNA following a 30 min salt pulse, to determine the rapid response effect, ribosome profiling and RNAseq would need to be conducted with cells treated with an acute osmotic stress for shorter periods of time (i.e., 1 min, 5 min, etc.). This would allow us to determine if the Neurospora translational response following an osmotic stress is similar to that found in both mammals and yeast.

Translational Regulation Following a Light Pulse

Light regulates many molecular and physiological processes in *N. crassa* (143), ranging from growth to conidiation. Previous work has shown extensive control of gene expression following a light pulse, through binding of the WCC to various transcription factors, which in turn bind to downstream genes and transcription factors creating a network of transcriptional regulation (20, 134). However, nothing was known about the effect of light on translational regulation.

To determine if light alters mRNA translation, I performed a light induction experiment on WT cells kept in DD or exposed to varying times of light. Using preliminary sequencing analysis, I found 36 highly significant genes that had constitutive mRNAs that were translational up- or down-regulated. Similar to our osmotic stress experiment, genes were enriched for metabolic processes suggesting that following exposure to light, specific metabolic genes are being translationally regulated. Light is also a stress for

Neurospora; thus, the overall trend is that upon exposure of cells to stress, rapid changes in the levels of primary metabolism can help to overcome the stress.

Translational Regulation by the Clock

The circadian clock regulates many biological functions and physiological processes in diverse organisms (1). Much work in Neurospora has focused on cataloging rhythmic mRNAs, and determining the mechanisms involved in clock regulation of transcription (20, 70, 71, 134). However, little is known about clock regulation of translation in Neurospora or any other clock model system.

To better understand how the clock might regulate mRNA translation, I performed ribosome profiling and RNAseq experiments over a circadian time course with WT and Δ*frq* cells. To determine which mRNAs were rhythmically regulated at the translation level through clock-control of eEF-2, I conducted the same experiments in Δ*rck-2* cells. We are still awaiting sequencing data for the 2nd Δ*frq* and Δ*rck-2* DD12 - 32 replicates, as well as most of the DD28 – 48 time points, and therefore only included the data for the first 6 time points (DD12 – DD32) from 3 WT replicates and 1 Δ*rck-2* replicate.

Generally, when comparing the overlap between WT replicates from combined or individual time points, there was little correlation, relative to the osmotic and light stress replicates. I also saw the least overlap between replicates for time points DD12 and DD32, although the reason for this is unknown. The low correlation between replicates

could be due to the differences in sequencing depth/coverage. My original time course replicates (rep. 1 and 2, DD12 – 32) were sequenced with 8 samples per flow cell lane, resulting in low depth of coverage. However, all subsequent sequencing has involved fewer multiplexed samples (approx. 4 per lane), leading to higher coverage and an increase in the number of reads for rep. 3. Future work will involve re-sequencing the low depth of coverage replicates, if enough sample remains, otherwise new time course experiments will be performed.

From preliminary data analyses, I found that few genes (88) overlapped when comparing rhythmically cycling mRNAs to mRNAs with rhythmic ribosomal occupancy. This discrepancy can be explained by the high false discovery rate (FDR) since our q-values were generally 0.5 or higher. JTK cycle is an excellent script for analyzing rhythmic sequencing data, however it does have its limits. To increase the number of identified cycling genes and decrease the FDR, the algorithm requires a 2 h sampling resolution over 2 consecutive days. Unfortunately, I was unable to sample this often due to the cost of the experiments (144). An example of an improperly called gene by JTK cycle is *ccg-1* (NCU03753), which is known to be transcriptionally rhythmic. In our ribosome profiling data set, this gene is called rhythmic, however in the RNAseq data set *ccg-1*, is called arrhythmic (Table A5). When the rest of the sequencing data arrives, I will reanalyze the data to see if *ccg-1* is still called arrhythmic. If so, there are alternative scripts and algorithms to analyze the data, such as Detection of Differential Rhythmicity (DODR) (145, 146).

Despite not having all of the data, I continued with the analysis of the rhythmic ribosome profiling to generate a list of preliminary candidates for further study. 549 constitutively expressed genes in WT cells had cycling mRNA ribosomal occupancy, and these were enriched for glycogen anabolism. Of the 549 mRNAs rhythmically regulated by translation, the majority of these peaked during the subjective evening/night time, which coordinates with an increase in anabolic functions as previously described (70, 71). The 549 mRNAs regulated by translation were examined further, and I identified 419 that were controlled by clock signaling to RCK-2/eEF-2.

Future work for all 3 experiments, osmotic stress, light induction, and circadian clock control of translation, will involve deeper analysis of the sequencing data. For the circadian data set, once all of the data is received, I will reanalyze the data with JTK cycle, and use alternate scripts to validate the results (i.e., DODR). In all 3 data sets, deeper analyses will be performed to determine the translational efficiencies of the mRNAs, as well as to investigate the role of the translationally regulated mRNAs in metabolism. I will also determine if there are any unique motifs, with specialized sequences or secondary structures for these mRNAs. There may also be novel upstream open reading frames (uORFs) that are controlling initiation for these mRNAs. For RCK-2/eEF-2 translationally regulated mRNAs, I will examine the levels of mRNA and whether this has any effect on their specificity. If these mRNAs are highly expressed, they may have increased sensitivity to elongation inhibition. There may also be unique domains within the coding sequence that effect elongation rates. If unique motifs are

identified, mutations will be made in those domains to determine if they are responsible for osmotic, light, and/or clock regulation of translation. We are also currently validating the ribosome profiling data using *luc* translational and transcriptional fusions of several candidate genes.

To determine the biological significance of Neurospora regulation of translation after an osmotic stress, light stress, or over a circadian time course, we can examine if WT strains outcompete motif deleted/mutated strains, as well as the Δ*rck-2* strain. These strains would be exposed to (i) osmotic stresses with differing concentrations and durations; (ii) light of various intensities and duration; and (iii) stresses presented at different times of the day. From these experiments, it may be possible to determine the biological significance for Neurospora regulation of translation.

In summary, once we have a better idea of the mechanism for how certain mRNAs are selected for translational regulation, and given that both translation and circadian clock mechanisms are highly conserved, this work will offer fundamental insights into translation control by the clock, and will provide a platform to extend these studies into mammalian clocks. Determining the circadian proteome will lead to a better understanding of clock control of cellular metabolism, and why some drugs are more effective or toxic at specific times of the day.

Materials and Methods

Strains and Growth Conditions

Vegetative growth conditions were as previously described (119). The *N. crassa* wild-type (WT) FGSC#4200 (*mat a*, 74-OR23-IV) and FGSC#11545 (*mat a*, Δ*rck-2::hph*) strains were used for all analyses. Verification of gene deletion for the Δ*rck-2* strain was accomplished by PCR, and the Δ*rck-2* strain containing the hph construct was maintained on Vogel's minimal media, supplemented with 200 μg/mL of hygromycin B (#80055-286, VWR, Radner, PA). All experiments were conducted using germinated conidia as previously described (123, 134, 147). Briefly, for the salt and light induction experiments, $1X10^6$ conidia were added to 500 mL of 1X Vogel's minimal media pH 6.0, containing 2% glucose and grown for 4 h at 25° C in LL with orbital shaking (100 rpm). The cultures were then transferred to DD for 24 h at 25° C with orbital shaking. 4% NaCl was added to the salt induction samples 30 min prior to harvest. For the light induction samples, cultures were transferred to LL for 15, 30, 45, 60, and 120 min at 25° C prior to harvest. For the DD12 – 32 time course experiments, $1X10^5$ conidia were added to 500 mL of 1X Vogel's minimal media pH 6.0, containing 2% glucose and grown for 4 h at 25° C in LL with orbital shaking. Cultures were transferred to DD every 4 h for the indicated times at 25° C. For the DD28 – 48 time course experiments, $1X10^4$ conidia were added to 500 mL of 1X Vogel's minimal media pH 6.0, containing 2% glucose and grown for 2 h at 25° C in LL with orbital shaking. Cultures were transferred to DD every 4 h for the indicated times at 25° C. All samples were harvested onto filter paper by vacuum filtration, and washed with ice-cold DEPC water. The resulting

mycelial pad was cut into pieces (approx. 100 mg/piece) and placed into a 50 mL conical tube, snap-frozen in liquid nitrogen, and stored at -80° C.

Protein Extraction and Western Blotting

To assay FRQ protein levels, protein was extracted as previously described (122) with the following modification: the extraction buffer consisted of 50 mM HEPES pH 7.4, 137 mM NaCl, 10% glycerol, 5 mM EDTA, 10 mM NaF, 1 mM PMSF, 1 mM sodium ortho-vanadate, and 1 mM β-glycerophosphate. Protein concentration was determined using the Bradford assay (#500-0112, Bio-Rad Laboratories, Hercules, CA). Protein samples (50 μg) were separated on 10% SDS/PAGE gels and blotted to an Immobilon-P nitrocellulose membrane (#IPVH00010, Millipore, Billerica, MA) according to standard methods. FRQ was detected using mouse monoclonal anti-FRQ primary antibody (Supernatant from clone 3G11-1B10-E2, a gift from M. Brunner's lab) in 7.5% milk, 1X TBS, 0.1% Tween-20 at a concentration of 1:200 and anti-mouse IgG-Peroxidase secondary antibody (#170-6516, BioRad Laboratories) at a concentration of 1:10,000.

Reverse Transcription Quantitative PCR (RT-qPCR)

Total RNA was extracted as previously described (148) using 750 μL of extraction buffer (0.1 M NaOAc pH 5.3, 1% SDS, 10 mM EDTA), 500 μL acid phenol:chloroform, and approx. 200 μL glass beads (#11079105, BioSpec Products Inc., Bartlesville, OK). Total RNA was quantified using a NanoDrop spectrophotometer (Thermo Fisher

Scientific Inc., Waltham, MA) and RNA quality was assessed by denaturing gel electrophoresis.

Synthesis of cDNA was performed as previously described (82). Briefly, total RNA (4 μg) was treated with 1 μL TURBO™ DNase (#AM1907, Thermo Fisher Scientific Inc., Waltham, MA for 30 min at 37° C to remove genomic DNA, and the reaction was stopped using 1 μL DNase inactivation reagent at room temperature (RT) for 2 min. Following centrifugation, the supernatant was transferred into a fresh tube and the RNA was quantified using a NanoDrop spectrophotometer. DNA-free total RNA (1 μg) was used as the template for first-strand cDNA synthesis as described by Wei et al., 2013. Quantitative PCR (qPCR) was performed as described (82) using 3 μL of cDNA, 1X SYBR® Green I (#S-7563, Thermo Fisher Scientific Inc., Waltham, MA), 0.25 U of TaKaRa™ rTaq DNA polymerase (#R001A, EMD Millipore Corporation, Billerica, MA), and 500nM of each primer. PCR was performed using an Applied Biosystems 7300 real-time PCR machine (Thermo Fisher Scientific Inc., Waltham, MA).

RNAseq

Total RNA was isolated from frozen mycelia, and poly(A) mRNA was purified from 125 μg of total RNA as previously described (134, 147) using oligo $d(T)_{25}$ magnetic beads (#S1419S, New England Biolabs, Ipswich, MA). Isolated mRNA was enriched using Epicentre Terminator™ 5'-phosphate-dependent exonuclease (#TER51020,

Illumina (Epicentre), Madison, WI). cDNA and sequencing libraries were prepared as previously described (134, 147).

Ribosome Profiling

Ribosome profiling was carried out as previously described (149) using frozen mycelia. Briefly, 2 g of frozen mycelia were added to pre-chilled grinding vials, along with 2 mL of lysis beads made by dripping lysis buffer into liquid nitrogen. Samples were pulverized in a SPEX CertiPrep 6850 Freezer/Mill® (#6850, SPEX SamplePrep, Metuchen, NJ) using a 10 min pre-cooling cycle, followed by 3X 2 min grind cycles, with 1 min re-cooling between each cycle. Pulverized cells were transferred to pre-chilled 50 mL polycarbonate centrifuge tubes and allowed to thaw on ice (approx. 30 min), and then centrifuged at 4° C for 15 min at 16,000 rpm using a JA-20 rotor. The supernatant (approx. 2 mL) was carefully removed, avoiding both the pellet and lipid upper layer, and placed in a pre-chilled 15 mL conical tube. Cell extract was quantified by measuring the A260 of the extract using a Varian Cary® 50 UV-Vis Spectrophotometer (Agilent Technologies, Santa Clara, CA). 50 A260 units of extract were brought to a final volume of 300 µL with lysis buffer, which consists of 20 mM Tris-Cl (pH 7.5), 150 mM NaCl, 5 mM $MgCl_2$, 1 mM DTT, 1% Triton X-100, 25 U/mL Turbo DNase (#AM2238, Thermo Fisher Scientific Inc., Waltham, MA), and 100 µg/mL cycloheximide; and treated with 1.875 µL of RNase I (#AM2294, Thermo Fisher Scientific Inc., Waltham, MA) for 45 min at RT with gentle mixing. The extract was immediately transferred to a pre-chilled 3.5 mL, 13 X 51 mm polycarbonate

ultracentrifuge tube, 0.9 mL of a 1M sucrose cushion underlay was added, and the ribosomes were pelleted by centrifugation at 70,000 rpm at 4° C for 4 h. All subsequent steps to step 46 were followed as described by Ingolia et al., 2012. The rRNA depletion step was not performed, but instead after heat-inactivation of CircLigase (#CL4111K, Illumina (Epicentre), Madison, WI), 2.0 µL of GlycoBlue™ (#AM9515, Thermo Fisher Scientific Inc., Waltham, MA), 6.0 µL 5 M NaCl, 74 µL of DEPC water, and 150 µL of isopropanol were added to each tube and precipitation was carried out overnight at -80° C. The DNA was pelleted by centrifugation for 30 min at 20,000 g at 4° C; samples were washed with 70% ethanol and allowed to air-dry for 10 min. The pellet was then resuspended in 5.0 µL of 10 mM Tris (pH 8.0), and PCR amplification/barcode addition were performed as described (149). Sequencing libraries were quantified and checked for quality on an Agilent 2100 Bioanalyzer using a DNA high-sensitivity chip (Agilent, Santa Clara, CA) per the manufacturer's instructions. Sequencing was carried out on an Illumina HiSeq 3000 (Illumina, Inc., San Diego, CA).

Read Processing

Ribosome profiling reads were trimmed using Cutadapt to remove all adapter sequences. Before alignment, all sets of reads were individually, and as a group, analyzed using FastQC to check read quality and length for both ribosome profiling and RNA-seq data. Trimmed ribosome profiling reads were then aligned to *N. crassa* assembly 12 using Tophat2 with Bowtie1. RNA-seq reads were aligned to *N. crassa* assembly 12 using Tophat2 with Bowtie2. A maximum of 2 mismatches were allowed for any one read for

both ribosome profiling read alignment and RNA-seq read alignment. To determine the amount of ribosome profiling and RNA-seq reads that mapped to the 5' or 3' UTR, CDS, or other regions of the genome, read sets were concatenated into one file and mapped to the *N. crassa* assembly 12 CDS annotation using "--unaligned" and "--aligned" as outputs. The unaligned reads were then mapped to the *N. crassa* assembly 12 gene annotation, and the percent of reads that mapped to the CDS, the remainder of the genes, and unmapped reads was determined.

Quantification and Analysis

Quantification of FPKM values was done using Cuffdiff and output was analyzed in R studio as previously described (135). Briefly, cummeRbund was used to compare FPKM values between data sets, generate scatter matrices, and compare each salt induced (30 min), light pulse (15, 30, 45, 60, and 120 min) to time 0 min. For the time course experiments, cummeRbund was used to compare FPKM values between data sets and generate scatter matrices. JTK cycle was then used to analyze the time course data and identify rhythmically cycling genes (138), with the following script modification: line 14 was changed to *periods <- 5:7* (to identify genes with a period range of 20 – 28) and line 15 was changed to *jtk.init(periods,4)* (indicating the amount of time between time points). These data produced tables that were able to be extracted and sent to MySQL. MySQL was used to extract all statistically significant FPKM changes ($q < 0.2$ and $p < 0.05$) for the subsequent data tables. Extracted data were analyzed using R studio in order to produce more specific data plots. Heat maps with Euclidean clustering were

generated using R studio and heatmap.2 with hclust and colors were specified using colorRampPalette. A list of the commands and script used for all sequencing data are provided in Appendix B.

CHAPTER IV

SUMMARY

The results presented in this dissertation have provided additional insight into the stress response and circadian clock regulation of translation in Neurospora. I have demonstrated that following an osmotic stress, the p38-like OS-2 MAPK phosphorylates the conserved serine/threonine kinase RCK-2, which in turn phosphorylates the highly conserved eEF-2. Using ribosome profiling, coupled with RNAseq, I show that this leads to regulation of a specific set of mRNAs that are enriched for metabolic processes. I also demonstrate that following a light pulse, there are a specific set of mRNAs that are being regulated in their ribosomal occupancy. These mRNAs are also enriched for metabolic processes.

I show that the clock signals through the OS pathway to generate rhythms in phosphorylation of RCK-2, which in turn results in rhythmic phosphorylation of eEF-2. Clock signaling to eEF-2 leads to repression of translation during the subjective daytime, with higher levels of translation occurring during the subjective evening (Figure 27). I have also shown that clock regulation of eEF-2 does not globally regulate all mRNAs, since not all proteins cycle in abundance. However, there are specific mRNAs that are being translationally regulated by the clock, as well as by clock-control of eEF-2. Some of these mRNAs regulate anabolism and peak in the evening, the time when anabolic processes are highest (70, 71). Translation of mRNA is the most energy-demanding

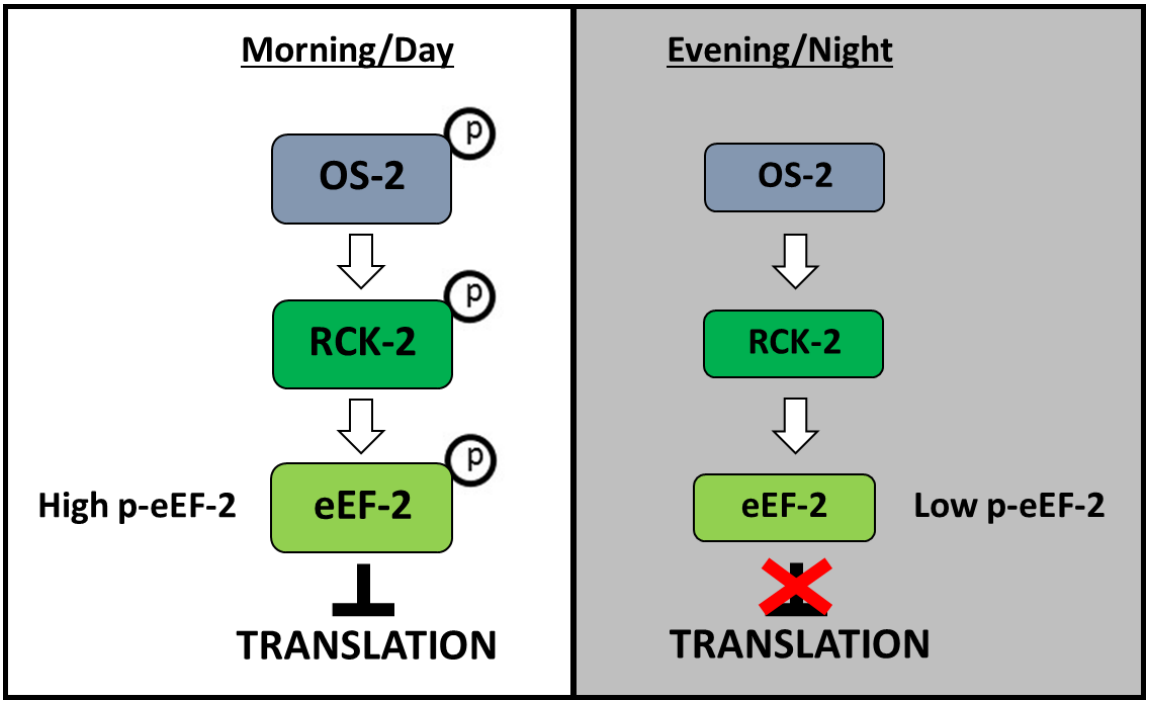

Figure 27. Model for circadian regulation of translation.

process in a cell. I speculate that repression of translation during the daytime allows Neurospora to conserve energy during the osmotically stressful daytime, freeing energy for use in translation during the evening when the environmental conditions are more conducive to growth and development. As such, I predict that nighttime mRNA translation provides an adaptive advantage to the organism. To test this idea, one could examine if WT strains outcompete RCK-2 deletion strains, which lack clock control of eEF-2 activity, under conditions in which varying types of osmotic stresses are given during the day.

Stress Response Regulation of mRNA Translation in Neurospora

Translational Regulation Following an Osmotic Stress

The ability of cells to quickly respond to osmotic stress is essential for survival. Cellular pathways are activated that lead to transcriptional activation of genes needed for survival, or if the osmotic stress is too great, apoptosis will be triggered (150, 151). Organisms have learned to adapt to osmotically stressful situations. In Neurospora, the OS pathway is activated following an osmotic stress and the terminal MAPK OS-2 interacts with key transcription factors and kinases to activate genes needed to survive the stress, and to inactivate most other genes to conserve energy (26). I identified Neurospora RCK-2 and eEF-2 and showed that they are part of the stress response pathway (chapter II). Overall, it makes sense to alter translation after an acute stress is encountered as this would be the most rapid way to turn on genes needed to survive the stress, and turn off genes that are not essential for survival. Interestingly, I found that following an osmotic stress, specific mRNAs are regulated at the translational level and these primarily encode for metabolic processes (chapter III). Yet, several questions still remain.

I previously observed that induction of RCK-2 protein and phosphorylation require OS-2, however when we compared WT and Δ*os-2* protein extracts on the same western gel, the overall abundance of RCK-2 was dramatically reduced in Δ*os-2* cells (chapter II). While exposure times to detect RCK-2 from WT extracts ranged from 2 – 10 s, exposure times to detect RCK-2 from Δ*os-2* extracts ranged from 1 – 2 m. These data suggested

that not only is OS-2 regulating induction and phosphorylation of RCK-2, but also the overall abundance of RCK-2 protein. Consistent with low levels of RCK-2 protein in Δ*os-2*, I found that the level of *rck-2* mRNA is significantly lower in Δ*os-2* cells, suggesting that the components of the OS pathway positively regulate *rck-2* expression. Previous work in our lab has shown that after an osmotic stress, OS-2 interacts with and activates a transcription factor, ASL-1, that in turn regulates downstream stress response genes (26). Thus, one explanation for the reduced abundance of RCK-2 in Δ*os-2* cells is that ASL-1 binds to the promoter of *rck-2*, or to another gene that encodes a transcription factor that regulates the expression of *rck-2*. To test this hypothesis, ASL-1 could be tagged with V5, followed by ChIP-seq to determine which genes are bound by ASL-1. If *rck-2* is not one of the direct targets of ASL-1, I would next examine the possibility that other transcription factors or chromatin modifying genes regulated by ASL-1 are responsible for the low levels of *rck-2* mRNA.

Following an osmotic stress, eEF-2 phosphorylation is induced and in the absence of *rck-2* and/or *os-2* this phosphorylation is reduced (chapter II). However, I still observed low level phosphorylation of eEF-2 in the individual and doubly mutant strains, suggesting that other kinase(s) can phosphorylate eEF-2. It is known that in mammals, eEF-2 kinase, which regulates eEF-2, is activated by environmental stress, hypoxia, and nutrient status (53). While we were unable to identify a Neurospora eEF-2 kinase, it is possible that kinases associated with activation of mammalian eEF-2 kinase, including TOR-dependent kinases, AMP-kinase, or cyclic AMP dependent protein kinase A, could

be directly phosphorylating eEF-2. To determine what other kinase(s) may regulate eEF-2, I would first examine in knockouts, or knockdowns (for essential genes) of the candidate kinases if levels of P-eEF-2 are reduced, and if so, I would generate a double mutant strain containing a mutation in the candidate kinase, and deletion of RCK-2. If I find that eEF-2 is not phosphorylated in the double mutant when cells are stressed by salt, hypoxia, or nutrient depravation, I would then carry out an *in vitro* phosphorylation assay using purified eEF-2 and the candidate kinase from *N. crassa*. If all of the candidate kinases are ruled out as being able to phosphorylate eEF-2, I would perform an IP with eEF-2 following an osmotic stress. However, in many cases, interactions between kinases and their substrates are transient, and therefore difficult to IP. If I am successful and able to pull down RCK-2 as a control with eEF-2, I would then use mass spectrometry to identify possible candidate kinases that are associated with eEF-2. Knockouts, or knockdowns of these candidates would then be used to validate if they are indeed necessary for phosphorylation of eEF-2 as described above. It is also possible that phosphates play a role in rhythmic accumulation of P-eEF-2, although this has not been examined. In mammals, protein phosphatase 2A (PP2A) converts P-eEF-2 to an active form (152, 153). To test if PP2A plays a role in Neurospora cells, we could examine the levels of P-eEF-2 in an available *rgb-1* mutant in Neurospora, which encodes for the regulatory subunit of PP2A (154).

Specific mRNAs enriched for metabolic processes are being regulated at the level of translation, in cells given an acute osmotic stress (chapter III). A subset of these

translationally regulated mRNAs are controlled by RCK-2/eEF-2 and are also enriched for metabolism. However, the mechanism for this specificity is unknown. Further analysis of the ribosome profiling sequencing data may reveal unique motifs with specialized sequences or secondary structures for these mRNAs. There may also be novel upstream open reading frames (uORFs) that are controlling initiation for these mRNAs. For the mRNAs whose translational regulation is due to RCK-2/eEF-2, the levels of mRNA could be affecting their specificity. If these mRNAs are highly expressed, they may have increased sensitivity to elongation inhibition. There may also be unique domains within the coding sequence that effect elongation rates.

I also showed that mRNAs are up- and down-regulated at the translational level. Further analysis of the sequencing data may reveal that induced mRNAs have different motifs/codon usage than repressed mRNAs. Once the mechanism(s) is/are identified, further work would include mutating these regulatory elements to determine if they are indeed required for specificity. This work could then be expanded to other organisms to see if this is a conserved mechanism for mRNA regulation of translation following an osmotic stress. The question still remains, why would these mRNAs be enriched for metabolic processes? It is known that reactive oxygen species (ROS) are generated by metabolism (155, 156). I speculate that following an osmotic stress, in addition to conserving energy, Neurospora reduces translation of metabolic genes to decrease ROS production, which in turn would increase the chance for survivability/adaptation. This idea could be tested by examining ROS production in the RCK-2 deletion strain that

cannot rhythmically control the levels of P-eEF-2 following varying types of osmotic stresses. If my hypothesis is correct, the levels of ROS would be lower in WT cells versus Δ*rck-2* cells under these conditions.

Translational Regulation Following a Light Pulse

Light provides energy for growth and development, but also is damaging to DNA. Therefore, organisms have evolved to respond to light in many different ways, including producing photo protective proteins such as melanin in mammalian cells, and carotenoids in plants and fungi. Following a light pulse, in Neurospora, a complex transcription factor network is activated to extensively regulate the expression of many genes (20). However, nothing was known about translational regulation following light exposure. I identified specific mRNAs that were only regulated in ribosomal occupancy in response to a light pulse, and these mRNAs, similar to the osmotic translationally regulated mRNAs, were enriched for metabolic processes (chapter III). Further sequencing analysis should shed light on the mechanism for this regulation by identifying unique motifs, secondary structures, etc., as described above. Validation of the mechanism(s) would follow as previously described, and would serve as the basis to extend these studies into other organisms to determine if this is a conserved mechanism for mRNA regulation of translation following a light pulse. Similar to osmotic stress, light stress in Neurospora can lead to rapid regulation of gene expression by shutting down translation of specific mRNAs involved in metabolism, which would be predicted to reduce ROS production to help overcome the adverse effects of the stress.

Circadian Regulation of mRNA Translation in Neurospora

Circadian clocks allow organisms to anticipate daily environmental cycles, and regulate physiology and behavior to optimize the timing of resource allocation for improved fitness (157). For example, our heart rate and blood pressure increase in anticipation of waking up each morning (158). In preparation for eating, our liver and fat cells maximize the production of metabolizing and energy storage proteins (159-161). Our capacity for learning and memory, and the onset of sleep, are clock-controlled (158). The clock also provides a mechanism to predict and prepare for daily changes in environmental and genotoxic stress (22, 162, 163). As a consequence of the widespread influence of the clock on physiology, disruption of the clock, either through mutation, or by living against the clock (e.g. shift work), significantly impacts our health (164), and through clock regulation of metabolism, many drugs are more effective or more toxic depending on the time of administration (165). Understanding the clock and how it regulates these diverse biological functions has been the focus of studies from all over the world for the past 60 years.

Neurospora has been one of the most valuable tools for circadian researchers, not just because of the rapid generation time, ease of genetic manipulation, or the amazing knockout library, but because of the high conservation of many of the genes and pathways in Neurospora (i.e., what is found in Neurospora can be applicable to higher eukaryotes). In Neurospora, the clock regulates gene expression, as well as diverse biological functions such as growth and development. Much work has focused on the

regulation of transcription, but growing evidence suggests a role for the clock in regulating translation. My work in Neurospora has focused on a mechanism for clock regulation of translation. I found that clock signaling through the p38-like OS pathway leads to rhythmic phosphorylation of RCK-2, which ultimately leads to phosphorylation of eEF-2 (chapter II). I was able to show *in vitro* that this regulation acts as a mechanism for clock-control of translation. Our *in vitro* studies used only a single optimized *luc* mRNA. However, once we have a better idea of the mechanism for how certain mRNAs are selected for regulation by eEF-2, we can validate the mechanism by using selected and non-selected RNAs, as well as RNAs with mutations in the unique sequences, in the *in vitro* translation system. Furthermore, while I was able to show that RCK-2 accounts for 60% of the levels of P-eEF-2, we still do not know how much of the total amount of eEF-2 is phosphorylated by stress or by the clock. Although I attempted to answer this question, I was unable to do so because the antibody available to detect total eEF-2 only recognizes non-phosphorylated eEF-2. Thus, I was unable to use the same antibody to accurately quantitate the amounts of unphosphorylated and phosphorylated eEF-2 in cells. In the future, a new antibody could be generated that can detect both forms; eEF-2 could be tagged and the phosphorylated and unphosphorylated forms separated using Phos-Tag™ gels; or alternatively, eEF-2 phosphorylation levels could be measured by quantitative mass spectrometry.

To identify the circadian proteome, with the caveat that there are post-translational modifications (PTMs) that regulate the stability, activity, interactions, etc. of proteins

(166, 167), and to determine how clock regulation of eEF-2 activity affects rhythmic translation *in vivo*, I adapted a previously described ribosome profiling protocol (149) for use with Neurospora cells. Ribosome profiling, coupled with RNAseq, showed that specific constitutively expressed mRNAs are being translationally regulated (chapter III). Some of these mRNAs encode metabolic processes, similar to the mRNAs enriched following osmotic and light stress. I also found that the majority (~ 60%) peak in the evening, the same time when anabolic processes occur in Neurospora. Further analysis will determine if these evening specific translationally regulated mRNAs have unique motifs with specialized sequences or secondary structures.

I found that a specific set of these constitutive mRNAs with rhythmic ribosomal occupancy require clock signaling through RCK-2/eEF-2 to maintain rhythmicity. Since not all of the rhythmic ribosomal occupancy mRNAs were affected, this would suggest there are other mechanisms for clock regulation of mRNA translation. One possibility is through clock regulation of translation initiation. I performed some preliminary experiments and found that eIF-2α, a key factor in translation initiation, is rhythmically phosphorylated, suggesting a possible mechanism for clock regulation of translation initiation. These preliminary experiments are currently being followed up by another graduate student in the lab, Shanta Karki. She demonstrated that the clock controls rhythms in accumulation of P-eIF-2α, and she showed that the Neurospora homolog of GCN2 kinase, CPC-3, is necessary for phosphorylation of P-eIF-2α. She just completed a circadian ribosome profiling experiment in cells deleted for CPC-3. Thus, once we

obtain the results from her experiment, we will be able to assess the contribution of rhythmic initiation control to rhythmic ribosome occupancy. If deletion of both RCK-2 and CPC-3 abolish rhythmic ribosome occupancy of all of the mRNAs, then we can conclude that these pathways are responsible for the bulk of rhythmic translation control. If we find that many of the mRNAs still show rhythmic occupancy, then future experiments will be needed to identify the mechanisms responsible for this activity, including examining the effects of deletion of other translation initiation, elongation, or termination factors on rhythmic ribosome occupancy.

To determine how clock signaling to RCK-2/eEF-2 specifically affects translationally regulated mRNAs, I could also determine the overall levels for mRNAs from the RNAseq data. It may be that highly expressed mRNAs, which are predicted to have increased ribosomal occupancy due to the abundance of mRNA availability, would have increased sensitivity to elongation inhibition. Since not all eEF-2 is phosphorylated, as previously indicated (chapter II), any change in the levels of P-eEF-2 could affect the rate of translation elongation of these mRNAs. Low abundance mRNAs, which are predicted to have decreased ribosomal occupancy, may escape this regulation. It is also possible that there may be unique domains within the coding sequence affecting codon usage. Future work would include mutating the identified motifs and/or regulatory elements, and assaying mutations in these elements for loss of rhythmicity *in vitro* and *in vivo*.

Another interesting possibility that has not been examined is if rhythmic ribosomal occupancy of mRNA provides a mechanism to control the peak phase of protein accumulation. In the future, to examine translational regulation of phase control, candidate genes that display a discordance between rhythmic mRNA peaks and peaks in ribosome occupancy can be selected. For each of these candidates, transcriptional and translational luciferase fusions in WT, Δ*frq*, and Δ*rck-2* strains can be generated and used to validate the phases of the mRNA rhythm and the protein rhythm. In cases where changes in phase that are dependent on eEF-2 phosphorylation rhythms are validated, possible signature motifs that confer delays in translation rates associated with elongation can be screened. If found, these motifs can be mutated to validate their role in phase regulation, and once confirmed, used to screen the remainder of the genome. For example, if the majority of genes showing phase shifts between the mRNA and protein have an unusual codon bias (168), mutants in which the codon bias in one of these genes is altered could be assessed for changes in the phase of rhythmic protein accumulation relative to the mRNA.

Lastly, I would like to comment on the technical limitations of analyses of genome-wide rhythmic RNA and ribosome occupancy studies. While the development of next-generation sequencing has revolutionized and accelerated studies of global gene regulation, problems in statistical analyses due to depth of sequence analyses, limitations in the numbers of replicates and time points can greatly limit the usefulness of the results. To try to overcome these issues, John Hogenesh's group has carried out

computational simulations on RNA-seq data to create standards for the field (144). They found that 2 h sampling resolution over 2 consecutive days increases the number of identified rhythmic transcripts and results in fewer false positives. Unfortunately, we were unable to sample this often due to the cost of the experiments. Thus, new bioinformatics tools are needed to overcome such limitations in experimental design, and low sequence depth inherent in ribosome profiling data.

In summary, components of translation, stress response pathways, and the circadian clock are all highly conserved. This work offers fundamental insights into mRNA translational regulation due to osmotic stress, light response, and control by the clock, providing a platform to extend these studies into mammalian stress response pathways and clocks. Determining the effects of the stress response proteome and circadian proteome will lead to a better understanding of how cellular metabolism is regulated, and may lead to a better understanding of how clock defects in humans can lead to heart disease and cancer, and could help predict drug targets that would benefit from selected time of day administration.

REFERENCES

1. Dunlap JC (1999) Molecular bases for circadian clocks. *Cell* 96(2):271-290.
2. Karlsson B, Knutsson A, & Lindahl B (2001) Is there an association between shift work and having a metabolic syndrome? Results from a population based study of 27,485 people. *Occupational and Environmental Medicine* 58(11):747-752.
3. Ishida N (2007) Circadian clock, cancer and lipid metabolism. *Neuroscience Research* 57(4):483-490.
4. DeMarian JJ (1729) Observation botanique. *L'Histoire de l'Academie Royale Scientifique*:47-48.
5. Dunlap JC, Loros JJ, & DeCoursey PJ. (2004). Chronobiology: Biological timekeeping. Sunderland, MA: Sinauer Associates, Inc.
6. Bell-Pedersen D, *et al.* (2005) Circadian rhythms from multiple oscillators: Lessons from diverse organisms. *Nat Rev Genet* 6(7):544-556.
7. Liu Y & Bell-Pedersen D (2006) Circadian rhythms in Neurospora crassa and other filamentous fungi. *Eukaryotic Cell* 5(8):1184-1193.
8. Ballario P, *et al.* (1996) White collar-1, a central regulator of blue light responses in Neurospora, is a zinc finger protein. *Embo J* 15(7):1650-1657.
9. Ballario P, Talora C, Galli D, Linden H, & Macino G (1998) Roles in dimerization and blue light photoresponse of the PAS and LOV domains of Neurospora crassa white collar proteins. *Molecular Microbiology* 29(3):719-729.

10. Sommer T, Chambers JA, Eberle J, Lauter FR, & Russo VE (1989) Fast light-regulated genes of Neurospora crassa. *Nucleic Acids Research* 17(14):5713-5723.

11. Froehlich AC, Liu Y, Loros JJ, & Dunlap JC (2002) White Collar-1, a circadian blue light photoreceptor, binding to the frequency promoter. *Science* 297(5582):815-819.

12. Linden H & Macino G (1997) White collar 2, a partner in blue-light signal transduction, controlling expression of light-regulated genes in Neurospora crassa. *Embo J* 16(1):98-109.

13. Crosthwaite SK, Dunlap JC, & Loros JJ (1997) Neurospora wc-1 and wc-2: transcription, photoresponses, and the origins of circadian rhythmicity. *Science* 276(5313):763-769.

14. Diernfellner A, *et al.* (2007) Long and short isoforms of Neurospora clock protein FRQ support temperature-compensated circadian rhythms. *FEBS Lett* 581(30):5759-5764.

15. Hurley JM, Larrondo LF, Loros JJ, & Dunlap JC (2013) Conserved RNA helicase FRH acts nonenzymatically to support the intrinsically disordered neurospora clock protein FRQ. *Molecular Cell* 52(6):832-843.

16. Querfurth C, *et al.* (2007) Posttranslational regulation of Neurospora circadian clock by CK1a-dependent phosphorylation. *Cold Spring Harb Symp Quant Biol* 72:177-183.

17. He Q, *et al.* (2003) FWD1-mediated degradation of FREQUENCY in Neurospora establishes a conserved mechanism for circadian clock regulation. *Embo J* 22(17):4421-4430.

18. Brunner M & Schafmeier T (2006) Transcriptional and post-transcriptional regulation of the circadian clock of cyanobacteria and Neurospora. *Genes Dev* 20(9):1061-1074.

19. Schafmeier T, *et al.* (2005) Transcriptional feedback of Neurospora circadian clock gene by phosphorylation-dependent inactivation of its transcription factor. *Cell* 122(2):235-246.

20. Smith KM, *et al.* (2010) Transcription factors in light and circadian clock signaling networks revealed by genomewide mapping of direct targets for neurospora white collar complex. *Eukaryotic Cell* 9(10):1549-1556.

21. Coulthard LR, White DE, Jones DL, McDermott MF, & Burchill SA (2009) p38(MAPK): Stress responses from molecular mechanisms to therapeutics. *Trends Mol Med* 15(8):369-379.

22. Vitalini MW, *et al.* (2007) Circadian rhythmicity mediated by temporal regulation of the activity of p38 MAPK. *Proceedings of the National Academy of Sciences of the United States of America* 104(46):18223-18228.

23. Woelfle MA, Ouyang Y, Phanvijhitsiri K, & Johnson CH (2004) The adaptive value of circadian clocks: An experimental assessment in cyanobacteria. *Current Biology : CB* 14(16):1481-1486.

24. Dodd AN, *et al.* (2005) Plant circadian clocks increase photosynthesis, growth, survival, and competitive advantage. *Science* 309(5734):630-633.

25. Lamb TM, Goldsmith CS, Bennett L, Finch KE, & Bell-Pedersen D (2011) Direct transcriptional control of a p38 MAPK pathway by the circadian clock in Neurospora crassa. *Plos One* 6(11).

26. Lamb TM, Finch KE, & Bell-Pedersen D (2012) The Neurospora crassa OS MAPK pathway-activated transcription factor ASL-1 contributes to circadian rhythms in pathway responsive clock-controlled genes. *Fungal Genet Biol* 49(2):180-188.

27. Vitalini MW, de Paula RM, Park WD, & Bell-Pedersen D (2006) The rhythms of life: Circadian output pathways in Neurospora. *Journal of Biological Rhythms* 21(6):432-444.

28. Koike N, *et al.* (2012) Transcriptional architecture and chromatin landscape of the core circadian clock in mammals. *Science* 338(6105):349-354.

29. Menet JS, Rodriguez J, Abruzzi KC, & Rosbash M (2012) Nascent-Seq reveals novel features of mouse circadian transcriptional regulation. *Elife* 1:e00011.

30. Duffield GE (2003) DNA microarray analyses of circadian timing: The genomic basis of biological time. *J Neuroendocrinol* 15(10):991-1002.

31. Partch CL, Green CB, & Takahashi JS (2014) Molecular architecture of the mammalian circadian clock. *Trends Cell Biol* 24(2):90-99.

32. Nagel DH & Kay SA (2012) Complexity in the wiring and regulation of plant circadian networks. *Current Biology : CB* 22(16):R648-657.

33. Kojima S, Shingle DL, & Green CB (2011) Post-transcriptional control of circadian rhythms. *J Cell Sci* 124(Pt 3):311-320.

34. Staiger D & Koster T (2011) Spotlight on post-transcriptional control in the circadian system. *Cell Mol Life Sci* 68(1):71-83.

35. Belanger V, Picard N, & Cermakian N (2006) The circadian regulation of Presenilin-2 gene expression. *Chronobiol Int* 23(4):747-766.

36. Robinson BG, Frim DM, Schwartz WJ, & Majzoub JA (1988) Vasopressin mRNA in the suprachiasmatic nuclei: Daily regulation of polyadenylate tail length. *Science* 241(4863):342-344.

37. Cagampang FR, Yang J, Nakayama Y, Fukuhara C, & Inouye ST (1994) Circadian variation of arginine-vasopressin messenger RNA in the rat suprachiasmatic nucleus. *Brain Res Mol Brain Res* 24(1-4):179-184.

38. Baggs JE & Green CB (2003) Nocturnin, a deadenylase in Xenopus laevis retina: A mechanism for posttranscriptional control of circadian-related mRNA. *Current Biology : CB* 13(3):189-198.

39. Garbarino-Pico E, *et al.* (2007) Immediate early response of the circadian polyA ribonuclease nocturnin to two extracellular stimuli. *Rna* 13(5):745-755.

40. Reddy AB, *et al.* (2006) Circadian orchestration of the hepatic proteome. *Current Biology : CB* 16(11):1107-1115.

41. Jouffe C, *et al.* (2013) The circadian clock coordinates ribosome biogenesis. *PLoS Biology* 11(1):e1001455.

42. Robles MS, Cox J, & Mann M (2014) In-vivo quantitative proteomics reveals a key contribution of post-transcriptional mechanisms to the circadian regulation of liver metabolism. *PLoS Genet* 10(1):e1004047.

43. Atger F, *et al.* (2015) Circadian and feeding rhythms differentially affect rhythmic mRNA transcription and translation in mouse liver. *Proceedings of the National Academy of Sciences of the United States of America* 112(47):E6579-6588.

44. van Ooijen G & Millar AJ (2012) Non-transcriptional oscillators in circadian timekeeping. *Trends Biochem Sci* 37(11):484-492.

45. Mittag M, Lee DH, & Hastings JW (1994) Circadian expression of the luciferin-binding protein correlates with the binding of a protein to the 3' untranslated region of its mRNA. *Proceedings of the National Academy of Sciences of the United States of America* 91(12):5257-5261.

46. Huang Y, Genova G, Roberts M, & Jackson FR (2007) The LARK RNA-binding protein selectively regulates the circadian eclosion rhythm by controlling E74 protein expression. *Plos One* 2(10):e1107.

47. Lee K, Loros JJ, & Dunlap JC (2000) Interconnected feedback loops in the Neurospora circadian system. *Science* 289(5476):107-110.

48. Zhang Y, Lamm R, Pillonel C, Lam S, & Xu JR (2002) Osmoregulation and fungicide resistance: The Neurospora crassa os-2 gene encodes a HOG1 mitogen-activated protein kinase homologue. *Applied and Environmental Microbiology* 68(2):532-538.

49. Bilsland-Marchesan E, Arino J, Saito H, Sunnerhagen P, & Posas F (2000) Rck2 kinase is a substrate for the osmotic stress-activated mitogen-activated protein kinase Hog1. *Molecular and Cellular Biology* 20(11):3887-3895.

50. Teige M, Scheikl E, Reiser V, Ruis H, & Ammerer G (2001) Rck2, a member of the calmodulin-protein kinase family, links protein synthesis to high osmolarity MAP kinase signaling in budding yeast. *Proceedings of the National Academy of Sciences of the United States of America* 98(10):5625-5630.

51. Swaminathan S, Masek T, Molin C, Pospisek M, & Sunnerhagen P (2006) Rck2 is required for reprogramming of ribosomes during oxidative stress. *Molecular Biology of the Cell* 17(3):1472-1482.

52. Warringer J, Hult M, Regot S, Posas F, & Sunnerhagen P (2010) The HOG pathway dictates the short-term translational response after hyperosmotic shock. *Molecular Biology of the Cell* 21(17):3080-3092.

53. Kaul G, Pattan G, & Rafeequi T (2011) Eukaryotic elongation factor-2 (eEF2): Its regulation and peptide chain elongation. *Cell Biochem Funct* 29(3):227-234.

54. Nakamura J, *et al.* (2009) Overexpression of eukaryotic elongation factor eEF2 in gastrointestinal cancers and its involvement in G2/M progression in the cell cycle. *Int J Oncol* 34(5):1181-1189.

55. Chen CY, *et al.* (2011) Sumoylation of eukaryotic elongation factor 2 is vital for protein stability and anti-apoptotic activity in lung adenocarcinoma cells. *Cancer Sci* 102(8):1582-1589.

56. Bagaglio DM, *et al.* (1993) Phosphorylation of elongation factor 2 in normal and malignant rat glial cells. *Cancer Research* 53(10 Suppl):2260-2264.

57. Parmer TG, *et al.* (1999) Activity and regulation by growth factors of calmodulin-dependent protein kinase III (elongation factor 2-kinase) in human breast cancer. *Br J Cancer* 79(1):59-64.

58. Calberg U, Nilsson A, Skog S, Palmquist K, & Nygard O (1991) Increased activity of the eEF-2 specific, Ca2+ and calmodulin dependent protein kinase III during the S-phase in Ehrlich ascites cells. *Biochemical and Biophysical Research Communications* 180(3):1372-1376.

59. Bagaglio DM & Hait WN (1994) Role of calmodulin-dependent phosphorylation of elongation factor 2 in the proliferation of rat glial cells. *Cell Growth Differ* 5(12):1403-1408.

60. Celis JE, Madsen P, & Ryazanov AG (1990) Increased phosphorylation of elongation factor 2 during mitosis in transformed human amnion cells correlates with a decreased rate of protein synthesis. *Proceedings of the National Academy of Sciences of the United States of America* 87(11):4231-4235.

61. Park S, *et al.* (2008) Elongation factor 2 and fragile X mental retardation protein control the dynamic translation of Arc/Arg3.1 essential for mGluR-LTD. *Neuron* 59(1):70-83.

62. Weatherill DB, *et al.* (2011) Compartment-specific, differential regulation of eukaryotic elongation factor 2 and its kinase within Aplysia sensory neurons. *J Neurochem* 117(5):841-855.

63. Sudo T, Kawai K, Matsuzaki H, & Osada H (2005) p38 mitogen-activated protein kinase plays a key role in regulating MAPKAPK2 expression. *Biochemical and Biophysical Research Communications* 337(2):415-421.

64. Redpath NT, Foulstone EJ, & Proud CG (1996) Regulation of translation elongation factor-2 by insulin via a rapamycin-sensitive signalling pathway. *Embo J* 15(9):2291-2297.

65. Perentesis JP, *et al.* (1992) Saccharomyces cerevisiae elongation factor 2. Genetic cloning, characterization of expression, and G-domain modeling. *J Biol Chem* 267(2):1190-1197.

66. Redpath NT, Price NT, Severinov KV, & Proud CG (1993) Regulation of elongation factor-2 by multisite phosphorylation. *European Journal of Biochemistry / FEBS* 213(2):689-699.

67. Ruys SPD, *et al.* (2012) Identification of autophosphorylation sites in eukaryotic elongation factor-2 kinase. *Biochem J* 442:681-692.

68. Knebel A, Haydon CE, Morrice N, & Cohen P (2002) Stress-induced regulation of eukaryotic elongation factor 2 kinase by SB 203580-sensitive and -insensitive pathways. *Biochem J* 367(Pt 2):525-532.

69. Hizli AA, *et al.* (2013) Phosphorylation of eukaryotic elongation factor 2 (eEF2) by cyclin A-cyclin-dependent kinase 2 regulates its inhibition by eEF2 kinase. *Molecular and Cellular Biology* 33(3):596-604.

70. Hurley JM, *et al.* (2014) Analysis of clock-regulated genes in Neurospora reveals widespread posttranscriptional control of metabolic potential. *Proceedings of the National Academy of Sciences of the United States of America* 111(48):16995-17002.

71. Sancar C, Sancar G, Ha N, Cesbron F, & Brunner M (2015) Dawn- and dusk-phased circadian transcription rhythms coordinate anabolic and catabolic functions in Neurospora. *BMC Biol* 13:17.

72. Zhang R, Lahens NF, Ballance HI, Hughes ME, & Hogenesch JB (2014) A circadian gene expression atlas in mammals: implications for biology and medicine. *Proceedings of the National Academy of Sciences of the United States of America* 111(45):16219-16224.

73. Beckwith EJ & Yanovsky MJ (2014) Circadian regulation of gene expression: At the crossroads of transcriptional and post-transcriptional regulatory networks. *Current Opinion in Genetics & Development* 27:35-42.

74. Lipton JO, *et al.* (2015) The Circadian Protein BMAL1 Regulates translation in response to S6K1-mediated phosphorylation. *Cell* 161(5):1138-1151.

75. Cheng P, He Q, He Q, Wang L, & Liu Y (2005) Regulation of the Neurospora circadian clock by an RNA helicase. *Genes & Development* 19(2):234-241.

76. He Q, Cha J, Lee HC, Yang Y, & Liu Y (2006) CKI and CKII mediate the FREQUENCY-dependent phosphorylation of the WHITE COLLAR complex to close the Neurospora circadian negative feedback loop. *Genes & Development* 20(18):2552-2565.

77. Schafmeier T, Kaldi K, Diernfellner A, Mohr C, & Brunner M (2006) Phosphorylation-dependent maturation of Neurospora circadian clock protein from a nuclear repressor toward a cytoplasmic activator. *Genes & Development* 20(3):297-306.

78. Heintzen C & Liu Y (2007) The Neurospora crassa circadian clock. *Advances in Genetics* 58:25-66.

79. Froehlich AC, Loros JJ, & Dunlap JC (2003) Rhythmic binding of a WHITE COLLAR-containing complex to the frequency promoter is inhibited by FREQUENCY. *Proceedings of the National Academy of Sciences of the United States of America* 100(10):5914-5919.

80. Bilsland E, Molin C, Swaminathan S, Ramne A, & Sunnerhagen P (2004) Rck1 and Rck2 MAPKAP kinases and the HOG pathway are required for oxidative stress resistance. *Molecular Microbiology* 53(6):1743-1756.

81. de Paula RM, Lamb TM, Bennett L, & Bell-Pedersen D (2008) A connection between MAPK pathways and circadian clocks. *Cell Cycle* 7(17):2630-2634.

82. Wei J, Zhang Y, Ivanov IP, & Sachs MS (2013) The stringency of start codon selection in the filamentous fungus Neurospora crassa. *J Biol Chem* 288(13):9549-9562.

83. Wang Z, Fang P, & Sachs MS (1998) The evolutionarily conserved eukaryotic arginine attenuator peptide regulates the movement of ribosomes that have translated it. *Molecular and Cellular Biology* 18(12):7528-7536.

84. Yu CH, *et al.* (2015) Codon usage influences the local rate of translation elongation to regulate co-translational protein folding. *Molecular Cell* 59(5):744-754.

85. Tunon MJ, Gonzalez P, Lopez P, Salido GM, & Madrid JA (1992) Circadian rhythms in glutathione and glutathione-S transferase activity of rat liver. *Arch Int Physiol Biochim Biophys* 100(1):83-87.

86. Cao R, *et al.* (2015) Light-regulated translational control of circadian behavior by eIF4E phosphorylation. *Nature Neuroscience* 18(6):855-862.

87. Cao R, *et al.* (2013) Translational control of entrainment and synchrony of the suprachiasmatic circadian clock by mTOR/4E-BP1 signaling. *Neuron* 79(4):712-724.

88. Cornu M, *et al.* (2014) Hepatic mTORC1 controls locomotor activity, body temperature, and lipid metabolism through FGF21. *Proceedings of the National Academy of Sciences of the United States of America* 111(32):11592-11599.

89. Lim C & Allada R (2013) ATAXIN-2 activates PERIOD translation to sustain circadian rhythms in Drosophila. *Science* 340(6134):875-879.

90. Zhang Y, Ling J, Yuan C, Dubruille R, & Emery P (2013) A role for Drosophila ATX2 in activation of PER translation and circadian behavior. *Science* 340(6134):879-882.

91. Bradley S, Narayanan S, & Rosbash M (2012) NAT1/DAP5/p97 and atypical translational control in the Drosophila Circadian Oscillator. *Genetics* 192(3):943-957.

92. Morf J, *et al.* (2012) Cold-inducible RNA-binding protein modulates circadian gene expression posttranscriptionally. *Science* 338(6105):379-383.

93. Kojima S, *et al.* (2007) LARK activates posttranscriptional expression of an essential mammalian clock protein, PERIOD1. *Proceedings of the National Academy of Sciences of the United States of America* 104(6):1859-1864.

94. Aitken CE & Lorsch JR (2012) A mechanistic overview of translation initiation in eukaryotes. *Nature Structural & Molecular Biology* 19(6):568-576.

95. Richter JD & Coller J (2015) Pausing on polyribosomes: Make way for elongation in translational control. *Cell* 163(2):292-300.

96. Liu B & Qian SB (2014) Translational reprogramming in cellular stress response. *Wiley Interdiscip Rev RNA* 5(3):301-315.

97. Zarubin T & Han J (2005) Activation and signaling of the p38 MAP kinase pathway. *Cell Research* 15(1):11-18.

98. Knebel A, Morrice N, & Cohen P (2001) A novel method to identify protein kinase substrates: EEF2 kinase is phosphorylated and inhibited by SAPK4/p38delta. *The EMBO Journal* 20(16):4360-4369.

99. Redpath NT, Foulstone EJ, & Proud CG (1996) Regulation of translation elongation factor-2 by insulin via a rapamycin-sensitive signalling pathway. *The EMBO Journal* 15(9):2291-2297.

100. Wang X, *et al.* (2001) Regulation of elongation factor 2 kinase by p90(RSK1) and p70 S6 kinase. *The EMBO Journal* 20(16):4370-4379.

101. Althausen S, *et al.* (2001) Changes in the phosphorylation of initiation factor eIF-2alpha, elongation factor eEF-2 and p70 S6 kinase after transient focal cerebral ischaemia in mice. *Journal of Neurochemistry* 78(4):779-787.

102. Browne GJ, Finn SG, & Proud CG (2004) Stimulation of the AMP-activated protein kinase leads to activation of eukaryotic elongation factor 2 kinase and to its phosphorylation at a novel site, serine 398. *The Journal of Biological Chemistry* 279(13):12220-12231.

103. Horman S, *et al.* (2002) Activation of AMP-activated protein kinase leads to the phosphorylation of elongation factor 2 and an inhibition of protein synthesis. *Current Biology : CB* 12(16):1419-1423.

104. Redpath NT & Proud CG (1993) Cyclic AMP-dependent protein kinase phosphorylates rabbit reticulocyte elongation factor-2 kinase and induces calcium-independent activity. *The Biochemical Journal* 293 (Pt 1):31-34.

105. Williams JA, Su HS, Bernards A, Field J, & Sehgal A (2001) A circadian output in Drosophila mediated by neurofibromatosis-1 and Ras/MAPK. *Science* 293(5538):2251-2256.

106. Hayashi Y, Sanada K, Hirota T, Shimizu F, & Fukada Y (2003) p38 Mitogen-activated Protein Kinase Regulates Oscillation of Chick Pineal Circadian Clock. *J. Biol. Chem.* 278(27):25166-25171.

107. Pizzio G, Hainich E, Ferreyra G, Coso O, & Golombek D (2003) Circadian and photic regulation of ERK, JNK and p38 in the hamster SCN. *Neurochemistry* 14(2):1417-1419.

108. Cao R, Anderson FE, Jung YJ, Dziema H, & Obrietan K (2011) Circadian regulation of mammalian target of rapamycin signaling in the mouse suprachiasmatic nucleus. *Neuroscience* 181:79-88.

109. Nikaido SS & Takahashi JS (1998) Day/night differences in the stimulation of adenylate cyclase activity by calcium/calmodulin in chick pineal cell cultures: evidence for circadian regulation of cyclic AMP. *Journal of Biological Rhythms* 13(6):479-493.

110. Lamia KA, *et al.* (2009) AMPK regulates the circadian clock by cryptochrome phosphorylation and degradation. *Science* 326(5951):437-440.

111. Janich P, Arpat AB, Castelo-Szekely V, Lopes M, & Gatfield D (2015) Ribosome profiling reveals the rhythmic liver translatome and circadian clock regulation by upstream open reading frames. *Genome Research* 25(12):1848-1859.

112. Jang C, Lahens NF, Hogenesch JB, & Sehgal A (2015) Ribosome profiling reveals an important role for translational control in circadian gene expression. *Genome Research* 25(12):1836-1847.

113. Bass J (2012) Circadian topology of metabolism. *Nature* 491(7424):348-356.

114. Froy O (2013) Circadian aspects of energy metabolism and aging. *Ageing Research Reviews* 12(4):931-940.

115. Burkeen JF, Womac AD, Earnest DJ, & Zoran MJ (2011) Mitochondrial calcium signaling mediates rhythmic extracellular ATP accumulation in suprachiasmatic nucleus astrocytes. *The Journal of Neuroscience : The Official Journal of the Society for Neuroscience* 31(23):8432-8440.

116. Yamazaki S, Ishida Y, & Inouye S (1994) Circadian rhythms of adenosine triphosphate contents in the suprachiasmatic nucleus, anterior hypothalamic area and caudate putamen of the rat--negative correlation with electrical activity. *Brain Research* 664(1-2):237-240.

117. Marpegan L, *et al.* (2011) Circadian regulation of ATP release in astrocytes. *The Journal of Neuroscience : The Official Journal of the Society for Neuroscience* 31(23):8342-8350.

118. Lakin-Thomas PL, Bell-Pedersen D, & Brody S (2011) The genetics of circadian rhythms in Neurospora. *Adv Genet* 74:55-103.

119. Loros JJ, Denome SA, & Dunlap JC (1989) Molecular cloning of genes under control of the circadian clock in Neurospora. *Science* 243(4889):385-388.

120. Honda S & Selker EU (2009) Tools for fungal proteomics: multifunctional neurospora vectors for gene replacement, protein expression and protein purification. *Genetics* 182(1):11-23.

121. Gooch VD, *et al.* (2008) Fully codon-optimized luciferase uncovers novel temperature characteristics of the Neurospora clock. *Eukaryotic Cell* 7(1):28-37.

122. Garceau NY, Liu Y, Loros JJ, & Dunlap JC (1997) Alternative initiation of translation and time-specific phosphorylation yield multiple forms of the essential clock protein FREQUENCY. *Cell* 89(3):469-476.

123. Davis RH & de Serres FJ (1970) Genetic and microbiological research techniques for Neurospora crassa. *Methods in Enzymology* 17:79-143.

124. Wang Z & Sachs MS (1997) Arginine-specific regulation mediated by the Neurospora crassa arg-2 upstream open reading frame in a homologous, cell-free in vitro translation system. *J Biol Chem* 272(1):255-261.

125. Zeenko VV, *et al.* (2008) An efficient in vitro translation system from mammalian cells lacking the translational inhibition caused by eIF2 phosphorylation. *Rna* 14(3):593-602.

126. Dyer BW, Ferrer FA, Klinedinst DK, & Rodriguez R (2000) A noncommercial dual luciferase enzyme assay system for reporter gene analysis. *Analytical Biochemistry* 282(1):158-161.

127. Larrondo LF, Olivares-Yanez C, Baker CL, Loros JJ, & Dunlap JC (2015) Circadian rhythms. Decoupling circadian clock protein turnover from circadian period determination. *Science* 347(6221):1257277.

128. Bennett LD, Beremand P, Thomas TL, & Bell-Pedersen D (2013) Circadian activation of the mitogen-activated protein kinase MAK-1 facilitates rhythms in clock-controlled genes in Neurospora crassa. *Eukaryotic Cell* 12(1):59-69.

129. Waskiewicz AJ & Cooper JA (1995) Mitogen and stress response pathways: MAP kinase cascades and phosphatase regulation in mammals and yeast. *Curr Opin Cell Biol* 7(6):798-805.

130. Fulda S, Gorman AM, Hori O, & Samali A (2010) Cellular stress responses: Cell survival and cell death. *Int J Cell Biol* 2010:214074.

131. Idnurm A & Heitman J (2005) Light controls growth and development via a conserved pathway in the fungal kingdom. *PLoS Biology* 3(4):e95.

132. de Nadal E, Ammerer G, & Posas F (2011) Controlling gene expression in response to stress. *Nat Rev Genet* 12(12):833-845.

133. Young MW & Kay SA (2001) Time zones: A comparative genetics of circadian clocks. *Nat Rev Genet* 2(9):702-715.

134. Wu C, *et al.* (2014) Genome-wide characterization of light-regulated genes in Neurospora crassa. *G3* 4(9):1731-1745.

135. Trapnell C, *et al.* (2012) Differential gene and transcript expression analysis of RNA-seq experiments with TopHat and Cufflinks. *Nature Protocols* 7(3):562-578.

136. Lauter FR & Russo VE (1991) Blue light induction of conidiation-specific genes in Neurospora crassa. *Nucleic Acids Research* 19(24):6883-6886.

137. Ingolia NT, Ghaemmaghami S, Newman JR, & Weissman JS (2009) Genome-wide analysis in vivo of translation with nucleotide resolution using ribosome profiling. *Science* 324(5924):218-223.

138. Hughes ME, Hogenesch JB, & Kornacker K (2010) JTK_CYCLE: an efficient nonparametric algorithm for detecting rhythmic components in genome-scale data sets. *Journal of Biological Rhythms* 25(5):372-380.

139. Noguchi R, *et al.* (2007) Identification of OS-2 MAP kinase-dependent genes induced in response to osmotic stress, antifungal agent fludioxonil, and heat shock in Neurospora crassa. *Fungal Genet Biol* 44(3):208-218.

140. Freitas FZ, *et al.* (2016) The SEB-1 Transcription Factor Binds to the STRE Motif in Neurospora crassa and Regulates a Variety of Cellular Processes Including the Stress Response and Reserve Carbohydrate Metabolism. *G3* 6(5):1327-1343.

141. Rajasekhar VK, *et al.* (2003) Oncogenic Ras and Akt signaling contribute to glioblastoma formation by differential recruitment of existing mRNAs to polysomes. *Molecular Cell* 12(4):889-901.

142. Halbeisen RE & Gerber AP (2009) Stress-dependent coordination of transcriptome and translatome in yeast. *PLoS Biology* 7(5):e1000105.

143. He Q & Liu Y (2005) Molecular mechanism of light responses in Neurospora: from light-induced transcription to photoadaptation. *Genes Dev* 19(23):2888-2899.

144. Li J, Grant GR, Hogenesch JB, & Hughes ME (2015) Considerations for RNA-seq analysis of circadian rhythms. *Methods Enzymol* 551:349-367.

145. Luck S & Westermark PO (2016) Circadian mRNA expression: Insights from modeling and transcriptomics. *Cell Mol Life Sci* 73(3):497-521.

146. Thaben PF & Westermark PO (2016) Differential rhythmicity: Detecting altered rhythmicity in biological data. *Bioinformatics*.

147. Sachs MS & Yanofsky C (1991) Developmental expression of genes involved in conidiation and amino acid biosynthesis in Neurospora crassa. *Dev Biol* 148(1):117-128.

148. Yarden O, Plamann M, Ebbole DJ, & Yanofsky C (1992) cot-1, a gene required for hyphal elongation in Neurospora crassa, encodes a protein kinase. *Embo J* 11(6):2159-2166.

149. Ingolia NT, Brar GA, Rouskin S, McGeachy AM, & Weissman JS (2012) The ribosome profiling strategy for monitoring translation in vivo by deep sequencing of ribosome-protected mRNA fragments. *Nature Protocols* 7(8):1534-1550.

150. Bortner CD, Scoltock AB, Sifre MI, & Cidlowski JA (2012) Osmotic stress resistance imparts acquired anti-apoptotic mechanisms in lymphocytes. *J Biol Chem* 287(9):6284-6295.

151. Dmitrieva NI, Michea LF, Rocha GM, & Burg MB (2001) Cell cycle delay and apoptosis in response to osmotic stress. *Comp Biochem Physiol A Mol Integr Physiol* 130(3):411-420.

152. Redpath NT & Proud CG (1989) The tumour promoter okadaic acid inhibits reticulocyte-lysate protein synthesis by increasing the net phosphorylation of elongation factor 2. *Biochem J* 262(1):69-75.

153. Gschwendt M, Kittstein W, Mieskes G, & Marks F (1989) A type 2A protein phosphatase dephosphorylates the elongation factor 2 and is stimulated by the phorbol ester TPA in mouse epidermis in vivo. *FEBS Lett* 257(2):357-360.

154. Yang Y, *et al.* (2004) Distinct roles for PP1 and PP2A in the Neurospora circadian clock. *Genes Dev* 18(3):255-260.

155. Apel K & Hirt H (2004) Reactive oxygen species: Metabolism, oxidative stress, and signal transduction. *Annu Rev Plant Biol* 55:373-399.

156. Ha H & Lee HB (2000) Reactive oxygen species as glucose signaling molecules in mesangial cells cultured under high glucose. *Kidney Int Suppl* 77:S19-25.

157. Sharma VK (2003) Adaptive significance of circadian clocks. *Chronobiol Int* 20(6):901-919.

158. Kyriacou CP & Hastings MH (2010) Circadian clocks: Genes, sleep, and cognition. *Trends Cogn Sci* 14(6):259-267.

159. Green CB, Takahashi JS, & Bass J (2008) The meter of metabolism. *Cell* 134(5):728-742.

160. Froy O (2010) Metabolism and circadian rhythms--implications for obesity. *Endocr Rev* 31(1):1-24.

161. Kovac J, Husse J, & Oster H (2009) A time to fast, a time to feast: The crosstalk between metabolism and the circadian clock. *Mol Cells* 28(2):75-80.

162. Miki T, Matsumoto T, Zhao Z, & Lee CC (2013) p53 regulates Period2 expression and the circadian clock. *Nat Commun* 4:2444.

163. Antoch MP & Kondratov RV (2010) Circadian proteins and genotoxic stress response. *Circ Res* 106(1):68-78.

164. Karatsoreos IN (2012) Effects of circadian disruption on mental and physical health. *Curr Neurol Neurosci Rep* 12(2):218-225.

165. Griffett K & Burris TP (2013) The mammalian clock and chronopharmacology. *Bioorg Med Chem Lett* 23(7):1929-1934.

166. Proietto M, Bianchi MM, Ballario P, & Brenna A (2015) Epigenetic and posttranslational modifications in light signal transduction and the circadian clock in Neurospora crassa. *Int J Mol Sci* 16(7):15347-15383.

167. Liu Y (2005) Analysis of posttranslational regulations in the Neurospora circadian clock. *Methods Enzymol* 393:379-393.

168. Zhou M, *et al.* (2013) Non-optimal codon usage affects expression, structure and function of clock protein FRQ. *Nature* 495(7439):111-115.

APPENDIX A

Table A1. Strains used for this study.

Strain	Genotype	Cross	FGSC#	DBP#	Reference
Wild type	*mat A*, 74-OR23-IV		2489		
Wild type	*mat a*, 74-OR23-IV		4200		
ras-1^{bd}	*mat A, ras-1^{bd}*		1858		
Δ*mus-51*	*mat a*, Δ*mus-51::bar^{+}*		9718		
Δ*os-2*	*mat A*, Δ*os-2::hph*		17933		
Δ*frq*	*mat A*, Δ*frq:: bar^{+}*			1228	Bennett et al, 2013
Δ*frq*	*mat A, ras-1^{bd}* Δ*frq:: hph*		7490		
Δ*rck-2*	*mat A*, Δ*rck-2:: hph*		11545		
Δ*rck-2*	*mat A, ras-1^{bd}* Δ*rck-2:: hph*	FGSC11545 x FGSC1858		1116	This study
Δ*rck-2*, Δ*os-2*	*mat A*, Δ*rck-2:: hph*, Δ*os-2:: hph*	DBP1116 x FGSC17933		1394	This study
RCK-2::HA	*mat A, rck-2::3xHA::hph*	FGSC2489 x FGSC9718		1254	This study
RCK-2::HA	*mat a, rck-2::3xHA::hph*	FGSC2489 x FGSC9718		1255	This study
RCK-2::HA, *ras-1^{bd}*	*mat a, ras-1^{bd}, rck2::3xHA::hph*	FGSC1858 x FGSC9718		1251	This study
RCK-2::HA, Δ*os-2*	*mat a, rck2::3xHA::hph,* Δ*os-2:: hph*	DBP1251 x FGSC17933		1264	This study
RCK-2::HA, Δ*frq*	*mat a, rck2::3xHA::hph,* Δ*frq:: bar^{+}*	DBP1255 x DBP1228		1301	This study

Table A2. Constitutively expressed mRNAs that are induced at the ribosomal occupancy level in WT cells following an osmotic stress.

Locus	Symbol	Name
NCU00264		hypothetical protein
NCU00675		efr-3
NCU00835		hypothetical protein
NCU00855		hypothetical protein
NCU01158		hypothetical protein
NCU01191		hypothetical protein
NCU01215		thioesterase
NCU01312	rca-1	regulator of conidiation in Aspergillus-1
NCU01398		thiol methyltransferase
NCU01417		propionate-CoA ligase
NCU01519		hypothetical protein
NCU01559		hypothetical protein
NCU01741	sna-1	SNARE complex subunit
NCU01808	cyc-1	cytochrome c
NCU01944		hypothetical protein
NCU01981	eif1	translation factor sui1
NCU02176		hypothetical protein
NCU02317		hypothetical protein
NCU02358		SDS23
NCU03202		hypothetical protein
NCU03406		hypothetical protein
NCU03451		hypothetical protein
NCU03693		oxidoreductase
NCU03699		zinc finger containing protein
NCU04043	dyn-4	hypothetical protein
NCU04139		hypothetical protein
NCU04174		hypothetical protein
NCU04289		hypothetical protein
NCU04628		hypothetical protein
NCU04665		hypothetical protein
NCU04718		hypothetical protein
NCU04776		hypothetical protein
NCU04847	div-9	cyclin

Table A2. Continued.

Locus	Symbol	Name
NCU04940		reticulon-4-interacting protein 1
NCU05351		hypothetical protein
NCU05561		copper metallothionein
NCU05624		L-asparaginase
NCU05637		hypothetical protein
NCU06273		hypothetical protein
NCU06467		hypothetical protein
NCU06586		AN1 zinc finger protein
NCU06763		hypothetical protein
NCU06811		hypothetical protein
NCU06928		hypothetical protein
NCU07042		alcohol dehydrogenase
NCU07817	ncw-3	non-anchored cell wall protein-3
NCU07953	aod-1	alternative oxidase-1
NCU08199		6-hydroxy-D-nicotine oxidase
NCU08824	mol-3	molybdopterin binding domain-containing protein
NCU08942		G-patch DNA repair protein
NCU09135		phosphatidylinositol phospholipase C
NCU09169		NmrA family transcriptional regulator
NCU09567		myo-inositol-1(or 4)-monophosphatase
NCU09632		hypothetical protein
NCU09787		hypothetical protein
NCU10125		hypothetical protein
NCU10500		F-box domain-containing protein
NCU10622		hypothetical protein
NCU16323	mito	mitochondrial
NCU16459	mito	mitochondrial
NCU16656	mito	mitochondrial
NCU16688	mito	mitochondrial
NCU16778	mito	mitochondrial
NCU16997	mito	mitochondrial
NCU17216	mito	mitochondrial

Table A3. Constitutively expressed mRNAs that are repressed at the ribosomal occupancy level in WT cells following an osmotic stress.

Locus	Symbol	Name
NCU00010		heavy metal tolerance protein
NCU00064		hypothetical protein
NCU00265		hypothetical protein
NCU00309	wsc2-1	WSC domain-containing protein
NCU00321		hypothetical protein
NCU00401		hypothetical protein
NCU00712	erg-14	3-hydroxy-3-methylglutaryl-coenzyme A reductase
NCU00722		amidohydrolase
NCU00729		hypothetical protein
NCU00738	cdp-2	hypothetical protein
NCU00811		hypothetical protein
NCU00911	gt2-2	polysaccharide synthase Cps1p
NCU01036	sp	DUF907 domain-containing protein
NCU01116	gsl-10	ceramide glucosyltransferase
NCU01119	erg-5	lanosterol synthase
NCU01143	msp-8	DEAD/DEAH box helicase
NCU01253		hypothetical protein
NCU01353	gh16-1	mixed-linked glucanase
NCU01378		acetoacetyl-CoA synthase
NCU01382		hypothetical protein
NCU01418	ccg-6	clock-controlled gene-6
NCU01457		ubiquitin C-terminal hydrolase
NCU01477		hypothetical protein
NCU01720		hypothetical protein
NCU01752	ncw-2	non-anchored cell wall protein-2
NCU01772	rpo-10	DNA-directed RNA polymerase III polypeptide
NCU01910		hypothetical protein
NCU01998		septin
NCU02014		hypothetical protein
NCU02059	39905	endothiapepsin
NCU02073		hypothetical protein
NCU02089		hypothetical protein
NCU02124		dienelactone hydrolase
NCU02184	chit-1	hypothetical protein
NCU02211		hypothetical protein
NCU02247	dim-2	DNA methyltransferase Dim-2
NCU02668		cell wall synthesis protein-Penicillium chrysogenum
NCU02770		hypothetical protein
NCU02940		hypothetical protein
NCU02946		mitochondrial carrier domain-containing protein
NCU02949		hypothetical protein
NCU02965	dno-1	origin recognition complex subunit 1
NCU02994		hypothetical protein
NCU03045		cellular morphogenesis protein

Table A3. Continued.

Locus	Symbol	Name
NCU03497	trm-51	plasma membrane iron permease
NCU03593	kal-1	kaleidoscope-1
NCU03596	chol-7	CRAL/TRIO domain-containing protein
NCU03600		GTP-binding protein EsdC
NCU03686	tah-3	hypothetical protein
NCU03928		hypothetical protein
NCU03955		phospholipase D1
NCU04080	ptr-5	palmitoyltransferase SWF1
NCU04088		hypothetical protein
NCU04092		N-acylethanolamine amidohydrolase
NCU04131		hypothetical protein
NCU04350	chs-7	chitin synthase 6
NCU04352	chs-5	chitin synthase C
NCU04373		hypothetical protein
NCU04468	aap-6	proline-specific permease
NCU04741	dash-7	hypothetical protein
NCU05062		hypothetical protein
NCU05132	gt4-1	hypothetical protein
NCU05137	ncw-1	non-anchored cell wall protein-1
NCU05138	gt25-1	hypothetical protein
NCU05163		hypothetical protein
NCU05294		C6 finger domain-containing protein
NCU05404		endoglucanase
NCU05545		hypothetical protein
NCU05789	gh16-6	secreted glucosidase
NCU05808		serine/threonine protein kinase
NCU05878	gt31-1	hypothetical protein
NCU05895		calcofluor white hypersensitive protein
NCU06007		hypothetical protein
NCU06057	gim-1	GPI mannosyltransferase 1
NCU06085		LCCL domain-containing protein
NCU06182	nrc-1	nonrepressor of conidiation-1
NCU06308	cyt-5	DNA-directed RNA polymerase
NCU06374		multispanning membrane protein
NCU06375		hetallophosphoesterase domain-containing protein
NCU06499		hypothetical protein
NCU06508	com	ophatidylinositol anchor phosphoethanolamine tra
NCU06509		hypothetical protein
NCU06596		hypothetical protein
NCU06722	trp-5	tryptophanyl-tRNA synthetase
NCU06737		hypothetical protein
NCU06781	gh72-2	1,3-beta-glucanosyltransferase Gel2
NCU06870	gsl-1	serine palmitoyl CoA transferase subunit LcbA
NCU06983		hypothetical protein

Table A3. Continued.

Locus	Symbol	Name
NCU07265		hypothetical protein
NCU07277	acw-8	anchored cell wall protein-8
NCU07313		chromosome transmission fidelity protein 18
NCU07359		hypothetical protein
NCU07366		lucosamine-fructose-6-phosphate aminotransferase
NCU07504	apg-11	ajor facilitator superfamily transporter protein MFS
NCU07881		hypothetical protein
NCU07999	gpip-2	GPI ethanolamine phosphate transferase 1
NCU08027		nucleoside diphosphatase
NCU08131	gh13-1	alpha-amylase
NCU08132	gh13-10	alpha-1,3-glucan synthase Ags2
NCU08283		integral membrane channel protein
NCU08343		RGS domain-containing protein
NCU08350		hypothetical protein
NCU08364		choline sulfatase
NCU08391		hypothetical protein
NCU08407		MFS transporter
NCU08425		major facilitator superfamily transporter MFS_1
NCU08606		cell cycle inhibitor Nif1
NCU08610		hypothetical protein
NCU08632		hypothetical protein
NCU08685	ad-6	phosphoribosylformylglycinamidine synthase
NCU08820		hypothetical protein
NCU08855		hypothetical protein
NCU08889		hypothetical protein
NCU08909	gh72-5	beta-1,3-glucanosyltransferase
NCU09104		hypothetical protein
NCU09133	acw-7	hypothetical protein
NCU09313	sec10	exocyst complex component Sec10
NCU09326	gh17-4	hypothetical protein
NCU09492		hypothetical protein
NCU09503		hypothetical protein
NCU09542		impact family protein
NCU09552		topoisomerase 1-associated factor 1
NCU09562		hypothetical protein
NCU09658		hypothetical protein
NCU09874		hypothetical protein
NCU10270		hypothetical protein
NCU11030	cyp450-30	hypothetical protein
NCU16968	mito	mitochondrial
NCU17155	mito	mitochondrial

Table A4. Constitutively expressed mRNAs whose induction at the ribosomal occupancy level requires RCK-2/eEF-2 following an osmotic stress.

Locus	Symbol	Name
NCU00264		hypothetical protein
NCU00855		hypothetical protein
NCU01808	cyc-1	cytochrome c
NCU04139		hypothetical protein
NCU04718		hypothetical protein
NCU05351		hypothetical protein
NCU06811		hypothetical protein
NCU07817	ncw-3	non-anchored cell wall protein-3
NCU07953	aod-1	alternative oxidase-1
NCU09169		NmrA family transcriptional regulator
NCU09567		myo-inositol-1(or 4)-monophosphatase
NCU16778	mito	mitochondrial
NCU16997	mito	mitochondrial

Table A5. Constitutively expressed mRNAs whose repression at the ribosomal occupancy level requires RCK-2/eEF-2 following an osmotic stress.

Locus	Symbol	Name
NCU00309	wsc2-1	WSC domain-containing protein
NCU00401		hypothetical protein
NCU00722		amidohydrolase
NCU00738	cdp-2	hypothetical protein
NCU00911	gt2-2	polysaccharide synthase Cps1p
NCU01036	sp	DUF907 domain-containing protein
NCU01477		hypothetical protein
NCU01720		hypothetical protein
NCU01910		hypothetical protein
NCU01998		septin
NCU02059	39905	endothiapepsin
NCU02124		dienelactone hydrolase
NCU02211		hypothetical protein
NCU02247	dim-2	DNA methyltransferase Dim-2
NCU02770		hypothetical protein
NCU02946		mitochondrial carrier domain-containing protein
NCU03045		cellular morphogenesis protein
NCU03600		GTP-binding protein EsdC
NCU03928		hypothetical protein
NCU03955		phospholipase D1
NCU04080	ptr-5	palmitoyltransferase SWF1
NCU04088		hypothetical protein
NCU04092		N-acylethanolamine amidohydrolase
NCU04131		hypothetical protein
NCU04350	chs-7	chitin synthase 6
NCU04352	chs-5	chitin synthase C
NCU04741	dash-7	hypothetical protein
NCU05132	gt4-1	hypothetical protein

Table A5. Continued.

Locus	Symbol	Name
NCU05163		hypothetical protein
NCU05294		C6 finger domain-containing protein
NCU05545		hypothetical protein
NCU05808		serine/threonine protein kinase
NCU05878	gt31-1	hypothetical protein
NCU06007		hypothetical protein
NCU06085		LCCL domain-containing protein
NCU06374		multispanning membrane protein
NCU06375		metallophosphoesterase domain-containing protein 2
NCU06499		hypothetical protein
NCU06722	trp-5	tryptophanyl-tRNA synthetase
NCU07313		chromosome transmission fidelity protein 18
NCU08027		nucleoside diphosphatase
NCU08132	gh13-10	alpha-1,3-glucan synthase Ags2
NCU08350		hypothetical protein
NCU08364		choline sulfatase
NCU08391		hypothetical protein
NCU08606		cell cycle inhibitor Nif1
NCU08610		hypothetical protein
NCU08909	gh72-5	beta-1,3-glucanosyltransferase
NCU09104		hypothetical protein
NCU09492		hypothetical protein
NCU09503		hypothetical protein
NCU09542		impact family protein
NCU09552		topoisomerase 1-associated factor 1
NCU09562		hypothetical protein
NCU10270		hypothetical protein
NCU11030	cyp450-30	hypothetical protein

Table A6. Constitutively expressed mRNAs that are induced at the ribosomal occupancy level in WT cells following a light pulse.

Locus	Symbol	Name
NCU00204		hypothetical protein
NCU08173		hypothetical protein
NCU05594		L-galactose dehydrogenase
NCU08057		short chain dehydrogenase/reductase
NCU03506		hypothetical protein
NCU08943		3-oxoacyl-(acyl-carrier-protein) reductase
NCU01348		agmatinase
NCU01510		meiotically up-regulated 190 protein
NCU00281	gt1-2	UDP-glucose,sterol transferase
NCU05377		integral membrane protein
NCU07745		hypothetical protein
NCU09830	abc-4	ABC multidrug transporter
NCU01088		hypothetical protein
NCU04635		hypothetical protein
NCU01451		hypothetical protein

Table A7. Constitutively expressed mRNAs that are repressed at the ribosomal occupancy level in WT cells following a light pulse.

Locus	Symbol	Name
NCU08020	pms-1	DNA mismatch repair protein
NCU09356		hypothetical protein
NCU08405		hypothetical protein
NCU01417		propionate-CoA ligase
NCU07339		hypothetical protein
NCU06476		hypothetical protein
NCU03092		nuclear localization sequence binding protein
NCU10045	ce8-1	pectinesterase
NCU02994		hypothetical protein
NCU07736		PEP5
NCU02867		hypothetical protein
NCU09520		hypothetical protein
NCU08228		UDP-glucose dehydrogenase
NCU06132		siderophore iron transporter
NCU09007		hypothetical protein
NCU05704		hypothetical protein
NCU03496		hypothetical protein
NCU04665		hypothetical protein
NCU06061		oxidoreductase
NCU09681		hypothetical protein
NCU07535	sah-3	hypothetical protein

Table A8. List of constitutively expressed mRNAs that have rhythmic ribosomal occupancy in WT cells.

Locus	Symbol	Name	Locus	Symbol	Name
NCU00033		integral membrane protein	NCU01167		hypothetical protein
NCU00050		pyruvate dehydrogenase X component	NCU01184	msp-9	pre-mRNA splicing factor cwc2
NCU00064		hypothetical protein	NCU01212		hypothetical protein
NCU00077	mus-52	mutagen sensitive-52	NCU01213	sod-2	superoxide dismutase-2
NCU00083		hypothetical protein	NCU01243		C6 finger domain-containing protein
NCU00088		4-nitrophenylphosphatase	NCU01272	mpr-6	mitochondrial presequence protease
NCU00133	ctc-1	FACT complex subunit pob-3	NCU01276		N-acetyltransferase 5
NCU00168		1-acylglycerol-3-phosphate O-acyltransferase	NCU01291		hypothetical protein
NCU00193	gt22-1	GPI mannosyltransferase 3	NCU01302		hydrolase
NCU00205		hypothetical protein	NCU01317	crp-45	60S ribosomal protein L12
NCU00210		nuclear cap binding protein subunit 2	NCU01356		hypothetical protein
NCU00251	cpr-7	hypothetical protein	NCU01362		INO80 chromatin remodeling complex
NCU00263		serin endopeptidase	NCU01365		ATP dependent DNA ligase domain-containing protein
NCU00277		hypothetical protein	NCU01382		hypothetical protein
NCU00322		hypothetical protein	NCU01391		hypothetical protein
NCU00346		EBDP2	NCU01411		MFS multidrug resistance transporter
NCU00349		hypothetical protein	NCU01434		hypothetical protein
NCU00356		nucleoside transporter	NCU01459	ts	hypothetical protein
NCU00372		hypothetical protein	NCU01503		pre-rRNA processing protein Tsr1
NCU00373		hypothetical protein	NCU01549		hypothetical protein
NCU00379		hypothetical protein	NCU01563		RNA polymerase II holoenzyme cyclin-like subunit
NCU00424		Spo76 protein	NCU01597		hypothetical protein
NCU00435		SNF7 family protein	NCU01613	pp-2	protein arginine N-methyltransferase HSL7
NCU00438		adenosine deaminase	NCU01614		hypothetical protein
NCU00453	trm-3	sodium/hydrogen exchanger 3	NCU01615		hypothetical protein
NCU00459		hypothetical protein	NCU01640	rpn-4	C2H2 transcription factor
NCU00485		hypothetical protein	NCU01653		hypothetical protein
NCU00488		protein phosphatase PP2A regulatory subunit A	NCU01678		amine oxidase
NCU00559		hypothetical protein	NCU01680	pma-1	plasma membrane ATPase-1
NCU00616		hypothetical protein	NCU01696	paa-2	mRNA cleavage factor complex component Pcf11
NCU00643	ard-1	L-arabinitol 4-dehydrogenase	NCU01697		hypothetical protein
NCU00646		methyltransferase LaeA	NCU01706		MYB DNA-binding domain-containing protein
NCU00648	aap-5	choline transporter	NCU01734		hypothetical protein
NCU00679		hypothetical protein	NCU01750		hypothetical protein
NCU00681		GTPase activating protein	NCU01793		RNA binding domain-containing protein
NCU00721	aap-24	proline-specific permease	NCU01794		hypothetical protein
NCU00727		hypothetical protein	NCU01831		RNA polymerase TFIIH complex subunit Ssl1
NCU00740		hypothetical protein	NCU01835		hypothetical protein
NCU00741		gliotoxin biosynthesis protein GliK	NCU01839	cea-7	carboxylesterase
NCU00755		hypothetical protein	NCU01851		hypothetical protein
NCU00762	gh5-1	endoglucanase 3	NCU01902	chi-1	glucosamine 6-phosphate N-acetyltransferase
NCU00790	hak-1	high affinity potassium transporter-1	NCU01908		hypothetical protein
NCU00795	trm-14	membrane bound cation transporter	NCU01944		hypothetical protein
NCU00833		hypothetical protein	NCU01992	cvc-3	coatomer subunit gamma
NCU00860	trm-37	ZIP family zinc transporter	NCU01994		bZIP transcription factor
NCU00861		hypothetical protein	NCU02034	rid-1	RIP defective
NCU00881	ham-7	hypothetical protein	NCU02055		uridine nucleosidase Urh1
NCU00913	gwt1	GPI-anchored wall transfer protein 1	NCU02067	mdm12	mitochondrial inheritance component mdm12
NCU00931		lysyl-tRNA synthetase	NCU02159		hypothetical protein
NCU00948		hypothetical protein	NCU02160	rac-1	small GTPase RAC
NCU00981		ribosome biogenesis protein nsa-2	NCU02169		hypothetical protein
NCU00992		hypothetical protein	NCU02201		laccase
NCU00995		hypothetical protein	NCU02250	oli	oligomycin-resistant
NCU01010		hypothetical protein	NCU02264	pfo-3	prefoldin subunit 3
NCU01082		hypothetical protein	NCU02272		hypothetical protein
NCU01119	erg-5	lanosterol synthase	NCU02296	aln-1	allantoinase
NCU01121		hypothetical protein	NCU02311		hypothetical protein
NCU01135		hypothetical protein	NCU02315		hypothetical protein
NCU01147		tyrosine decarboxylase	NCU02326		hypothetical protein
NCU01149		cupin domain-containing protein	NCU02353	cpr-3	hypothetical protein

Table A8. Continued.

Locus	Symbol	Name	Locus	Symbol	Name
NCU02355		hypothetical protein	NCU03573	spc-3	hypothetical protein
NCU02362		hypothetical protein	NCU03590		hypothetical protein
NCU02371	rbd2	rhomboid protein 2	NCU03600		GTP-binding protein EsdC
NCU02385		hypothetical protein	NCU03610		NEDD8-conjugating enzyme UBC12
NCU02415		zinc metalloproteinase	NCU03645		hypothetical protein
NCU02428	rbg-24	nucleolar essential protein 1	NCU03719		RING finger protein
NCU02460		syntaxin family protein	NCU03732		SIS1
NCU02482	tca-2	2-methylcitrate synthase	NCU03751		hypothetical protein
NCU02496	div-12	M-phase inducer phosphatase 3	NCU03752		EBP domain-containing protein
NCU02536	coq-6	ubiquinone biosynthesis monooxygenase COQ6	NCU03753	ccg-1	clock controlled protein CCG-1
NCU02559		hypothetical protein	NCU03769	naf-2	hypothetical protein
NCU02561		hypothetical protein	NCU03782		DNA-directed RNA polymerase II subunit RPB11
NCU02578	sin3	paired amphipathic helix protein Sin3a	NCU03804	cna-1	serine/threonine-protein phosphatase 2B catalytic subunit
NCU02614	nup-13	peptidyl-prolyl cis-trans isomerase H	NCU03816		hypothetical protein
NCU02631	drc-1	DNA replication complex GINS protein psf-1	NCU03829		hypothetical protein
NCU02651		hypothetical protein	NCU03838	trf-2	transcription elongation factor spt-4
NCU02663		L-lysine 2,3-aminomutase	NCU03850		ureidoglycolate hydrolase
NCU02678		hypothetical protein	NCU03868		hypothetical protein
NCU02679	cea-1	carboxylesterase	NCU03880		phosphorylcholine transferase
NCU02682		hypothetical protein	NCU03884		hypothetical protein
NCU02705		F1F0 ATP synthase assembly protein Atp10	NCU03906		BSD domain-containing protein
NCU02717	msp-17	pre-mRNA-splicing factor clf-1	NCU03908		fmp-52
NCU02743	vps26	vacuolar protein sorting protein 26	NCU03937		intermediate filament protein
NCU02748		rRNA-processing protein utp23	NCU03940		questionable protein
NCU02753		WD repeat-containing protein	NCU03964		hypothetical protein
NCU02780		U2 small nuclear ribonucleoprotein B	NCU03977		hypothetical protein
NCU02789		hypothetical protein	NCU04001	ff-7	female fertility-7
NCU02811	ham-8	hypothetical protein	NCU04034		hypothetical protein
NCU02830		ARF GTPase activator	NCU04054	Bml	tubulin beta chain
NCU02852		cytochrome P450	NCU04061		hypothetical protein
NCU02869		hypothetical protein	NCU04065	trm-7	potassium channel protein
NCU02877		hypothetical protein	NCU04085		hypothetical protein
NCU02896	ada-3	hypothetical protein	NCU04092		N-acylethanolamine amidohydrolase
NCU02913		DNA repair protein rad5	NCU04135		hypothetical protein
NCU02975		hypothetical protein	NCU04158	nmr	nitrogen metabolite regulation
NCU03019		hypothetical protein	NCU04171	mrp-21	50S ribosomal protein L5
NCU03023		phenol 2-monooxygenase	NCU04175		hypothetical protein
NCU03061		translation initiation factor RLI1	NCU04196		tRNA (adenine-N(1)-)-methyltransferase catalytic subunit trm61
NCU03068	pdx-3	glycerol-3-phosphate phosphatase 1	NCU04222		hypothetical protein
NCU03070		hypothetical protein	NCU04260		oxidoreductase domain-containing protein
NCU03136		hypothetical protein	NCU04267		hypothetical protein
NCU03142		hypothetical protein	NCU04282		hypothetical protein
NCU03158		alpha/beta hydrolase	NCU04283		hypothetical protein
NCU03166	ad-3A	phosphoribosylaminoimidazole-succinocarboxamide synthase	NCU04347		pyruvate formate lyase activating enzyme
NCU03208		hypothetical protein	NCU04427		hypothetical protein
NCU03233		hypothetical protein	NCU04440		hypothetical protein
NCU03245		hypothetical protein	NCU04466		cyanamide hydratase
NCU03265		hypothetical protein	NCU04470		HD domain-containing protein
NCU03283		2-keto-4-pentenoate hydratase	NCU04479		LAP2
NCU03298		hypothetical protein	NCU04484		hypothetical protein
NCU03310	phb-2	prohibitin-2	NCU04485		pre-rRNA processing protein Esf1
NCU03316	prr-2	pH-response regulator protein palC	NCU04538		hypothetical protein
NCU03355	mpr-2	calpain-5	NCU04572		hypothetical protein
NCU03359	iap-1	intermembrane space AAA protease IAP-1	NCU04576		hypothetical protein
NCU03401		hypothetical protein	NCU04593		Lcc9
NCU03413		hypothetical protein	NCU04600		protein phosphatase 2C isoform gamma
NCU03546		hypothetical protein	NCU04633		RING finger protein
NCU03561	mic-15	mitochondrial carrier protein	NCU04643		peptide-N4-(N-acetyl-beta-glucosaminyl)asparagine amidase A
NCU03564		flap structure-specific endonuclease	NCU04662	apg-4	autophagy protein 5
NCU03566		short chain dehydrogenase/reductase	NCU04710		hypothetical protein

Table A8. Continued.

Locus	Symbol	Name	Locus	Symbol	Name
NCU04724		VHS domain-containing protein	NCU05958		hypothetical protein
NCU04732		hypothetical protein	NCU05966		DNA repair protein
NCU04737	nst-1	chromatin regulatory protein sir2	NCU05977		dihydrodipicolinate synthase
NCU04744		dihydrodipicolinate synthetase	NCU05978		hypothetical protein
NCU04770		TATA-binding protein	NCU05990		cell surface receptor/MFS transporter
NCU04788		cytosolic Fe-S cluster assembling factor NBP35	NCU05999		CaaX farnesyltransferase beta subunit Ram1
NCU04809		MFS phospholipid transporter	NCU06012		hypothetical protein
NCU04811		hypothetical protein	NCU06019		hypothetical protein
NCU04824		hypothetical protein	NCU06026	qa-Y	quinate-Y
NCU04830		hypothetical protein	NCU06034		hypothetical protein
NCU04856	gln-2	glutamine synthetase	NCU06056		hypothetical protein
NCU04886		MFS multidrug transporter	NCU06059		hypothetical protein
NCU04889		hypothetical protein	NCU06078		hypothetical protein
NCU04905		hypothetical protein	NCU06083		hypothetical protein
NCU04959	gh16-4	secreted glucosidase	NCU06102		hypothetical protein
NCU04963		high-affinity glucose transporter	NCU06149	drh-10	ATP-dependent RNA helicase dhh-1
NCU04984		hypothetical protein	NCU06180		hypothetical protein
NCU05006	cyp450-8	cytochrome P450	NCU06182	nrc-1	nonrepressor of conidiation-1
NCU05035		hypothetical protein	NCU06196		hypothetical protein
NCU05054		hypothetical protein	NCU06264	mus-53	mutagen sensitive-53
NCU05115		hypothetical protein	NCU06284	vps35	vacuolar protein sorting-associated protein 35
NCU05135		hypothetical protein	NCU06299		hypothetical protein
NCU05159	ce5-2	acetylxylan esterase	NCU06302		hypothetical protein
NCU05168	pmb	arginine transporter	NCU06317		stress response RCI peptide
NCU05188		FAD monooxygenase	NCU06328		hypothetical protein
NCU05250		hypothetical protein	NCU06393		hypothetical protein
NCU05259		acyl-CoA desaturase 1	NCU06403		hypothetical protein
NCU05260		protein kinase domain-containing protein	NCU06423		hypothetical protein
NCU05271		hypothetical protein	NCU06425		hypothetical protein
NCU05293		rRNA processing protein Rrp8	NCU06439		zinc finger protein
NCU05298	nit-3	nitrate nonutilizer-3	NCU06440	pca-4	proteasome component PRE6
NCU05301		methyltransferase	NCU06453		hypothetical protein
NCU05315		hypothetical protein	NCU06551		hypothetical protein
NCU05385		hypothetical protein	NCU06604		hypothetical protein
NCU05394		MFS transporter	NCU06607		hypothetical protein
NCU05460		hypothetical protein	NCU06615		hypothetical protein
NCU05518		peroxisomal copper amine oxidase	NCU06655		lipid particle protein
NCU05540		hypothetical protein	NCU06664		recombination hotspot-binding protein
NCU05550		hypothetical protein	NCU06687	gsy-1	glycogen synthase-1
NCU05554	un-25	60S ribosomal protein L13	NCU06700		alpha/beta hydrolase
NCU05555		hypothetical protein	NCU06706		killer toxin sensitivity protein
NCU05557		hypothetical protein	NCU06738	sec31	protein transporter sec-31
NCU05609		hypothetical protein	NCU06762	gt34-1	alpha-1,6-mannosyltransferase subunit
NCU05628		hypothetical protein	NCU06782		zinc metalloproteinase
NCU05629		hypothetical protein	NCU06783		ATP citrate lyase
NCU05641		hypothetical protein	NCU06785		ATP-citrate synthase subunit 1
NCU05653		carbonic anhydrase	NCU06790		hypothetical protein
NCU05689	cox-4	cytochrome c oxidase polypeptide IV	NCU06799	vad-5	fungal specific transcription factor
NCU05695		hypothetical protein	NCU06826		hypothetical protein
NCU05784		hypothetical protein	NCU06867		hypothetical protein
NCU05794		hypothetical protein	NCU06869	paa-9	cleavage and polyadenylylation specificity factor
NCU05796		trafficking protein particle complex subunit 3	NCU06889		hypothetical protein
NCU05802	msp-31	ATP-dependent RNA helicase A	NCU06912		hypothetical protein
NCU05842		hypothetical protein	NCU06913		hypothetical protein
NCU05858		fatty acid oxygenase	NCU06918		purine permease
NCU05870		hypothetical protein	NCU06928		hypothetical protein
NCU05872		hypothetical protein	NCU06949	spr-6	subtilisin-like proteinase Mp1
NCU05908	mpr-4	hypothetical protein	NCU06965		hypothetical protein
NCU05915		hypothetical protein	NCU06998	rnp-6	scavenger mRNA decapping enzyme
NCU05931		hypothetical protein	NCU07042		alcohol dehydrogenase

Table A8. Continued.

Locus	Symbol	Name	Locus	Symbol	Name
NCU07061		hypothetical protein	NCU08376		hypothetical protein
NCU07064		L-galactonate dehydratase	NCU08390		hypothetical protein
NCU07066	mus-44	mating-type switching protein swi10	NCU08407		MFS transporter
NCU07113		hypothetical protein	NCU08408		btn-1
NCU07138		hypothetical protein	NCU08468	bud6	actin-interacting protein
NCU07166		hypothetical protein	NCU08469		hypothetical protein
NCU07205	nit-10	nitrate transporter CRNA	NCU08475		hypothetical protein
NCU07210		hypothetical protein	NCU08489	trm-36	transporter SMF1/ESP1
NCU07262	trm-29	hypothetical protein	NCU08523		hypothetical protein
NCU07279		hypothetical protein	NCU08535		acetyl-CoA carboxylase
NCU07301		hypothetical protein	NCU08541		hypothetical protein
NCU07338	gt32-2	alpha-1,6-mannosyltransferase Och1	NCU08554	ssp-1	peptidyl-prolyl cis-trans isomerase ssp-1
NCU07343		major facilitator family transporter	NCU08607		endoplasmic reticulum-Golgi intermediate compartment protein 3
NCU07380	eif3d	eukaryotic translation initiation factor 3	NCU08623		hypothetical protein
NCU07388		hypothetical protein	NCU08644		hypothetical protein
NCU07468		NAD dependent epimerase/dehydratase	NCU08695		hypothetical protein
NCU07479		hypothetical protein	NCU08705		hypothetical protein
NCU07502		hypothetical protein	NCU08764		hypothetical protein
NCU07533	39911	secreted aspartic proteinase	NCU08796		hypothetical protein
NCU07538		hypothetical protein	NCU08826		hypothetical protein
NCU07549	mrp-52	mitochondrial ribosomal protein L43	NCU08836		hypothetical protein
NCU07556	crf8-1	TBP associated factor	NCU08853		hypothetical protein
NCU07568		hypothetical protein	NCU08868	tgl-3	hypothetical protein
NCU07588		hypothetical protein	NCU08872		hypothetical protein
NCU07655	nup-29	hypothetical protein	NCU08874		BET3 family protein
NCU07656		hypothetical protein	NCU08879		hypothetical protein
NCU07678		hypothetical protein	NCU08887		hypothetical protein
NCU07681	vma-9	vacuolar ATPase subunit e	NCU08923		zinc knuckle domain-containing protein
NCU07699		hypothetical protein	NCU08930	nuo21.3a	NADH:ubiquinone oxidoreductase 21.3kD subunit a
NCU07737		salicylate hydroxylase	NCU08938	mag-1	DNA-3-methyladenine glycosylase
NCU07756	tca-11	succinate dehydrogenase cytochrome b560 subunit	NCU08952		translation regulator GCD7
NCU07802		hypothetical protein	NCU08962		hypothetical protein
NCU07837	csb	DNA repair protein Rhp26/Rad26	NCU08976		fatty acid elongase
NCU07850	nor-1	NADPH oxidase regulator NoxR	NCU08981		dml-1
NCU07886		hypothetical protein	NCU08989		ADP-ribosylation factor 1
NCU07887	rdr-1	ribonucleoside-diphosphate reductase small subunit	NCU09012		hypothetical protein
NCU07888		hypothetical protein	NCU09064		hypothetical protein
NCU07891		hypothetical protein	NCU09069		hypothetical protein
NCU07942		hypothetical protein	NCU09099		hypothetical protein
NCU07945	tah-4	fungal specific transcription factor	NCU09123	camk-1	Ca/CaM-dependent kinase-1
NCU08005		NADPH-adrenodoxin reductase Arh1	NCU09125		hypothetical protein
NCU08006		hypothetical protein	NCU09132	tba-1	alpha tubulin
NCU08015		hypothetical protein	NCU09163		hypothetical protein
NCU08023		cytohesin-2	NCU09167		hypothetical protein
NCU08064		meiotically up-regulated 190 protein	NCU09195	gpr-6	vacuolar membrane PQ loop repeat protein
NCU08091		hypothetical protein	NCU09199		tyrosinase
NCU08099		hypothetical protein	NCU09230	cys-16	cysteine-16
NCU08117		hypothetical protein	NCU09237		KH domain RNA binding protein
NCU08127	gh76-3	hypothetical protein	NCU09247		hypothetical protein
NCU08151		DNA kinase/phosphatase Pnk1	NCU09300		RNA Polymerase II CTD phosphatase Fcp1
NCU08170		hypothetical protein	NCU09312		di-trans,poly-cis-decaprenylcistransferase
NCU08184		hypothetical protein	NCU09314		hypothetical protein
NCU08227		hypothetical protein	NCU09321		sucrose transporter
NCU08232	gt32-1	alpha-1,6-mannosyltransferase Och1	NCU09348		hypothetical protein
NCU08251		hypothetical protein	NCU09349	drh-13	ATP-dependent RNA helicase has-1
NCU08260		hypothetical protein	NCU09371		6,7-dimethyl-8-ribityllumazine synthase
NCU08281		hypothetical protein	NCU09378	rpo-20	DNA-directed RNA polymerase II polypeptide
NCU08294	nit-4	nitrate nonutilizer-4	NCU09393		hypothetical protein
NCU08307		hypothetical protein	NCU09395		hypothetical protein
NCU08316		DUF221 domain-containing protein	NCU09401		hypothetical protein
NCU08342	csn-7	COP9 signalosome complex subunit 7a	NCU09433		hypothetical protein
NCU08347		hypothetical protein	NCU09438		translation repressor/antiviral protein Ski3
NCU08366		hypothetical protein	NCU09456		dimethylaniline monooxygenase

Table A8. Continued.

Locus	Symbol	Name
NCU09458		MFS transporter
NCU09465	dph-3	diphthamide biosynthesis protein 3
NCU09472		hypothetical protein
NCU09516	mus-41	DNA repair protein rad-5
NCU09606		hypothetical protein
NCU09629		hypothetical protein
NCU09657		hypothetical protein
NCU09702	gh5-6	endo-beta-1,6-galactanase
NCU09707	cpn-8	hypothetical protein
NCU09724		hypothetical protein
NCU09767		membrane transporter
NCU09786		hypothetical protein
NCU09792		UDP-galactose transporter Gms1
NCU09800		taurine dioxygenase
NCU09831		hypothetical protein
NCU09842	mak-1	mitogen-activated protein kinase MKC1
NCU09897	vma-5	vacuolar membrane ATPase-5
NCU09900		hypothetical protein
NCU09910		hypothetical protein
NCU09977		hypothetical protein
NCU09990		hypothetical protein
NCU10021	hgt-1	MFS monosaccharide transporter
NCU10027		hypothetical protein
NCU10101		hypothetical protein
NCU10304		hypothetical protein
NCU10400		phospholipase PldA
NCU10610		hypothetical protein
NCU10651		chitin binding protein
NCU10658		hypothetical protein
NCU10760		jumonji domain-containing protein 5
NCU10810		mRNA splicing protein
NCU10905		SH3 domain-containing protein
NCU10906		hypothetical protein
NCU10987		MFS transporter Fmp42
NCU11095		hypothetical protein
NCU11252		cyclin Pch1
NCU11307		CCC1
NCU11314		CaaX prenyl proteinase Rce1
NCU11409		ATP-dependent RNA helicase chl-1
NCU12033	gh18-11	class III chitinase
NCU12068		hypothetical protein
NCU12099		hypothetical protein
NCU12104		hypothetical protein
NCU12151		hypothetical protein
NCU16390	mito	mitochondrial
NCU16411	mito	mitochondrial
NCU16497	mito	mitochondrial
NCU16572	mito	mitochondrial
NCU16597	mito	mitochondrial
NCU16648	mito	mitochondrial
NCU16704	mito	mitochondrial
NCU16716	mito	mitochondrial
NCU16720	mito	mitochondrial
NCU16722	mito	mitochondrial
NCU16779	mito	mitochondrial
NCU16807	mito	mitochondrial
NCU16941	mito	mitochondrial
NCU16967	mito	mitochondrial
NCU17116	mito	mitochondrial
NCU17123	mito	mitochondrial
NCU17138	mito	mitochondrial
NCU17249	mito	mitochondrial
NCU17252	mito	mitochondrial

Table A9. List of constitutively expressed mRNAs that have rhythmic ribosomal occupancy due to RCK-2/eEF-2.

Locus	Symbol	Name	Locus	Symbol	Name
NCU00033		integral membrane protein	NCU01563		RNA polymerase II holoenzyme cyclin-like subunit
NCU00064		hypothetical protein	NCU01597		hypothetical protein
NCU00088		4-nitrophenylphosphatase	NCU01613	pp-2	protein arginine N-methyltransferase HSL7
NCU00133	ctc-1	FACT complex subunit pob-3	NCU01614		hypothetical protein
NCU00168		1-acylglycerol-3-phosphate O-acyltransferase	NCU01615		hypothetical protein
NCU00193	gt22-1	GPI mannosyltransferase 3	NCU01640	rpn-4	C2H2 transcription factor
NCU00205		hypothetical protein	NCU01678		amine oxidase
NCU00210		nuclear cap binding protein subunit 2	NCU01680	pma-1	plasma membrane ATPase-1
NCU00251	cpr-7	hypothetical protein	NCU01697		hypothetical protein
NCU00263		serin endopeptidase	NCU01706		MYB DNA-binding domain-containing protein
NCU00277		hypothetical protein	NCU01793		RNA binding domain-containing protein
NCU00346		EBDP2	NCU01794		hypothetical protein
NCU00356		nucleoside transporter	NCU01831		RNA polymerase TFIIH complex subunit Ssl1
NCU00372		hypothetical protein	NCU01835		hypothetical protein
NCU00373		hypothetical protein	NCU01839	cea-7	carboxylesterase
NCU00379		hypothetical protein	NCU01908		hypothetical protein
NCU00424		Spo76 protein	NCU01944		hypothetical protein
NCU00435		SNF7 family protein	NCU01992	cvc-3	coatomer subunit gamma
NCU00438		adenosine deaminase	NCU01994		bZIP transcription factor
NCU00459		hypothetical protein	NCU02034	rid-1	RIP defective
NCU00485		hypothetical protein	NCU02055		uridine nucleosidase Urh1
NCU00488		protein phosphatase PP2A regulatory subunit A	NCU02067	mdm12	mitochondrial inheritance component mdm12
NCU00648	aap-5	choline transporter	NCU02159		hypothetical protein
NCU00679		hypothetical protein	NCU02160	rac-1	small GTPase RAC
NCU00681		GTPase activating protein	NCU02201		laccase
NCU00721	aap-24	proline-specific permease	NCU02264	pfo-3	prefoldin subunit 3
NCU00727		hypothetical protein	NCU02272		hypothetical protein
NCU00740		hypothetical protein	NCU02315		hypothetical protein
NCU00741		gliotoxin biosynthesis protein GliK	NCU02355		hypothetical protein
NCU00755		hypothetical protein	NCU02362		hypothetical protein
NCU00762	gh5-1	endoglucanase 3	NCU02371	rbd2	rhomboid protein 2
NCU00790	hak-1	high affinity potassium transporter-1	NCU02385		hypothetical protein
NCU00795	trm-14	membrane bound cation transporter	NCU02415		zinc metalloproteinase
NCU00833		hypothetical protein	NCU02428	rbg-24	nucleolar essential protein 1
NCU00860	trm-37	ZIP family zinc transporter	NCU02460		syntaxin family protein
NCU00861		hypothetical protein	NCU02482	tca-2	2-methylcitrate synthase
NCU00881	ham-7	hypothetical protein	NCU02496	div-12	M-phase inducer phosphatase 3
NCU00913	gwt1	GPI-anchored wall transfer protein 1	NCU02559		hypothetical protein
NCU00931		lysyl-tRNA synthetase	NCU02561		hypothetical protein
NCU00948		hypothetical protein	NCU02578	sin3	paired amphipathic helix protein Sin3a
NCU00995		hypothetical protein	NCU02631	drc-1	DNA replication complex GINS protein psf-1
NCU01010		hypothetical protein	NCU02651		hypothetical protein
NCU01082		hypothetical protein	NCU02678		hypothetical protein
NCU01119	erg-5	lanosterol synthase	NCU02682		hypothetical protein
NCU01135		hypothetical protein	NCU02705		F1F0 ATP synthase assembly protein Atp10
NCU01147		tyrosine decarboxylase	NCU02717	msp-17	pre-mRNA-splicing factor clf-1
NCU01149		cupin domain-containing protein	NCU02743	vps26	vacuolar protein sorting protein 26
NCU01167		hypothetical protein	NCU02748		rRNA-processing protein utp23
NCU01184	msp-9	pre-mRNA splicing factor cwc2	NCU02753		WD repeat-containing protein
NCU01213	sod-2	superoxide dismutase-2	NCU02780		U2 small nuclear ribonucleoprotein B
NCU01243		C6 finger domain-containing protein	NCU02789		hypothetical protein
NCU01272	mpr-6	mitochondrial presequence protease	NCU02830		ARF GTPase activator
NCU01276		N-acetyltransferase 5	NCU02852		cytochrome P450
NCU01317	crp-45	60S ribosomal protein L12	NCU02869		hypothetical protein
NCU01362		INO80 chromatin remodeling complex	NCU02877		hypothetical protein
NCU01382		hypothetical protein	NCU02975		hypothetical protein
NCU01411		MFS multidrug resistance transporter	NCU03019		hypothetical protein
NCU01459	ts	hypothetical protein	NCU03068	pdx-3	glycerol-3-phosphate phosphatase 1
NCU01503		pre-rRNA processing protein Tsr1	NCU03142		hypothetical protein
NCU01549		hypothetical protein	NCU03158		alpha/beta hydrolase

Table A9. Continued.

Locus	Symbol	Name	Locus	Symbol	Name
NCU03166	ad-3A	phosphoribosylaminoimidazole-succinocarboxamide synthase	NCU04724		VHS domain-containing protein
NCU03208		hypothetical protein	NCU04732		hypothetical protein
NCU03233		hypothetical protein	NCU04737	nst-1	chromatin regulatory protein sir2
NCU03245		hypothetical protein	NCU04770		TATA-binding protein
NCU03265		hypothetical protein	NCU04788		cytosolic Fe-S cluster assembling factor NBP35
NCU03283		2-keto-4-pentenoate hydratase	NCU04809		MFS phospholipid transporter
NCU03298		hypothetical protein	NCU04811		hypothetical protein
NCU03316	prr-2	pH-response regulator protein palC	NCU04824		hypothetical protein
NCU03355	mpr-2	calpain-5	NCU04830		hypothetical protein
NCU03359	iap-1	intermembrane space AAA protease IAP-1	NCU04886		MFS multidrug transporter
NCU03401		hypothetical protein	NCU04889		hypothetical protein
NCU03413		hypothetical protein	NCU04905		hypothetical protein
NCU03546		hypothetical protein	NCU04959	gh16-4	secreted glucosidase
NCU03561	mic-15	mitochondrial carrier protein	NCU04963		high-affinity glucose transporter
NCU03566		short chain dehydrogenase/reductase	NCU04984		hypothetical protein
NCU03573	spc-3	hypothetical protein	NCU05054		hypothetical protein
NCU03590		hypothetical protein	NCU05159	ce5-2	acetylxylan esterase
NCU03600		GTP-binding protein EsdC	NCU05168	pmb	arginine transporter
NCU03610		NEDD8-conjugating enzyme UBC12	NCU05188		FAD monooxygenase
NCU03645		hypothetical protein	NCU05250		hypothetical protein
NCU03732		SIS1	NCU05259		acyl-CoA desaturase 1
NCU03752		EBP domain-containing protein	NCU05260		protein kinase domain-containing protein
NCU03753	ccg-1	clock controlled protein CCG-1	NCU05271		hypothetical protein
NCU03769	naf-2	hypothetical protein	NCU05293		rRNA processing protein Rrp8
NCU03782		DNA-directed RNA polymerase II subunit RPB11	NCU05301		methyltransferase
NCU03804	cna-1	serine/threonine-protein phosphatase 2B catalytic subunit	NCU05315		hypothetical protein
NCU03816		hypothetical protein	NCU05460		hypothetical protein
NCU03838	trf-2	transcription elongation factor spt-4	NCU05540		hypothetical protein
NCU03850		ureidoglycolate hydrolase	NCU05550		hypothetical protein
NCU03880		phosphorylcholine transferase	NCU05555		hypothetical protein
NCU03884		hypothetical protein	NCU05609		hypothetical protein
NCU03906		BSD domain-containing protein	NCU05628		hypothetical protein
NCU03908		fmp-52	NCU05629		hypothetical protein
NCU03937		intermediate filament protein	NCU05641		hypothetical protein
NCU03940		questionable protein	NCU05653		carbonic anhydrase
NCU03977		hypothetical protein	NCU05695		hypothetical protein
NCU04001	ff-7	female fertility-7	NCU05784		hypothetical protein
NCU04061		hypothetical protein	NCU05794		hypothetical protein
NCU04092		N-acylethanolamine amidohydrolase	NCU05796		trafficking protein particle complex subunit 3
NCU04158	nmr	nitrogen metabolite regulation	NCU05802	msp-31	ATP-dependent RNA helicase A
NCU04171	mrp-21	50S ribosomal protein L5	NCU05858		fatty acid oxygenase
NCU04175		hypothetical protein	NCU05870		hypothetical protein
NCU04196		tRNA (adenine-N(1)-)-methyltransferase catalytic subunit trm61	NCU05872		hypothetical protein
NCU04222		hypothetical protein	NCU05908	mpr-4	hypothetical protein
NCU04260		oxidoreductase domain-containing protein	NCU05915		hypothetical protein
NCU04267		hypothetical protein	NCU05931		hypothetical protein
NCU04283		hypothetical protein	NCU05958		hypothetical protein
NCU04347		pyruvate formate lyase activating enzyme	NCU05966		DNA repair protein
NCU04466		cyanamide hydratase	NCU05977		dihydrodipicolinate synthase
NCU04470		HD domain-containing protein	NCU05978		hypothetical protein
NCU04479		LAP2	NCU05999		CaaX farnesyltransferase beta subunit Ram1
NCU04484		hypothetical protein	NCU06019		hypothetical protein
NCU04485		pre-rRNA processing protein Esf1	NCU06026	qa-Y	quinate-Y
NCU04572		hypothetical protein	NCU06034		hypothetical protein
NCU04576		hypothetical protein	NCU06056		hypothetical protein
NCU04600		protein phosphatase 2C isoform gamma	NCU06059		hypothetical protein
NCU04633		RING finger protein	NCU06083		hypothetical protein
NCU04643		peptide-N4-(N-acetyl-beta-glucosaminyl)asparagine amidase A	NCU06102		hypothetical protein
NCU04662	apg-4	autophagy protein 5	NCU06149	drh-10	ATP-dependent RNA helicase dhh-1
NCU04710		hypothetical protein	NCU06180		hypothetical protein

Table A9. Continued.

Locus	Symbol	Name	Locus	Symbol	Name
NCU06182	nrc-1	nonrepressor of conidiation-1	NCU07887	rdr-1	ribonucleoside-diphosphate reductase small subunit
NCU06196		hypothetical protein	NCU07888		hypothetical protein
NCU06264	mus-53	mutagen sensitive-53	NCU07891		hypothetical protein
NCU06284	vps35	vacuolar protein sorting-associated protein 35	NCU07942		hypothetical protein
NCU06302		hypothetical protein	NCU07945	tah-4	fungal specific transcription factor
NCU06317		stress response RCI peptide	NCU08005		NADPH-adrenodoxin reductase Arh1
NCU06328		hypothetical protein	NCU08006		hypothetical protein
NCU06393		hypothetical protein	NCU08023		cytohesin-2
NCU06403		hypothetical protein	NCU08064		meiotically up-regulated 190 protein
NCU06425		hypothetical protein	NCU08091		hypothetical protein
NCU06439		zinc finger protein	NCU08117		hypothetical protein
NCU06440	pca-4	proteasome component PRE6	NCU08127	gh76-3	hypothetical protein
NCU06453		hypothetical protein	NCU08151		DNA kinase/phosphatase Pnk1
NCU06551		hypothetical protein	NCU08170		hypothetical protein
NCU06604		hypothetical protein	NCU08184		hypothetical protein
NCU06607		hypothetical protein	NCU08227		hypothetical protein
NCU06615		hypothetical protein	NCU08232	gt32-1	alpha-1,6-mannosyltransferase Och1
NCU06655		lipid particle protein	NCU08251		hypothetical protein
NCU06664		recombination hotspot-binding protein	NCU08260		hypothetical protein
NCU06687	gsy-1	glycogen synthase-1	NCU08281		hypothetical protein
NCU06700		alpha/beta hydrolase	NCU08294	nit-4	nitrate nonutilizer-4
NCU06706		killer toxin sensitivity protein	NCU08307		hypothetical protein
NCU06738	sec31	protein transporter sec-31	NCU08316		DUF221 domain-containing protein
NCU06762	gt34-1	alpha-1,6-mannosyltransferase subunit	NCU08347		hypothetical protein
NCU06782		zinc metalloproteinase	NCU08366		hypothetical protein
NCU06783		ATP citrate lyase	NCU08376		hypothetical protein
NCU06785		ATP-citrate synthase subunit 1	NCU08390		hypothetical protein
NCU06790		hypothetical protein	NCU08408		btn-1
NCU06799	vad-5	fungal specific transcription factor	NCU08468	bud6	actin-interacting protein
NCU06826		hypothetical protein	NCU08469		hypothetical protein
NCU06867		hypothetical protein	NCU08475		hypothetical protein
NCU06869	paa-9	cleavage and polyadenylylation specificity factor	NCU08535		acetyl-CoA carboxylase
NCU06889		hypothetical protein	NCU08554	ssp-1	peptidyl-prolyl cis-trans isomerase ssp-1
NCU06918		purine permease	NCU08607		endoplasmic reticulum-Golgi intermediate compartment protein 3
NCU06928		hypothetical protein	NCU08623		hypothetical protein
NCU06949	spr-6	subtilisin-like proteinase Mp1	NCU08695		hypothetical protein
NCU06965		hypothetical protein	NCU08705		hypothetical protein
NCU07066	mus-44	mating-type switching protein swi10	NCU08764		hypothetical protein
NCU07138		hypothetical protein	NCU08796		hypothetical protein
NCU07166		hypothetical protein	NCU08826		hypothetical protein
NCU07205	nit-10	nitrate transporter CRNA	NCU08853		hypothetical protein
NCU07210		hypothetical protein	NCU08868	tgl-3	hypothetical protein
NCU07279		hypothetical protein	NCU08872		hypothetical protein
NCU07301		hypothetical protein	NCU08874		BET3 family protein
NCU07380	eif3d	eukaryotic translation initiation factor 3	NCU08923		zinc knuckle domain-containing protein
NCU07388		hypothetical protein	NCU08938	mag-1	DNA-3-methyladenine glycosylase
NCU07468		NAD dependent epimerase/dehydratase	NCU08952		translation regulator GCD7
NCU07502		hypothetical protein	NCU08962		hypothetical protein
NCU07533	39911	secreted aspartic proteinase	NCU08976		fatty acid elongase
NCU07538		hypothetical protein	NCU08981		dml-1
NCU07556	crf8-1	TBP associated factor	NCU09012		hypothetical protein
NCU07568		hypothetical protein	NCU09064		hypothetical protein
NCU07588		hypothetical protein	NCU09069		hypothetical protein
NCU07655	nup-29	hypothetical protein	NCU09099		hypothetical protein
NCU07656		hypothetical protein	NCU09123	camk-1	Ca/CaM-dependent kinase-1
NCU07678		hypothetical protein	NCU09125		hypothetical protein
NCU07699		hypothetical protein	NCU09132	tba-1	alpha tubulin
NCU07756	tca-11	succinate dehydrogenase cytochrome b560 subunit	NCU09167		hypothetical protein
NCU07802		hypothetical protein	NCU09195	gpr-6	vacuolar membrane PQ loop repeat protein
NCU07850	nor-1	NADPH oxidase regulator NoxR	NCU09199		tyrosinase

Table A9. Continued.

Locus	Symbol	Name
NCU09230	cys-16	cysteine-16
NCU09237		KH domain RNA binding protein
NCU09300		RNA Polymerase II CTD phosphatase Fcp1
NCU09312		di-trans,poly-cis-decaprenylcistransferase
NCU09314		hypothetical protein
NCU09321		sucrose transporter
NCU09348		hypothetical protein
NCU09349	drh-13	ATP-dependent RNA helicase has-1
NCU09371		6,7-dimethyl-8-ribityllumazine synthase
NCU09393		hypothetical protein
NCU09395		hypothetical protein
NCU09458		MFS transporter
NCU09516	mus-41	DNA repair protein rad-5
NCU09629		hypothetical protein
NCU09657		hypothetical protein
NCU09702	gh5-6	endo-beta-1,6-galactanase
NCU09707	cpn-8	hypothetical protein
NCU09724		hypothetical protein
NCU09767		membrane transporter
NCU09786		hypothetical protein
NCU09792		UDP-galactose transporter Gms1
NCU09800		taurine dioxygenase
NCU09831		hypothetical protein
NCU09842	mak-1	mitogen-activated protein kinase MKC1
NCU09897	vma-5	vacuolar membrane ATPase-5
NCU09900		hypothetical protein
NCU09910		hypothetical protein
NCU09990		hypothetical protein
NCU10021	hgt-1	MFS monosaccharide transporter
NCU10101		hypothetical protein
NCU10400		phospholipase PldA
NCU10610		hypothetical protein
NCU10651		chitin binding protein
NCU10658		hypothetical protein
NCU10760		jumonji domain-containing protein 5
NCU10810		mRNA splicing protein
NCU10987		MFS transporter Fmp42
NCU11095		hypothetical protein
NCU11307		CCC1
NCU11314		CaaX prenyl proteinase Rce1
NCU11409		ATP-dependent RNA helicase chl-1
NCU12033	gh18-11	class III chitinase
NCU12068		hypothetical protein
NCU12099		hypothetical protein
NCU12104		hypothetical protein
NCU12151		hypothetical protein
NCU16390	mito	mitochondrial
NCU16411	mito	mitochondrial
NCU16572	mito	mitochondrial
NCU16597	mito	mitochondrial
NCU16704	mito	mitochondrial
NCU16716	mito	mitochondrial
NCU16722	mito	mitochondrial
NCU16779	mito	mitochondrial
NCU16807	mito	mitochondrial
NCU17116	mito	mitochondrial
NCU17123	mito	mitochondrial
NCU17138	mito	mitochondrial
NCU17252	mito	mitochondrial

APPENDIX B

The following lines of code and script are used in Linux (operating system – Ubuntu 14.04 LTE). Examples are provided for each line of code, replace as needed. Note: Transcriptome (RNAseq) data is analyzed differently from ribosome profiling data, where applicable I have indicated the differences.

Gunzip
gunzip RP_WT_0min.fastq.gz

Bowtie
Download files from Broad website (N. crassa OR74A (NC12)):

supercontigs.fasta
genes.fasta
transcripts.fasta
transcripts.gtf

To install:
sudo apt-get install bowtie
sudo apt-get install bowtie2

To build index files:
bowtie-build supercontigs.fasta NC_12_supercontigs
bowtie-build transcripts.fasta NC_12_transcripts
bowtie-build genes.fasta NC_12_genes

Repeat, but with bowtie2-build instead of bowtie-build.

Linker Sequence
CTGTAGGCACCATCAAT

CutAdapt Code (Ribosome Profiling)
To install:
sudo apt-get install python-dev
sudo pip install cutadapt

To trim files:
cutadapt -a CTGTAGGCACCATCAAT -o RP_LP2_0min_trimmed RP_LP2_0min.fastq

FastQC
To install:
sudo apt-get install fastqc

To analyze trimmed files (Ribosome Profiling) or fastq files (Transcriptome):
fastqc
(This command will pop up a new screen, select your file from the pull down menu.)

TopHat Code (Transcriptome)
tophat2 -p 2 -G NC_12_transcripts.gtf -o RP_output/RP_LP2_0min NC_12_index
RP_LP2_0min.fastq

TopHat Using Bowtie1 (Ribosome Profiling)
tophat2 --bowtie1 -p 2 -G NC_12_transcripts.gtf -o RP_output/RP_LP2_0min NC_12
RP_LP2_0min_trimmed

SamTools
samtools sort accepted_hits.bam accepted_hits_sorted
samtools index accepted_hits_sorted.bam

CuffDiff Code
Multiple Replicates:

cuffdiff -p 10 -b NC_12_transcripts.fa -o RP_output/CuffDiffData -u
NC_12_transcripts.gtf -L
RP_LP_0,RP_LP_15,RP_LP_30,RP_LP_45,RP_LP_60,RP_LP_120
LP_1_Output/LP_0min/accepted_hits_sorted.bam,LP_2_Output/RP_LP2_0min/accepte
d_hits_sorted.bam
LP_1_Output/LP_15min/accepted_hits_sorted.bam,LP_2_Output/RP_LP2_15min/accep
ted_hits_sorted.bam
LP_1_Output/LP_30min/accepted_hits_sorted.bam,LP_2_Output/RP_LP2_30min/accep
ted_hits_sorted.bam
LP_1_Output/LP_45min/accepted_hits_sorted.bam,LP_2_Output/RP_LP2_45min/accep
ted_hits_sorted.bam
LP_1_Output/LP_60min/accepted_hits_sorted.bam,LP_2_Output/RP_LP2_60min/accep
ted_hits_sorted.bam
LP_1_Output/LP_120min/accepted_hits_sorted.bam,LP_2_Output/RP_LP2_120min/acc
epted_hits_sorted.bam

Single replicate:

cuffdiff -p 10 -b NC_12_transcripts.fa -o RP_SI_Output/RP_SI_CuffDiff -u
NC_12_transcripts.gtf -L RP_SI_WT_0,RP_SI_WT_30,RP_SI_dR_0,RP_SI_dR_30
RP_SI_Output/RP_SI_WT_0min/accepted_hits_sorted.bam
RP_SI_Output/RP_SI_WT_30min/accepted_hits_sorted.bam
RP_SI_Output/RP_SI_dR_0min/accepted_hits_sorted.bam
RP_SI_Output/RP_SI_dR_30min/accepted_hits_sorted.bam

Cufflinks
cufflinks -p 5 -o LP_60min_cuff -g NC_12_transcripts.gtf LP_60min/accepted_hits.bam

CuffMerge
cuffmerge -g NC_12_transcripts.gtf -o RP_LP_Merged RP_Transcripts.txt

The following code was used to generate heatmaps in R studio, an example is provided:

```
> data <- read.table("adv1_log2_values.csv", header=TRUE)

> dim(data)

[1] 54  4

> data[1:3, 1:4]

   gene_id   X0_log2  X15_log2  X60_log2
1 NCU07819 -11.71340 -10.80020 -10.32090
2 NCU07610 -10.41340 -11.00030  -9.86065
3 NCU09039  -8.27261  -9.00188  -7.62168

> row.names(data) <- data$gene_id

> data <- data[, -1]

> data[1:3, 1:3]

          X0_log2  X15_log2  X60_log2
NCU07819 -11.71340 -10.80020 -10.32090
NCU07610 -10.41340 -11.00030  -9.86065
NCU09039  -8.27261  -9.00188  -7.62168
```

```
> my_palette <- colorRampPalette(c("red", "yellow", "green"))(n = 299)
> myfun <- function(data) hclust(as.dist(1-cor(t(as.matrix(data)), method = "pearson")),
method = "average")
> heatmap.2(as.matrix(data),Colv=FALSE, dendrogram = "row", hclustfun = myfun,
col=my_palette, tracecol="red")
```

APPENDIX C

SPECIALIZED RIBOSOMES: A NEW FRONTIER IN GENE REGULATION

This appendix describes a submitted and accepted grant proposal sent to the Joint Genome Institute (JGI) that is a collaboration between the laboratories of Deborah Bell-Pedersen and Matthew Sachs at Texas A&M University.

The goal of the project is to define the "ribosome code" and if ribosomes have distinct compositions at different times of the day, leading to the translation of specific mRNAs. The idea being that ribosomes are not all the same, and the circadian clock plays a role in regulating the composition of ribosomal proteins (rproteins) and/or accessory proteins. To determine the role of the clock in the composition of ribosomes, ribosomes were isolated from WT and Δ*frq* cells harvested over a circadian time course. The isolated ribosomes will then be analyzed using mass spectrometry (mass spec). The mass spec data will be used to identify (i) rprotein composition; (ii) modifications to rproteins; and (iii) composition of associated accessory proteins. Further work will involve determining the mechanism(s) for clock regulation of rproteins, rpotein modifications, and accessory proteins. The final goal of the project is to identify which mRNAs are translated by ribosomes with unique ribosome compositions. Using ribosome profiling in WT cells and in cells with misexpressed rproteins, rproteins that have altered modification sites, and deleted/mutated accessory proteins; specific mRNAs will be identified that are translated by the heterogeneous ribosomes. This project will provide a better

understanding of the ribosome code, uncovering mechanisms that may be applicable to higher eukaryotes due to the high conservation of ribosomes.

My specific contribution to this proposal included isolating ribosomes from WT and Δ*frq* cells harvested every 4 h over a 36 h period (n = 3). Isolation of ribosomes for all samples was validated using SDS-PAGE gels and coomassie staining (Figure C1).

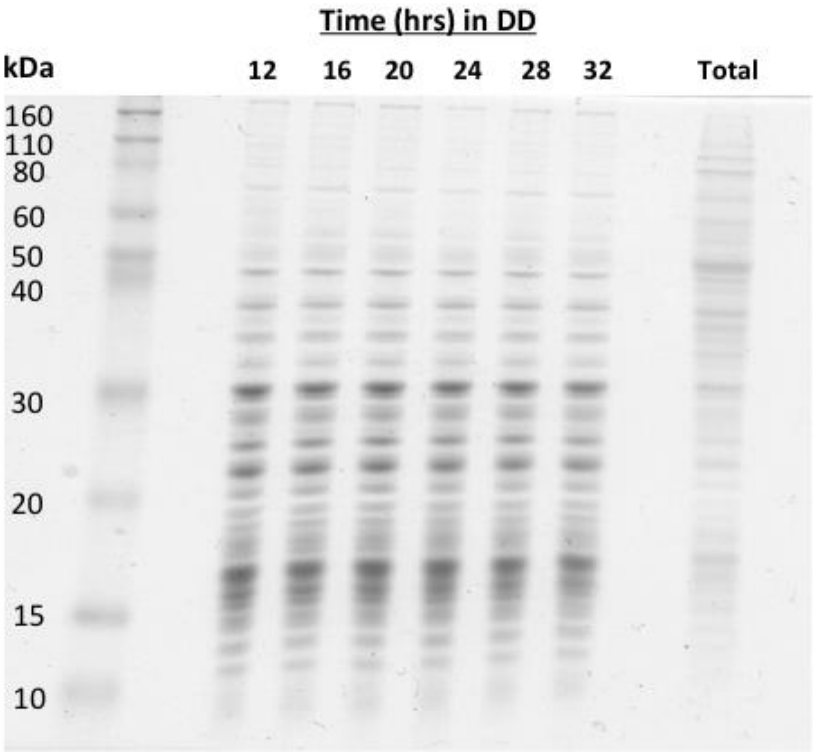

Figure C1. Validation of isolated ribosomes. SDS-PAGE gel of enriched ribosomes from WT cells harvested in the dark (DD) every 4 hrs. Molecular weight size markers are shown on the left and total protein extract on the right.